SEP. - DEC. 1998
Volume IV Number III

ISSN 0859 144X

THE ASEAN JOURNAL OF RADIOLOGY

Published by The Radiological Society and
The Royal College of Radiologists of Thailand,
Bangkok, Thailand

Supported through an educational grant from

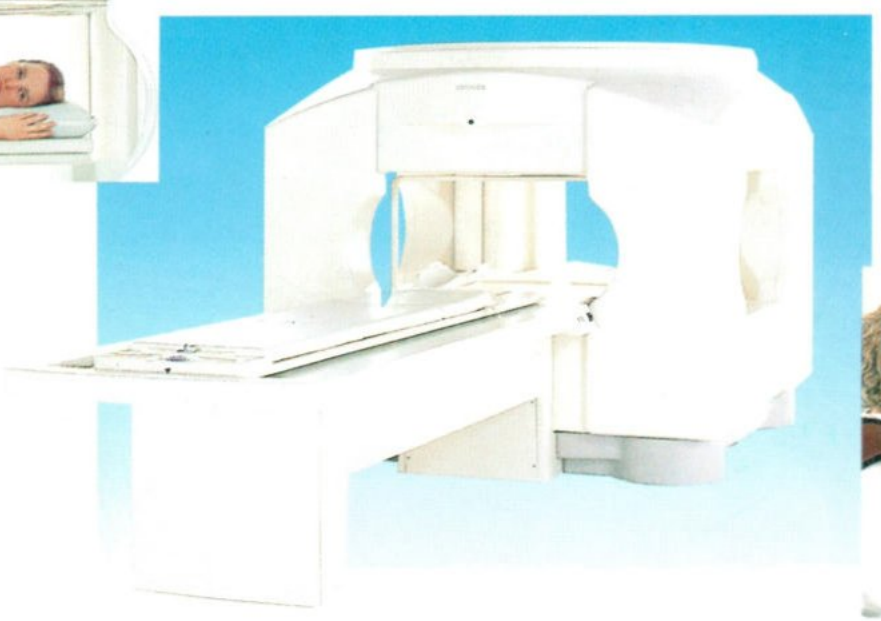

OPART

Superconducting Performance, OPEN MR Advantages.

The pioneer of open MR imaging, Toshiba has now developed a superconducting cryogenless magnet which sets new standards for open MR systems.

OPART takes advantage of the latest technology to provide exceptional image quality through a variety of fast scanning techniques.

A unique open magnet design offers all-round patient access, enabling even large, claustrophobic, and pediatric patients to be scanned with ease.

OPART Advantages

- Fast, flexible throughput for clinical productivity.
- Four sided patient accessibility, enhances patient comfort and throughput.
- A floating tabletop facilitates easy and accurate patient positioning for improved image quality.
- Icon driven computer platform, with user friendly software for true multitasking power.
- Long-term reliability and system upgradeability.
- Scanning is possible while the patient is still connected to ancillary MR compatible monitoring equipment.
- Exceptional performance across a variety of clinical applications.

TOSHIBA

GLOBAL IMAGING▪MEDICAL SYSTEMS

CMC BIOTECH

(SOLE DISTRIBUTOR)

CMC BIOTECH CO., LTD.

364 Muban Town-in-Town, Ladphrao 94 Ladphrao Road, Wangthonglang, Bangkok 10310

Tel. (662) 530-4995-6, 559-3261-2 559-2179-80, 538-4102, 538-0710 Fax : 539-6903

SEP. - DEC. 1998
Volume IV Number III

ISSN 0859 144X

THE ASEAN JOURNAL OF RADIOLOGY

Published by The Radiological Society and
The Royal College of Radiologists of Thailand,
Bangkok, Thailand

Supported through an educational grant from

BRACCO
INTERNATIONAL

ASDIR

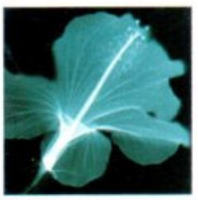

EDUCATION

Asian-Oceanian Seminars on Diagnostic and Interventional Radiology

1 9 9 9

Abdominal Imaging

February 12-13

Dhaka, Bangladesh

Programme Leader:

A.S.Q. Md. Sadeque

Musculo-Skeletal Radiology and Mammography

April 17-18

Singapore

Programme Leader:

J. Hoe

BRACCO

INTERNATIONAL

For further information please contact:
Huntington Communications Pte Ltd
47 Hill Street #07-03
S.C.C.C.I. Building
Singapore 179365
Tel: ++65-339 2883
Fax: ++65-339 2272
E-mail: hcompr@singnet.com.sg

http://www.bracco.com

1. The AAR Journal of Radiology publishes the papers on Radiological Sciences, such as research work, review articles, case reports, innovations in Medical Sciences related to all branches of Radiology, and letters to the editor. The aforementioned materials can be written in English only.

2. The authors have to submit 2 copies of the manuscript and a diskette: **to Prof. Dr. Kawee Tungsubutra,** 318 Kaweevej Hospital, Tarksin Road, Dhonburi, Bangkok 10600, Thailand. **or to the Associate Editors** at the Radiological Society of Malaysia, Indonesia, Philippine, Singapore and Brunei. The names and adresses of the Associate Editors in each country were published in the front page of this Journal.

3. The original copy to be submitted must be typed in a double space on one side of the page of 8.1/2"x 11.1/2" paper.

4. The format of the article must include :

a. Title page and address of the author (s)
b. Abstract
c. Introduction (Background)
d. Material and Method
e. Results and discussion (Tables and Illustrations)
f. Acknowledgement (if any)
g. References (Follow the Vancouver style developed by ICMJE)

5. We will provide 20 copies of reprints for the author (s) who submit (s) an article for publication in the AAR Journal.

6. The illustrations and tables must be clearly prepared with legends in English as they are the art works to be reproduced.

7. The authors are responsible for the contents of the article as to its facts and findings.

8. Ethics.

Paper reporting studies which might be interpreted as human experimentation (e.g. controlled trials) should conform to the standards of the Declaration of Helsinki (see British Medical Journal 1964:2:177) and should indicate that, approval that such studies may proceed, has been granted by the local or hospital Ethics Committee.

When reporting experiments on animals indicate whether the institution's or the National Research Council's guide for, or any national law on, the care and use of laboratory animals was followed.

THE ASEAN JOURNAL OF RADIOLOGY

Volume IV Number III SEP. - DEC. 1998

CONTENTS

THE ASEAN JOURNAL OF RADIOLOGY

Volume IV Number III SEP. - DEC. 1998

CONTENTS

GROWTH FRACTION DEFINED BY KI-67 IMMUNOSTAINING AS A SELECTION FOR COMBINED THERAPY OF RADIATION AND MITOMYCIN-C IN LOCALLY ADVANCED CERVICAL CANCERS

Badri C[1], Djakaria M[1], Sjamsudin S[2], Endang SRH[3]

ABSTRACT

OBJECTIVE To study the relationship between low growth fraction and hypoxic condition of the tumor that allows bioreductive agents, such as Mitomycin-C (MMC), to work more effectively in such environment. A prospective study was conducted at our institution between October 1994 and October 1996.

MATERIALS AND METHODS Sixty-one locally advanced cervical cancer patients with a low growth fraction as defined by Ki-67 immunostaining (Ki-67 index < 40%) were randomized into two groups. The first group of 30 patients were treated with irradiation alone and the second group of 31 patients were irradiated in combination with MMC. External irradiation was given with Linear accelerator or Co-60 to the whole pelvis, 180 cGy/fraction, 5 days a week, with a total dose of 5040 cGy in 5.5 weeks. This was followed by intracavitary afterloading irradiation within 2 weeks using High Dose Rate Co-60 sources, two applications, one week interval with a dose of 850 cGy at point A in each application. MMC was concurrently given as bolus injection on the first day of external irradiation and the first intracavitary application with a dose of body surface 15 mg/m^2 of each injection.

RESULTS Response of the tumors was determined within 3 months upon completion of irradiation. In the first group, complete response was achieved in 11 of 30 patients (36.6%), while in the second group, this was achieved in 26 of 31 patients (83.8%), showing significant difference between the two groups (p= 0.004). No marked difference of acute toxicity was observed.

CONCLUSIONS The results of the treatment suggested that low growth fraction tumors, which assumed as relatively hypoxic tumors, could be improved in their radiation response by Mitomycin-C.

Keywords Cervical cancer, Radiation response, Growth fraction, Ki-67 immunostaining, hypoxic tumor, Mitomycin-C.

[1] Department of Radiology,
[2] Department of Obstetrics and Gynecology,
[3] Department of Anatomic Pathology Faculty of Medicine, University of Indonesia Jakarta

BACKGROUND

Uterine cervical cancer (UCC) represents the most frequently encountered malignant tumor in women in various developing countries. The majority of patients admitted for treatment were at locally advanced stage, and the curative treatment could only be performed with radiation[1] whose results were not satisfactory yet. It was reported that the survival rate of the patients receiving radiation therapy alone was 50% at Stage IIb, 28% at Stage IIIb, and 10% at Stage IVa.[2,3] In developing countries, the survival rate of Stage III UCC patients proved to be lower, i.e., 22% for 5 years, and 25.2% for 3 years.[4,5]

One of the causes assumed to be responsible for the failure in radiation therapy is hypoxic condition for which hyperbaric oxygen, hypoxic radiosensitizer, treatment with bioreductive materials, and hyperthermia are used to overcome it.

One of the methods for treatment using bioreductive materials is a combined therapy of radiation and Mitomycin-C (MMC), i.e., a long known type of antibiotics and was already in use since 1956.[6] In either in vitro or in vivo experiments, MMC has been shown to enhance the results of radiation since this cytostatics works more effectively in hypoxic environtment of the tumor.[7] However, no desirable results have been achieved in its clinical application, particularly in treating UCC. The combined therapy for locally advanced UUC resulting in complete response ranged between 74.5 and 84.61%, which did not show significant difference from radiation therapy alone, i.e., 48.9% compared to 70%. Such is the case with survival rate which reached 73.08% compared to 60% in three years, and 59.6% compared to 42.0% in 30 to 72 months.[8,9] The fact that these results are not satisfactory yet may be due to the less selective administration of therapy, and in order to perform better selection, some reliable indicators will be necessary.

Mendehlson, 1960[10] showed that in a tumor tissue there is a proportion of proliferating cells called tumor growth fraction. The proliferating cells exist in the phases of a cell cycle, i.e., phases G_1, S, G_2, and M, while the non -proliferating cells (the quiescent cells) are at phase G_0. The determination of the size of growth fraction can be made by the use of various methods, such as through immunohistochemical examinations.

Gerdes, 1984[11] performed immunohistochemical examination by means of Ki-67 monoclonal antibody, and through this method the proliferating cells could be identified. These cells express Ki-67 antigen in its nuclear surface and could bind the correspondent monoclonal antibody such that it can be stained specifically. By comparing the number of proliferating cells and the total tumor cells, including quiescent cells, the size of tumor growth fraction may be identified and defined by Ki-67 index.

Nakano, 1993[12] used this technique in UCC patients and observed that the patients with Ki-67 of 33 %, or more, showed better response to radiation and more significant survival rate than the patients with Ki-67 less than 33%.

Thus, tumor growth fraction defined by Ki-67 can serve as predictor for radiation response and as prognostic factor in radiation therapy for UCC patients.

Sutherland, 1990[13] pointed out that hypoxic conditions could lead to changes at cellular level in tumor tissue. The condition of oxygen deficiency is generally accompanied by the nutritional deficiency and the occurrence of acid atmosphere in the environment of tumor cells. This

condition can result in inhibition to some of the proliferating cells that will terminate at phase G_1, and recede to phase G_0 such that tumor growth fraction is reduced, and thereby there is a likely correlation between hypoxia and low growth fraction.

Thus, it can be assumed that tumor growth fraction defined by Ki-67 index is an indicator for hypoxic tumor tissue.

Based on this assumption, values of Ki-67 index in locally advanced UCC may show the proportion of relatively hypoxic tumor group that is of some use for selecting therapy modality. The group with low Ki-67 index, which is considered to be relatively hypoxic, can be expected to yield favorable response to combined therapy of radiation and MMC, since the latter works more effectively in hypoxic conditions.

Hypotheses that can be formulated here is that the combined therapy of radiation and MMC in the patient group with low Ki-67 index provides better response to the tumor than the radiation therapy alone with insignificantly different toxicity.

The purpose of this study was to prove that the combined MMC and radiotherapy could enhance the results of radiation provided that this treatment is administered for the group of low growth fraction suspected to be hypoxic, and Ki-67 index can be used as the indicator for hypoxic conditions in locally advanced UCC.

MATERIALS AND METHODS

DESIGN

This study was a controlled clinical test, with basic design parallel for 2 groups of treatment in which each group served as the control group, respectively as:

a) Group of UCC patients with low growth fraction, receiving radiation therapy alone.
b) Group of UCC patients with low growth fraction, receiving combined therapy of radiation and MMC.

In this study, a number control variables were identified, i.e., age, clinical stage, histopathologic types, differentiation degree, type of growth fraction, tumor size, and Hb level. As control variables, which were also independent variables, were radiation treatment and combined treatment of radiation and MMC. Variables were dependent on response to tumor and therapy toxicity.

POPULATION AND SAMPLE

The population studied was all UCC patients at locally advanced stage according to the criteria established by FIGO (International Federation of Obstetrics and Gynecology) admitted for treatment at Division of Oncology, Department of Obstetrics and Gynecology, Faculty of Medicine University of Indonesia/Cipto Mangunkusumo General Hospital. In order to meet the criteria for the required sample size, all subjects fulfilling the criteria of the study were selected as samples through consecutive sampling.

INCLUSION CRITERIA

a) Performance status : 50-100 in Karnofsky scale [14]
b) Blood hemoglobin level : 10 g %, or higher
c) Number of lymphocyte : 4000/mm^3
d) Thrombocyte : > 100,000/mm^3
e) Renal and hepatic functions were normal
f) Lesion could be measured
g) Never receiving radiation and chemotherapy
h) No contraindications for therapy and chemotherapy.

EXCLUSION CRITERIA

a) Rejecting to participate in clinical tests
b) Cases with bleeding requiring immediate management
c) Age was > 70 years
d) Infection in pelvic cavity.

The calculation of sample size was done based on the assumption of the extent of radiation response in each group.
a) Group of low Ki-67 in radiation therapy alone : 35%
b) Group of low Ki-67 in combined therapy : 80%

The size of sample was counted using the calculation of response proportion in treatment group p (t) of 80%, and the control group p (c) of 35%, and by using the formula,[15] a sample of 22 subjects was obtained for each group.

Informed consent for medical intervention was obtained as necessary after the subjects of the study and their family were given explanation on the objective and steps of the study.

PATIENT SELECTION

Examinations were performed in patients suspected to develop locally advanced UCC admitted for treatment at the Oncology Polyclinic, Department of Obstetrics and Gynecology, Faculty of Medicine University of Indonesia/Cipto Mangunkusumo General Hospital, to determine the disease stage. Clinical and supporting examinations performed included thorax photos, intravenous pyelography, rectoscopy, cytoscopy, and laboratory examinations such as blood platelets, and renal and hepatic functions. Clinical stages were determined according to the system of FIGO of 1976.[16] Measurement of tumor size was performed with inspeculo, vaginal and rectal toucher. Patients with locally advanced Stage of IIb to IIIb meeting the inclusion criteria were included in the study. Patients at Stage IV were not included in the study since their management was subject to the prevailing protocols, and was not uniform.

Biopsy was performed in patients who met the criteria of the study for routine histopathologic and immunohistochemical examinations. Biopsy was performed at two sites opposite to the uterine cervix in order to obtain the more representative tissues. Both biopsy tissues were divided into two parts, i.e., the first part for routine histopathologic examination (Hematoxyllin-Eosin specimen), and the second one for immunohistochemistry using Ki-67 monoclonal antibody. Both types of examinations were performed at Department of Anatomic Pathology, Faculty of Medicine University of Indonesia/Cipto Mangunkusumo Hospital. Routine histopathologic examinations were done to identify histopathologic types and descriptions on the differentiation degree as specified in the protocol of routine histopathologic examinations established by the Working Group of Gynecologic Tumors, Faculty of Medicine University of Indonesia.

IMMUNOSTAINING EXAMINATION

All the fresh biopsy specimens were divided into two. One was fixed with 10% formaldehyde solution for conventional hematoxyllin and eosin staining and the other specimen was quickly frozen for Ki-67 immunostaining. The specimens were cut with a cryostat in 6 μm thickness, air dried, and fixed with cold 4% formaldehyde solution for 30 minutes. Then the sections were reacted with anti-Ki-67 monoclonal antibody.[17,18] (DAKO-PC; Dako, Copenhagen, Denmark) for an hour at room temperature. The sections were followed by reaction with biotinylated anti-mouse immunoglobulin G and avidin-biotin complex[19] (Vector Laboratories, Burlingame, CA) for 30 minutes. The sections

were reacted with 3.3-diaminobenzidine tetrahydrochloride (DAB, Dojin Chemicals, Tokyo) solution with 0.01% (w/v) hydrogenperoxide 23 for 2-5 minutes at room temperature and counterstained with hematoxylin. Control staining was done by incubating with phosphate-buffered saline, instead of anti-Ki-67 antiserum.

ASSESSMENT OF KI-67 INDEX

More than 1000 tumor cells per specimen were counted on three x 200 color photograph for calculation of the Ki-67 index. The Ki-67 index was estimated by the percentage of Ki-67 positive cancer cells among all the counted tumor cells.

The selection of threshold of Ki-67 index was determined on the basis of the reference of Nakano and Oka[20] who set up the margin of Ki-67 for low growth fraction to be 33% and 42%. In the present study, this margin was set at 40% based on the previous studies in 11 patients. It was found that Ki-67 ranged from 28.4% to 80.0% with a mean of 50.3% and a median of 49.9%. By using confidence interval of 95%, the percentage obtained was 40-60%, such that the lowest threshold of 40% was used.[21] The difference in the thresholds may be due to the varying clinical stages, geographic distribution, and different laboratory techniques used.

UCC patients at Stage IIb to IIIb who had been examined and whose diagnosis had been established were sent to Radiotherapy Unit for radiation planning. Patients were then divided into two groups, i.e., the group with Ki-67 of 40% or higher, and the group with Ki-67 index lower than 40%. In the latter group, randomization was performed, i.e., half of the patients were administered radiation alone, and the other half was given combined therapy of radiation and Mitomycin-C (MMC).

The group with Ki-67 index (40% would be treated the same way and reported in the future.

RADIATION TREATMENT

Radiation treatment was administered in two stages. The first stage was external radiation given to the whole pelvis, and the second stage was intracavitary radiation given in 1 to 2 weeks upon completion of external radiation. External radiotherapy was administered with radiation field, with superior border in lumbal IV and V vertebral rifts, and the inferior border was at the inferior border of pubis symphysis, and lateral border was 1.5 cm from linea inominata. A dose of 180 cGy fraction was administered 5 times per week, totaling 5040 cGy in 6.5 weeks. Radiation was given through antero-posterior field with linear accelerator of 10 or 4 megavolt instrument, or telecobalt-60 instrument.

At the end of external radiation, gynecologic examinations were performed to identify the response to radiation and to determine intracavitary radiation. Intracavitary radiation was performed when the at gynecologic examinations patients met the criteria, such as tumor had regressed in such a way that the applicator could be installed in the standard position. Intracavitary radiation was performed under spinal anesthesia if the first method failed. The applicator used was a rigid one; generally the applicator of RRTI (Rotterdam Radiotherapeutisch Instituut) model was applied with modified Manchester system.[22] The position of applicator was observed and improved with the aid of X-ray C-arm, and once it was well-positioned a calculation of isodose was performed to determine the required dose at point A, bladder, and rectum. The calculation of dose was done with Treatment Planning System and with Sidos-U computer from Siemens, or by using TSG-Radplan from IAEA that had both been calibrated with TLD.[23]

In general, intracavitary radiation was administered with High Dose Rate (HDR) afterloading techniques using Cobalt-60 source with HDR Selectron instrument (Nucletron). A dose of 850 cGy at point A was administered twice in one-week interval. In a number of patients, afterloading techniques were performed manually with Low Dose Rate (LDR), using Cs-137 source with a dose of 1300 cGy twice in one-week interval at point A. It was calculated that bladder and rectal doses did not exceed 80% of the dose at point A.

TUMOR RESPONSE

Tumor response was evaluated on the basis of the criteria of UICC[24] and determined at the end of radiation, in 1 month, and 3 months after completion of radiation. In addition to clinical examinations, biopsy interventions/histopathologic examinations were performed in 3 months after radiation.

Data were processed and analyzed with SPSS program with bivariate statistic test using Chi-square test for categorical variables and differentiation test of mean in continues variables. Furthermore, multivariate statistic test with logistic regression was used if bivariate statistic test was found to be significant.

RESULTS

From October 1, 1994 to November 30, 1996, 61 patients completed overall treatment and were evaluated up to 3 months after completion of radiation. The characteristics of 61 patients evaluated could be seen in (Table 1.)

TABLE 1. Patient's Characteistics

		No. of patients	%
Age	Mean	46.6	
	SD	9.3	
Stage	IIb.	38	62.2
	IIIa.	0	0
	IIIb.	23	37.7
Histologic type	Squamous cell Ca	48	78.6
	Adenocarcinoma	11	18.0
	Adenosquamous Ca	2	3.2
Histologic grade	Well differentiated	19	31.1
	Moderately differentiated	32	52.4
	Poorly differentiated	10	16.3
Tumor's size	< 4 cm	20	32.7
	4-6 cm	41	67.2
	> 6 cm	0	0
Hb level (pre-irradiation)	<12	37	60.6
	≥12	24	39.3
		61	100

Patients consisted of females aged between 26 and 69 years, with a mean of 46.6 years. The majority of them were at Stage IIb (62.2%). The most frequently found histopathologic type was squamous cell carcinoma (78.6%). However, the type of adenocarcinoma was found to be somewhat higher than the normal population, i.e., 18%, with the mostly frequently found differentiation of moderate degree (52.4%). Most of the patients had tumor measuring 4 - 6 cm (67.2%), and had Hb level < 12 g% (66.6%).

CHARACTERISTICS OF TREATMENT

Patients were divided into two types of treatment, i.e., 30 patients were treated with radiation alone, and another 31 patients with combined therapy of radiation and MMC.

TABLE 2. Characteristics of treatment

Type of treatment	No. of pts
Irradiation alone	30
Combined irradiation with MMC	31
Intracavitary irradation	
• High Dose Rate (HDR)	43
• Low dose rate (LDR)	18
• Intracavitary radiation dose	
Point A :	
HDR : mean 1700.0 cGy (TDF 50)	
LDR : mean 2600.0 cGy (TDF 50)	
Bladder :	
HDR : mean 1490,4 cGy (TDF 44)	
LDR : mean 1998,3 cGy (TDF 38)	
Rectum:	
HDR : mean 1351,3 cGy (TDF 39)	
LDR : mean 2003.5 cGy (TDF 38)	

TREATMENT OF INTRACAVITARY RADIATION

The majority of patients, i.e., 43 patients (70,5 %) received intracavitary radiation using HDR system, while another 18 patients (29,5 %) received manual afterloading application using LDR Cs-137 source. We resorted to this technique because HDR instrument was out of order for several months. The size and rate of the dose were calculated and tailored to HDR dose using Time Dose Fractionation (TDF) that was considered to have similar biological effects (Table 2). In the first group, the average dose administered was 2 x 850 cGy, or equivalent to TDF 50 at point A. The average bladder dose was 1490,4 cGy (TDF 44) and the rectal dose 1351,3 cGy (TDF 30). In the second group, dose at point A was 2 x 1300 cGy (TDF 50) with an average bladder dose of 1998,3cGy (TDF 38), and rectal dose of 2003.5 cGy (TDF 38).

TABLE 3. Distribution of variables according to type of treatment

	Irradiation		Irradiation + MMC		n	p
Variables	Risk (+)	Risk (-)	Risk (+)	Risk (-)		
Stage	10	20	13	18	61	NS
Histol. Type	6	24	7	24	61	NS
Tumor's size	19	11	9	22	61	0,02 (S)
Hb level	17	13	20	11	61	NS
Histol. Grade	4	26	10	21	61	NS

COMPARABILITY OF GROUPS

Of the various factors studied, some of them had the risks that may affect the evaluation of treatment impact. Thus, in order to avoid bias in two groups of treatment, i.e., the group of radiation therapy and the group of combined therapy of radiation and MMC, the risk factors must be divided evenly.

Variables evaluated to have risk factors were:

1) Clinical stage: positive risk was stage III, negative risk was stage II
2) Histologic types : positive risk was adeno-carcinoma, negative risk was squamous cell carcinoma.
3) Histologic grade: positive risk was the patients with unfavorable histologic grade, negative risk was those with moderate and favorable histologic grade.
4) Tumor size: Positive risk was tumor with a diameter of ≥ 4 cm, and negative risk was that with a diameter of < 4 cm.
5) Hb level: positive risk was the patients with Hb level < 12 g%, and negative risk was those with Hb ≥ 12 g%.

EVALUATION OF TUMOR RESPONSE

Evaluation of tumor response based on clinical examinations was performed in all patients at the end of radiation, in 1 month, and 3 months after completion of radiation according to the criteria of UICC. In all patients, either complete or partial response was found, and no response categorized as no change or progressive disease was encountered. In 27 patients, biopsy was performed in 3 months following radiation. The results of clinical examinations in the form of complete response were found in 22 patients, compatible with 18 patients with negative anatomic pathology, while there existed a remaining tumor in 5 patients, and 4 patients showed positive anatomic pathology. In terms of sensitivity, clinical examinations reached 80 %, while specitivity reached 81,8 %.

Sixty-one patients who completed radiation with a 3-month follow-up consisted of 2 groups of treatment, i.e.,

1) Group I (radiation therapy alone) with complete response : 11 patients (36.6%).
2) Group II (combined radiation therapy) with complete response : 26 patients (83.8%).

Thus, different type of treatment yielded different tumor response. In this case, the combined therapy provided more significant response than the radiation therapy alone. (Table 4).

TABLE 4. Response of tumor according to type of treatment

Type of treatment	Complete Response		Partial Response		Total	
	n	%	n	%	n	%
Irradiation + MMC	26	83,8	5	16,2	31	100
Irradiation	11	36,6	19	63,4	30	100
Total	37	60,6	24	39,4	61	100

MULTIVARIATE ANALYSIS

Multivariate analysis was performed because there existed significant influence of tumor size on treatment response in different treatment groups. For that reason, logistic regression test was done with the following determination of variables:

Dependent variable : treatment response.
Independent variables : types of treatment and tumor size.

In statistical test, it was evident that type of therapy significantly determined therapy response with factor of 4 times, while tumor size determined the response by 2 in patients with low fraction growth.

TOXICITY OF TREATMENT

Toxicity evaluated was acute toxicity during radiation and up to 3 months afterwards, and divided into 5 degrees, i.e., from 0 to IV using the criteria of ECOG. In the present study, toxicity degree was rendered to be a simpler one:

1) Mild toxicity, degree 0 - I
2) Moderate toxicity, degree II - III
3) Severe toxicity, degree IV

Toxicity of digestive tract was the most frequently found toxicity observed in 45 patients (74.5%); however, this toxicity was generally mild and mostly found in degree I. This was followed by hematologic toxicity that was observed in 31 patients (50.8%), and mostly occurred in decreased Hb (26 patients), followed by reduced leukocyte (24 patients), and mostly found in degree I. The next toxicity was observed in urinary tract that was found in 15 patients (24.5%), and mostly occurred in degree I. By contrast, patients suffering toxicity of degree III were 3, and no one suffered toxicity of degree IV (Table 5).

TABLE 5. Toxicity of treatment

Organ	n	%
Digestive tract	45	73,7
Hematological	31	50,8
Urinary tract	15	24,5
Others	3	4,9
Total	61	100

There was no significant difference in toxicity between the group of patients treated with radiation only or combined irradiation with MMC (Table 6).

TABLE 6. Comparison of toxicity according to type treatment

Toxicity	Irradiation	Irradiation + MMC	Total
Mild	24	21	45
Moderate	6	10	16
Total	30	31	61

DISCUSSION

It was evident that the radiation therapy alone in the group of patients with low Ki-67 index, i.e., less than 40%, resulted in unfavorable tumor response, i.e., complete response was found only in 11 of 30 patients (36.6%). As known, radiation response in UCC patients correlated with the tumor local control in the pelvis,[25] and the patient's survival rate.[26] With this less favorable prognosis, it would be appropriate to administer more intensive therapy. Combined therapy of radiation and MMC proved to provide more significant response in the group of patients with low Ki-67 index., i.e., 26 of 31 patients (83.8%) experienced complete response.

In addition, tumor growth fraction defined by Ki-67 index represented an independent predictor factor.[27] This was evident from biva- riate analysis, suggesting that tumor size played a part in radiation response. However, in multi- variate analysis, it showed that such influence was not significant. Other study [28] focusing on the group of patients with large tumor suggested a less satisfactory radiation response. Thus, tumor size constituted a prognostic factor with an adverse impact on UCC.

Previously, we assumed that there existed a close correlation between low growth fraction and hypoxic condition of the tumor tissue. This finding was based on an in vitro study[29] that was subsequently supported by the recent clinical studies.[30] With such assumption in mind, the group of patients with low growth fraction, suspected to be hypoxic, could be treated more definitely. Treatment modality adopted in this study was combined therapy of radiation and MMC that was considered to be more effective for hypoxic tumors. It proved that the combined therapy of radiation and MMC for the low growth fraction tumors yielded significantly better results than the radiation therapy alone, i.e., each with complete response of 83.8% and 36.6% respectively ($p = 0.004$).

With better results obtained from the combined therapy for UCC patients with low Ki-67 index, other treatments to overcome the problem of hypoxia was made possible, such as the use of hypoxic radiosensitizer, hyperthermia, and so forth, which in the past had not yielded satisfactory results. Such unsatisfactory results may be attributed to the fact that the treatment was performed in hypoxic tumors without cautious selection. Thus, the opportunity to perform a study with this mode of study may be more feasible. It is hoped that such a study could be performed in other tumors receiving radiation therapy as a curative treatment with hypoxic problems, such as nasopharynx cancer. There exists a number of

theories that correlate hypoxic condition with low growth fraction, such as: passive mechanism and active mechanism.

In passive mechanism, tumor cells situated more distant from blood vessels would suffer more oxygen and nutrition deficiency, and with adverse environmental impacts the metabolism of those cells would come to an end. Even if they still survive they would remain quiescent until the atmosphere improves. The weak cells would not survive, be necrotic and die.[31] Other theory held that in hypoxic condition due to disrupted vascularization or nutrition deficiency, a mechanism of cell preservation serving as genetic regulation would evolve to protect the cell from any possible threat. Here, the role of p^{53} as "watchman" was evident in regulating the cell's defense system. In severe hypoxic condition, p^{53} would direct the cells to perform apoptosis (programmed death). However, in milder hypoxic condition, through cyclin-dependent kinase inhibitor, i.e., p^{21}, p^{53} would inhibit various dependent kinases, i.e., CDK2, CDK4/6 and cdc2 that correlate with various cyclins, such as cyclins A, B, D, and E, which in turn change the activities of key proteins that control the cell's entry into cell cycles.[32] One of the inhibitions is to prevent cells that have completed mitosis from entering into phase G_1, such that those cells will recede into phase G_0, preventing them from proliferating and thereby reducing tumor growth fraction. Apoptosis itself could serve as predictor for the response to radiation, including locally advanced UCC.[33] This may be attributed to the extent of severity of hypoxic condition in the tumor tissue. Thus, the relationship between apoptosis and growth factor could provide important information on the severity of hypoxic condition.

To prove further the clinical relationship between growth fraction and hypoxic condition, a study on the pO_2 measurement using direct microelectrode[34] and immunohistochemistry using Ki-67 in the treatment of UCC is necessary. This will be more relevant if an examination on vascular density and intercapillary distance is also performed,[35] such as the relationship among the microenvironment factors resulting from tumor development and vascular changes may be proved. The recent report of the study performed by Nakano et al, 1997, suggested that there existed a correlation between pO_2 measured by microelectrode and tumor growth fraction defined by Ki-67 index.[36]

Clinical toxicity due to the combined application of radiation and MMC can be classified into acute and chronic toxicities. In the present study, acute toxicity did not reveal any significant increase between the group receiving combined radiation and the group with radiation alone.

In the previous studies,[37] effects of bone marrow depression in the administration of MMC were noticeable. However, these effects were not evident in the current study. This may be due to the fact that the dose administered was sufficient and the interval of administration was sufficiently long (approximately 8 weeks), such that hematologic toxicity of the first MMC administration had been lessened before the second administration. The dose given referred to the MMC administration in a prospective study on cervical and head and neck cancers, i.e., 15 mg/m^2 of body surface[38] in a 6-week interval for subsequent MMC administration. With such dose and method, the therapy response was sufficiently good with minimum toxicity. In addition, in this study radiation was administered with relatively lower dose per fraction, i.e., 180 cGy, administered 5 times a week during approximately 5.5. weeks with a total dose of 5040 cGy. Routine radiation was administered with a dose 200 cGy per fraction in the period of 5 weeks, with a total of 5000 cGy. The administration of different dose per fraction would result in different biological effects

if it was not compensated with identical amount of time of radiation and identical total dose. To achieve the similar biological effects, a TDF (Time Dose Fractionation) factor from Orton, 1973,[39] was used. In the current study, a TDF smaller than the conventional radiation was used. However, it was still within the limits of the radiation dose frequently administered conventionally to the pelvis area or parametria, i.e., between 4500 and 5000 cGy. It is hoped that with such dose, the radiation administered was effective, and thereby the cumulative toxicity from both treatment modalities could be reduced.

Clinical toxicity of chronic nature could not be assessed yet since the evaluation was made in 3 months after completion of therapy. In general, chronic toxicity in UCC was assessed after 6 months following the therapy. Chronic toxicity due to MMC was frequently observed in the lungs, heart and kidney. Nevertheless, those areas were not affected by radiation during the radiation of UCC, such that no cumulative toxicity occurred in those organs.

Based on the above findings, it was evident that the combined therapy of radiation and MMC could be practically applied. The possible barrier to be faced is that the examination with monclonal antibody Ki-67 requires frozen section that calls for a special management. Such special management requires a close coordination among the relevant departments, i.e., Departments of Obstetrics and Gynecology, Anatomic Pathology, and Radiology. The crucial problem is that how the biopsy tissue could be frozen in low temperature immediately after the tissue removal, and be kept in a low temperature before immunohistochemistry is performed. However, most of those barriers may be overcome, because currently the specimens using paraffin block can be made, as they have been performed for routine HE examination. The antibody used in this examination was MIB-1 monoclonal antibody or Ki-67 polyclonal antibody. Both antibodies have the same specificity in determining the size of growth fraction in the tumor with Ki-67 monoclonal antibody.[40]

CONCLUSIONS

In conclusion, the above findings suggested that the low growth fraction, which resulted in poor response to the radiation, yielded better results through the administration combined radiation and MMC. We assumed that the low tumor growth fraction provides important description on the hypoxic tumor tissue, such that MMC working more effectively in hypoxic condition will enhance the results of radiation. However, in order to prove conclusively that the growth fraction correlates with hypoxic condition, a further study employing, among others, O2 measurement with microelectrode will be necessary.

REFERENCES

1. Tobias JS. The role of Radiotherapy in the Management of Cancer : Overview. Ann Acad Med Singapore 1996; 25:371-9.
2. Annual Report on the results of Treatment in Gynecological Cancer. Vol 18. Kottmeier HL, Kolstad P, McGarrity KA, Peterson F, and Uifelder H editor. Stockholm: International Federation of Obstetrics and Gynecology 1982.
3. Hanks GE, Herring DF, Kramer S. Patterns of care outcome studies. Results of the national practice in cancer of the cervix. Cancer 1983; 51: 959.
4. Puriphat S, Chotivaganich C. Results of Radiation Therapy in Carcinoma of Cervix. Thai Cancer Journal 1984; 10: 115-121.
5. Nnatu SNN, Durosinmi - Etti FA. The Problems with the management of carcinoma of cervix in Nigeria - Lagos experience. East Afr Med J 1985; 62 (5): 347.

6. Hata T, Sano Y, Sugawara R. et al. Mitomycin, a new antibiotic from streptomyces. Int J Antibiot 1956; 9:141.
7. Rockwell S. and Kennedy KA.: Combination therapy with radiation and mitomycin C: pleliminary results with EMT6 tumor cells in vitro and i vivo. Int J Radiat Oncol Biol. Phys. 1982; 8:1035-1039.
8. Yongyut K, Pisit S, Piya P. High Dose Mitomycin-C with Concomitant Radiation Therapy in the Treatment of the Carcinoma of the Uterine Cervix. In : Azis MF, Kampono N, Sjamsudin S, eds. Cancer of the Uterine Cervix. Current Impact on Chemoirradiation Therapy. Jakarta : Department of Obstetrics and Gynaecology Faculty of Medicine University of Indonesia , 1988 : 31-37
9. Lorvidhaya V, Tonusin A, Charoeniam V, Punpae P, Changwiwit W, Isariyodom P. Induction Chemotherapy and Irradiation In Advanced Carcinoma of The Cervix . In : Azis MF, Kampono N, Sjamsudin S, eds. Cancer of the Uterine Cervix. Current Impact on Chemoirradiation Therapy. Jakarta : Department of Obstetrics and Gynaecology Faculty of Medicine University of Indonesia , 1988 : 47-52.
10. Mendelsohn ML. The growth fraction: A new concept applied to tumors. Science 1960; 132:1496.
11. Gerdes.J, Lemke H, Baisch H, Wacker HH, Schwab U, Stein H. Cell cycle analysis of a cell proliferation-associated human nuclear antigen defined by the monoclonal antibody Ki-67. J Immunol 1984; 133: 1710-1715.
12. Nakano T, Oka K. Differential values of Ki-67 index and mitotic index of proliferating cell population. An assessment of cell cycle and prognosis in radiation therapy for cervical cancer. Cancer 1993; 72:2401-8.
13. Sutherland R, Freyer J, Klieser MW et al. Cellular Growth and Metabolic Adaptations to Nutrient Stress Environments in Tumor Microregions. Int.J.Radiat. Oncol Biol Phys 1986; 12: 611-615.
14. Lorvidhaya V, Tonusin A, Charoeniam V, Punpae P, Changwiwit W, Isariyodom P. Iduction Chemotherapy and Irradiation In Advanced Carcinoma of The Cervix . In : Azis MF, Kampono N, Sjamsudin S, eds. Cancer of the Uterine Cervix. Current Impact on Chemoirradiation Therapy. Jakarta : Department of Obstetrics and Gynaecology Faculty of Medicine University of Indonesia , 1988 : 47-52.
15. Armitage P, and Gehan EA. Statistical methods for the identification and use of prognostic factors. Int. J. Cancer 1974; 13: 16-36.
16. International Federation of Gynecology and Obstetrics. Annual report on the results of treatment in carcinoma of the uterus, vagina and ovary. vol 16. Sweden Radiumhemmet, 1979
17. Setiawan I, Badri C. Pengalihan Catatan Registrasi Kanker ke Sistem Komputerisasi di Instalasi Radioterapi RSCM sebagai Penunjang Akurasi Data Insidensi Kanker. Jakarta: Instalasi Radioterapi RSCM, 1996
18. Tobias JS. The role of Radiotherapy in the Management of Cancer : Overview. Ann Acad Med Singapore 1996; 25:371-9.
19. Rockwell S. and Kennedy KA.: Combination therapy with radiation and mitomycin C: pleliminary results with EMT6 tumor cells in vitro and i vivo. Int J Radiat Oncol Biol. Phys. 1982; 8:1035-1039.
20. Nakano T, Oka K. Differential values of Ki-67 index and mitotic index of proliferating cell population. An assessment of cell cycle and prognosis in radiation therapy for cervical cancer. Cancer 1993; 72:2401-8.

21. Gardner MJ, Altman DG. Eds. Statistics with Confidence. Confidence intervals and statistical guidelines. London:The British Medical Journal, 1989; 71-9.
22. Aziz MF, Kampono N, Syamsuddin S, Djakaria M. Manual Pre Kanker dan Kanker Serviks Uterus, edisi ke satu, Jakarta Bagian Obstetri Ginekologi FKUI 1985 ; 1-7.
23. Tannock IF. The relation between cell proliferation and the vascular system in a transplanted mouse mammary tumour. Br J Cancer 1968;22:258-273.
24. Monfardini S, Brunner K, Crowther D, et al. editors. Manual of cancer chemotherapy. Geneva : UICC, 1981.
25. Shinleton HM, Gore H, Soong S-J, et al: Tumor recurrence and survival in stage Ib Cancer of the cervix. Am J Clin Oncol 1983; 6:265-272.
26. Suit HD, Westgate SJ. Impact of improved local control on survival. Int J Radiat Oncol Biol Phys 1986; 12:453-58
27. Brown DC and Gatter KC. Monoclonal antibody Ki-67 : its use in histopathology. Histopathology 1990; 17 : 489-503.
28. Nakano T, Oka K. MIB-1 and PC 10 Labeling Indices. Analysis of response to radiation therapy of patients with cervical adenocarcinoma compared with squamous cell carcinoma. Cancer 1996;77(11):2280-2285.
29. Schrape S, Jones DB, Wright DH. A comparison of three methods for the determination of growth fraction in non Hodgkin's lymphomas. Br J Cancer 1988; 55:283-286.
30. Nakano T, Ohno T. Correlation between oxygen tension measured by microelectrode and growth fraction defined by Ki-67 immunostaining in Cervical uterine cancer. 1997 (in press).
31. Thomlinson RH. Reoxygenation in tumors in relation to irradiation. Front Radiat Ther Oncol 1968; 3: 109-121.
32. International Federation of Gynecology and Obstetrics. Annual report on the results of treatment in carcinoma of the uterus, vagina and ovary. vol 16. Sweden Radiumhemmet, 1979
33. Graeber TG, Osmanian C, Jacks T et al. Hypoxia-mediated selection of cells with diminished apoptotic potential in solid tumours. Nature 1996; 379:88-91.
34. Hockel M, Knoop C, Schlenger K, Vorndran, Braussmann E, Mitze M et al. Intra tumoral pO2 predicts survival in advanced cancer of the uterine cervix. Radioth Oncol 1993; 26:45-50.
35. Metabolic microenvironment of human tumours: a review. Cancer Research, 1989; 49:6449-6465.
36. Malaise EP, Fertil B, Chavaudra N, Guichard M : Distribution of radiation sensitivities for human tumor cells of specific histological types: Comparison of in vitro to in vivo data. Int J Radiat Oncol Biol Phys 1986; 12 : 617 - 624.
37. Greene MH, Boice JD Jr, Greer BE, Blessing JA, Dembo AJ. Acute nonlymphocytic leukemia after therapy with alkylating agents for ovarian cancer. N Engl J Med. 1982 ; 307: 1416-1421.
38. Weissberg JB, Papac RJ, Son YH, et al. Randomized clinical trial of mitomycin-C or an adjuvant to radiotherapy in head and neck carcinoma. In J Radiat Oncol Biol Phys 1989; 1: 3.
39. Orton CG, Ellis F. A simplication in the use of the NSD concept, Br J Radiol. 1973; 56: 529 -537.
40. Key G. New Ki-67 equivalent murine monoclonal antibodies (MIB 1-3) prepared against recombinant parts of Ki-647 antigen. Anal Cell Pathol 1992; 4:181.

EXTRA LOBAR SEQUESTRATION: DEMONSTRATION OF BLOOD SUPPLY BY DOPPLER ULTRASOUND, CT AND MR ANGIOGRAPHY.

DR. M. PUVANESWARY,[1] DR. A. GILL,[2] DR. P. DAVIDSON[3]

ABSTRACT

Extralobar sequestration (ELS) is a congenital malformation with anomalous vessel(s) arising from the systemic circulation. ELS may be mimicked by other lesions such as cyst-adenomatoid malformation. Duplex ultrasound, CT and MR angiography suggested the correct diagnosis by demonstrating an anomalous artery arising from the abdominal aorta supplying the ELS.

CASE REPORT

A 25 year -old woman G1P1 at 18th week pregnancy demonstrated a cystic mass in the left hemithorax of the foetus. Follow-up ultrasonography demonstrated a complex mass with cystic and solid components occupying most of the left hemithorax and a diagnosis of Type 2 cyst adenomatoid malformation (CAM) of the lung was made. Early in the third trimester she developed polyhydraminos and the fetal heart was displaced toward the right hemithorax. Delivery was induced at term and a male infant weighing 3,640 gm was born. Apgar scores were 6 at 1 minute and 9 at 5 minutes, but the infant rapidly developed respiratory distress and was intubated and ventilated until surgery.

A chest radiograph revealed a large homogeneous soft tissue mass in the left hemithorax which displaced the heart and mediastinum to the right. Ultrasonography of the chest demonstrated a sharply defined crescentic predominantly echogenic mass with several small vessels. There was a suggestion of a vessel arising directly from the aorta and extending into the mass. Doppler interrogation demonstrated a systemic arterial waveform (Fig 1). Computed tomography of the chest showed a left posterior mediastinal mass extending across the midline with an anomalous artery arising from the abdominal aorta and extending into the mass (Fig 2). The heart was displaced to the right and there was a small left pneumothorax.

An MRI was performed on 1.5T superconducting system (Siemens). Axial T1-weighted TSE(693/12), sagittal TSE(587/12), coronal T2-weighted TSE(3894/112) and postcontrast axial TSE(693/12) and sagittal TSE(587/12) and 3D FISP gadolinium enhanced MR Angiography was performed. The T1-weighted image demonstrated

AUTHORS :
[1] Department of Medical Imaging John Hunter Hospital
[2] Department of Neonatology John Hunter Children's Hospital
[3] Department of Paediatric Surgery John Hunter Children's Hospital

ADDRESS FOR CORRESPONDENCE.
Dr M Puvaneswary
Department of Medical Imaging John Hunter Hospital Locked Bag 1, Hunter Regional Mail Centre N.S.W 2310 . AUSTRALIA

Fax (02) 49213415 Phone (02) 49213430 Email <pdavid@mail.newcastle.edu.au>

a large heterogeneous low signal intensity left posterior mediastinal mass measuring 8.2x4.5x6.4cm that crossed the midline. On T2-weighted sequences the mass was of high signal intensity with several cystic lesions. There was enhancement of the septae and marked peripheral homogeneous enhancement of the mass (Fig 3A). MR Angiography (Fig 3B) demonstrated an anomalous artery arising directly from the abdominal aorta just above the coeliac axis and ascending into the mass.

A provision diagnosis of extralobar sequestration was made and a thoracotomy with ligation of a feeding artery arising from the abdominal aorta at the level of the coeliac axis and resection of the extralobar sequestration was performed.

Histopathological examination confirmed an extralobar pulmonary sequestration. The patient recovered and remains well at eight months.

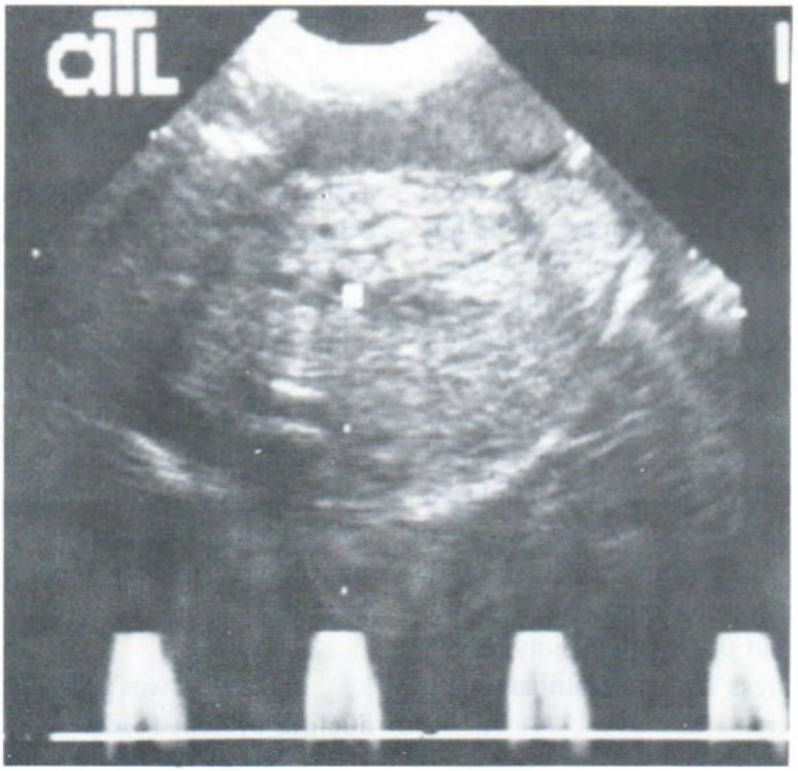

Fig 1 Doppler tracing from the vessel supplying the sequestration demonstrates a systemic arterial waveform.

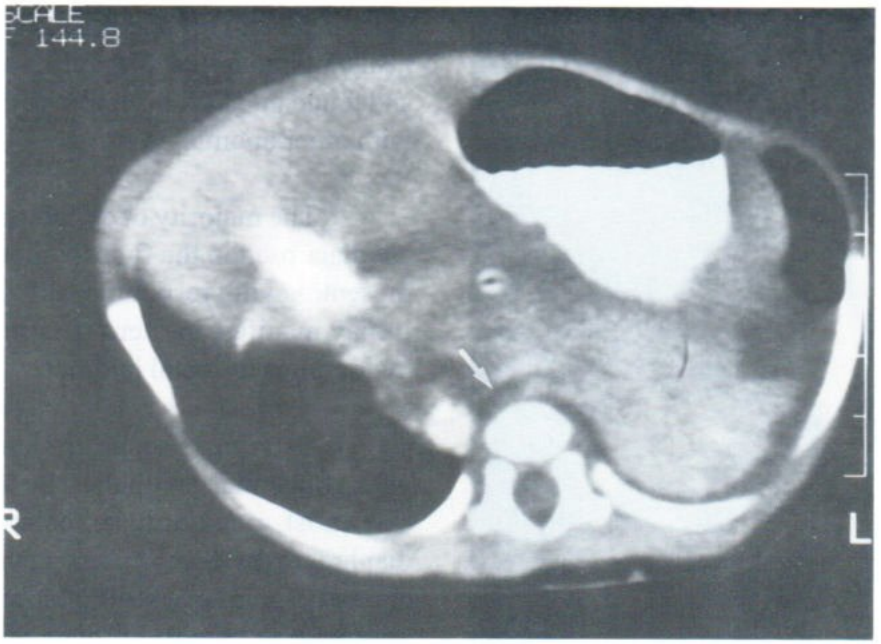

Fig 2 Axial contrast-enhanced CT demonstrates origin of anomalous artery from the abdominal aorta. (arrow)

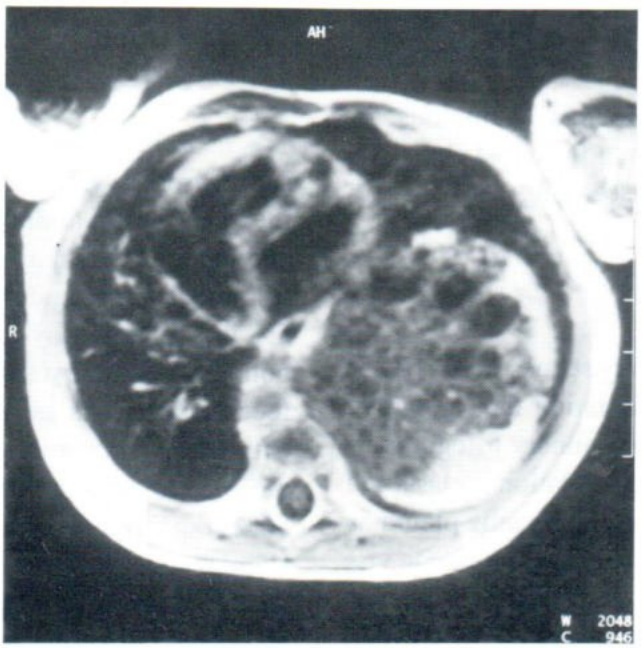

Fig(3A) Axial postcontrast MR image. Extralobar sequestration with areas of low signal intensity corresponding to cystic areas with enhancement of the wall. The heart is markedly displaced into the right hemithorax.

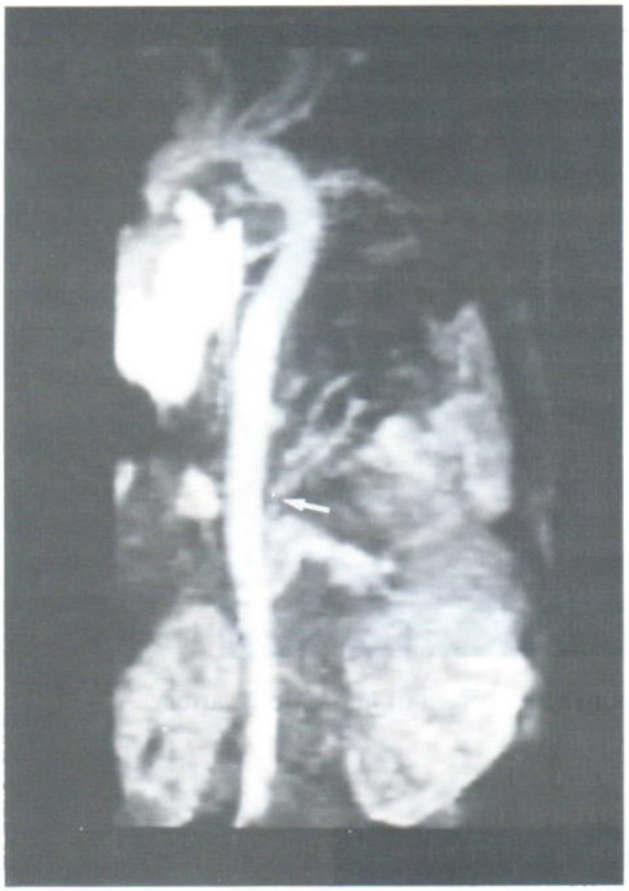

Fig(3B) MR angiogram depicts anomalous artery (arrow) arising from just above the celiac axis and ascending into the sequestration.

DISCUSSION

Extralobar pulmonary sequestration (ELS) is a rare congenital malformation that is part of the spectrum of broncho-pulmonary foregut malformations. Pulmonary sequestration is classified as intralobar being encased in the same pleura as the adjacent lung or extralobar with a separate visceral pleural investment. Pulmonary sequestration consists of lung tissue usually cystic which has no normal communication with the tracheobronchial tree or pulmonary artery. Extralobar sequestration make up 25% of pulmonary sequestration and 90% occur at the left base. They can also occur in the mediastinum, within the diaphragm, and in retroperitoneal sites. Retroperitoneally pulmonary sequestration are asymptomatic and found incidentally or at autopsy if unassociated with other anomalies.

The majority of extralobar sequestration's are diagnosed in the first six months of life, often presenting with respiratory distress and cyanosis. It may manifest in-utero if associated with polyhydramnios or foetal hydrops.

Extralobar sequestrations are associated with congenital anomalies in 50-65% of cases. The most commonly associated is congenital diaphragmatic hernia, diaphragmatic eventration or paralysis. In large sequestrations, or those found with a large congenital diaphragmatic hernia or pleural effusion, pulmonary hypoplasia may occur. Other anomalies found include bronchogenic cysts, pericardial defects, cyst-adenomatoid malformation, foregut duplication-with communication to the oesophagus or stomach, ectopic pancreas and vertebral anomalies.

Pulmonary sequestration drives its blood supply from a systemic artery arising directly from the thoracic or abdominal aorta in 80%. The anomalous artery may arise from the splenic, gastric, subclavian or intercostal artery in 15% and in 5% it is supplied by the pulmonary artery or by both the pulmonary and systemic circulation. The feeding artery is generally single but 20% of extralobar sequestrations are supplied by multiple arteries. Venous return is typically systemic in 80%, but drainage can be through the Azygos, Hemiazygos or venacava to the right atrium. The venous return is partly through the pulmonary vein in 20% of cases. Systemic arterial supply is not pathognomonic of sequestration. It can occur in other congenital conditions such as arteriovenous fistulae, pulmonary aplasia and systemic arteries can supply the normal lung parenchyma. In ELS the usual radiographic finding is a cystic or solid mass in the left lung base. Other findings include

normal appearing lung, hyperlucent areas, a combination of solid and cystic mass, or pneumonia.[1]

Typical sonographic findings are of a uniformly echogenic mass surrounded by a thin echogenic rim which distinguishes it from pulmonary consolidation and atelectasis.[2] Diagnosis is confirmed if a systemic feeding vessel is demonstrated and Doppler demonstrates a systemic arterial waveform. Antenatal sonography can demonstrate nonimmune hydrops foetalis, pleural effusions or maternal hydramnios. Pulmonary sequestration is identified as an echogenic mass separated from the lung.

The CT appearances show multicystic abnormalities with pulmonary cysts and emphysema which is probably due to air trapping from collateral ventilation. Dynamic, ultrafast high resolution CT demonstrate the anomalous artery supplying the sequestration.[3] The systemic arterial supply to sequestation is prone to partial or complete thrombosis. Calcification within the anomalous artery and sequestration has been demonstrated.[1]

MR angiography can similarly demonstrate systemic arterial supply to sequestration. MRI can demonstrate solid and mucous containing components of sequestration. However, emphysematous changes and calcification are not demonstrated.[4,5]

The definitive treatment for sequestration is surgical resection, and preoperative assessment of the presence and location of an anomalous systemic artery supply is the primary objective of imaging. Classification into intralobar and extralobar sequestration by the absence or presence of a separate pleural investment are not of primary importance for surgery. Therefore, all imaging techniques capable of demonstrating anomalous vessel are utilised to diagnose pulmonary sequestration. Non-invasive imaging technique include sonography, helical CT and MR angiography.

REFERENCES

1. Ikezoe J, Murayama S, Godwin J D,et al Bronchopulmonary sequestration: CT assesment. Radiology 1990;176:375-3792
2. Kaude J V and Laurin S. Ultrasonographic demonstration of systemic artery feeding extrapulmonary sequestration. Pediatr Radiol. 1984 ; 14: 226-227.3
3. Miller P A, Williamson B R J, Minor G R, et al. Pulmonary sequestration: Visualisation of the feeding artery by CT. J .Comput Assist Tomogr 1982;6
4. Doyle AJ. Demonstration of blood supply to pulmonary sequestration by MR Angiography. AJR. 1992;158:989-990 5
5. Brink D A and Balsara Z N. Prenatal ultrasound detection of intra-abdominal pulmonary sequestration with postnatal MRI correlation. Pediatr Radiol.1991; 21: 227

FOR MORE INFORMATION PLEASE CONTACT

PHILIPS MEDICAL SYSTEMS

- TEL. 745-4090 Ext. 3332
- FAX. 398-0792

Philips Electronics (Thailand) Ltd.
209/2 Sanpavuth Road, Prakanong, Bangkok 10260

PHILIPS

Let's make things better.

ANTERIOR CRUCIATE LIGAMENT INJURY : MR IMAGING WITH SURGICAL CORRELATION

Suphaneewan JAOVISIDHA M.D.[1], Nuanjitr SUCHARTNITIKUL M.D.[1]
Pimjai SIRIWONGPAIRAT M.D.[1], Chathchai POOKARNJANAMORAKOT M.D.[2]

ABSTRACT

OBJECTIVE. To determine the sensitivity, specificity, and accuracy of primary and secondary signs of ACL tear in MR imaging. **MATERIAL AND METHODS.** MR images of the knee in 31 patients who had surgical correlation were retrospectively reviewed by two radiologists who did not know the surgical results or the original interpretation. Surgery (open surgery or arthroscopy) demonstrated complete ACL tear in 9 patients and intact ACL in 22 patients. The appearance of ACL in sagittal T1/T2WI, coronal T1/T2WI, the anterior translation of tibia, the uncovered lateral meniscus sign, and the curvature of PCL were evaluated. **RESULTS.** The primary sign of ACL tear (abnormal morphology & signal intensity) had respective sensitivity, specificity, and accuracy of 100%, 86.3%, 90.3% on sagittal T1WI; 100%, 90.9%, 93.5% on sagittal T2WI; 75%, 95.2%, 89.7% on coronal T1WI; and 77.7%, 90.4%, 86.7% on coronal T2WI. The secondary signs of ACL tear had respective sensitivity, specificity, and accuracy of 77.7%, 100%, 93.1% for anterior translation of tibia at 5-mm cut off; 44.4%, 100%, 82.8% for uncovered lateral meniscus sign; and 87.5%, 90%, 89% for the buckling of PCL. CONCLUSION. Among the primary sign of ACL tear, an abnormal appearance of ACL on sagittal T2WI is most accurate. Anterior translation of tibia and uncovered lateral meniscus sign are secondary signs that have the highest specificity in diagnosing ACL tear.

INTRODUCTION

Magnetic resonance (MR) imaging is the most accurate and noninvasive technique for determining the status of anterior cruciate ligament (ACL).[1-6] The integrity of the ACL is, however, occasionally difficult to assess, particularly when the ACL is not entirely included on a single sagittal image.[7-10] In this situation, secondary sign of ACL tear may be useful to support the presumptive diagnosis of ACL tear. These signs refer to indirect findings on the MR imaging examination that suggest the presence of ACL tear because of either an inferred mechanism of injury or an instability pattern with ACL deficiency. We investigated the sensitivity, specificity, and accuracy of (a) abnormal morphologic features and signal intensity (SI) of ACL assessed on sagittal and coronal images and (b) secondary signs of ACL tear including anterior translation of tibia, uncovered lateral meniscus sign, and the curvature of posterior cruciate ligament (PCL).

MATERIAL & METHODS

Preoperative MR images were evaluated

[1] Department of Radiology, Ramathibodi Hospital, Mahidol University. Rama 6 street, Bangkok 10400, Thailand
[2] Department of Orthopedic Surgery, Ramathibodi Hospital, Bangkok, Thailand.

of 31 knees of patients whose ACL status had been surgically confirmed (by arthroscopy or open surgery) and in whom MR imaging had been performed in at least two planes. Twenty-two knees with intact ACL and 9 knees with complete ACL tear were proved surgically. MR images were retrospectively reviewed by two radiologists without knowledge of physical examination or surgical findings.

MR imaging examinations of the knee were performed with a 1.5-T magnet (Signa; GE Medical System, Milwaukee, WI). The knee was positioned in the extremity coil with the patient in supine position and the leg straightened. The machine was angled parallel to medial border of lateral femoral condyle. In sagittal plane, T1-, proton-density, and T2-weigthed images (T2WI) were obtained with spin echo (SE) using repetition time / echo time (TR [msec] / TE [msec]) 400/17, 4000/20-100, 3 signal average, 256x192 matrix, 20x15 - 22x16 cm field of view, and 3-mm slice thickness with 1-mm gap. In coronal plane, there were T1-weighted SE sequence using TR/TE 600-680/20 msec., and gradient recalled echo (GRE) sequence with TR/TE 600-680/20 msec., flip angle 25 degrees, 3 signal average.

Primary sign of ACL tear. The ACL was diagnosed as "normal" when it appeared as a band of fibers of low signal intensity on T1-, proton-density, and T2-WI. The normal orientation or slope of the ACL parallels to the femoral intercondylar roof. Abnormalities of both signal intensity (SI) and morphologic features referred to as primary MR imaging signs of ACL tear. The ACL was diagnosed as "torn" when focal or diffuse increased SI within the ligament was noted on T1-, proton-density, and T2-WI. Morphologic criteria used to support diagnosis of tear included an irregular, wavy contour of the ligament, a decreased slope of residual ACL, or an absence of ACL (Fig. 1).

Secondary sign of ACL tear. In this study, we used three secondary signs to support the diagnosis of ACL tear 1) anterior translation of tibia,[7] 2) uncovered lateral meniscus sign,[11] and 3) buckling of posterior cruciate ligament (PCL).[7] Anterior translation of tibia. The measurement was obtained at midsagittal plane of the lateral femoral condyle.[7] Two vertical lines were drawn tangent to posterior cortex or lateral femoral condyle and posterior cortex of lateral tibial plateau, and the distance was electronically measured and recorded as millimeters (Fig. 2). Uncovered lateral meniscus sign. Posterior displacement of the lateral meniscus compared with the posterior margin of lateral tibial plateau has been described as an indirect sign of complete ACL tear.[11,12] This sign was positive if a vertical line drawn tangently to the posteriormost cortical margin of lateral tibial plateau on sagittal image intersects any part of posterior horn of lateral meniscus. This sign was negative if this vertical line did not intersect the lateral meniscus (Fig. 3). Buckling of posterior cruciate ligament (PCL). The PCL was considered buckled if it demonstrated a sharp angulation apex posteriorly,[7] and was recorded as present or absent (Fig. 4).

Statistical Analysis. We performed Fisher Exact test to evaluate sensitivity, specificity, and accuracy of the primary sign and secondary sign of ACL tear, and performed Mann-Whitney U test to study the median value of anterior translation of tibia.

RESULT

Table 1 reveals the sensitivity, specificity, and accuracy of primary signs of ACL tear. Table 2 shows the results of secondary signs. Mann-Whitney U test revealed the median value of anterior translation of tibia to be 0.75 mm when the ACL was intact and 7.8 mm when the ACL was torn ($p < 0.0001$).

TABLE 1 Sensitivity, specificity, and accuracy of primary sign of ACL tear

Sequence	Sensitivity	Specificity	Accuracy	P-value
Sagittal T1	100	86.3	90.3	< 0.0001
Sagittal T2	100	90.9	93.5	< 0.00001
Coronal T1	75	95.2	89.7	< 0.001
Coronal T2	77.7	90.4	86.7	< 0.001

TABLE 2 Sensitivity, specificity, and accuracy of secondary sign of ACL tear

Sign	Sensitivity	Specificity	Accuracy	P-value
Anterior translation of tibia	77.7	100.0	93.1	——
Uncovered lateral meniscus	44.4	100.0	82.7	< 0.01
Buckling of PCL	87.5	90.0	89.0	< 0.01

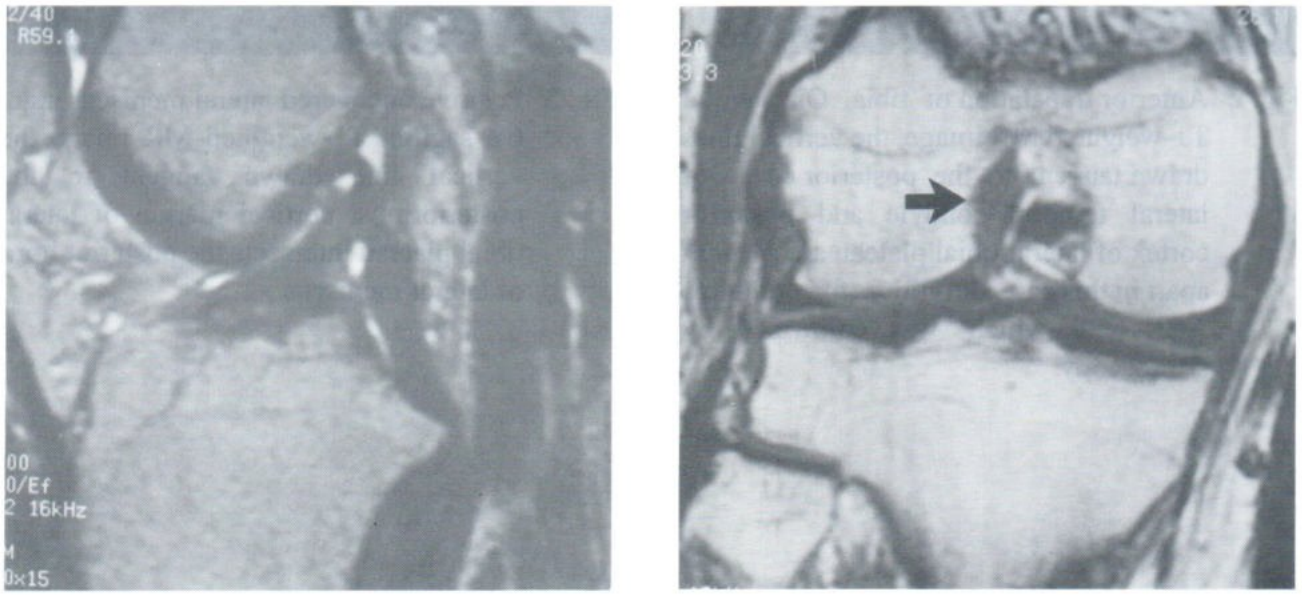

Fig. 1 Complete ACL tear. a) Sagittal T2-weighted MR image reveals focally increased SI in the mid portion of ACL. Decreased slope of the ACL is also observed. This is a 26-year-old male athlete presented with history of knee injury for 4 months. b) T1-weighted coronal MR image shows increased SI of the ACL in the intercondylar notch (black arrow). Decreased swelling of the ligament is due to timing of injury.

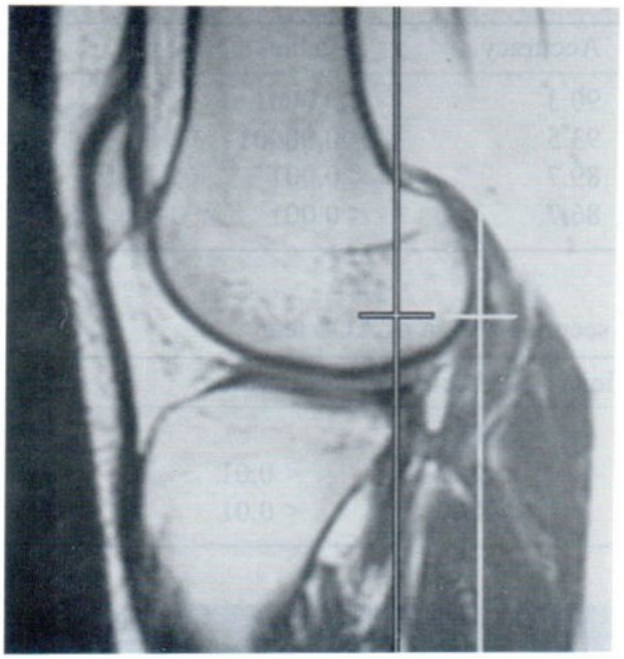

Fig. 2 Anterior translation of tibia. On sagittal T1-weighted MR image, the vertical lines drawn tangent to the posterior cortex of lateral femoral condyle and posterior cortex of lateral tibial plateau are 21 mm apart in this case, definitive for complete ACL tear which was confirmed by arthroscopy.

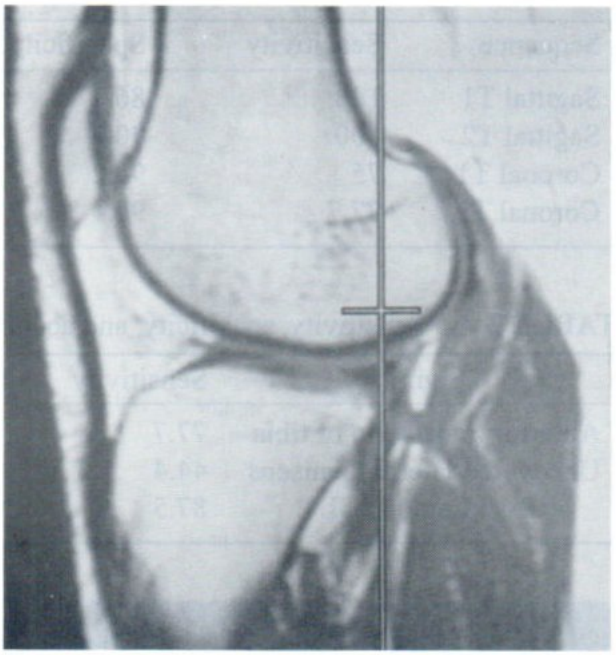

Fig. 3 Positive uncovered lateral meniscus sign. On sagittal T1-weighted MR image, the vertical line drawn tangent to the posteriormost cortical margin of lateral tibial plateau intersects the posterior horn of lateral meniscus.

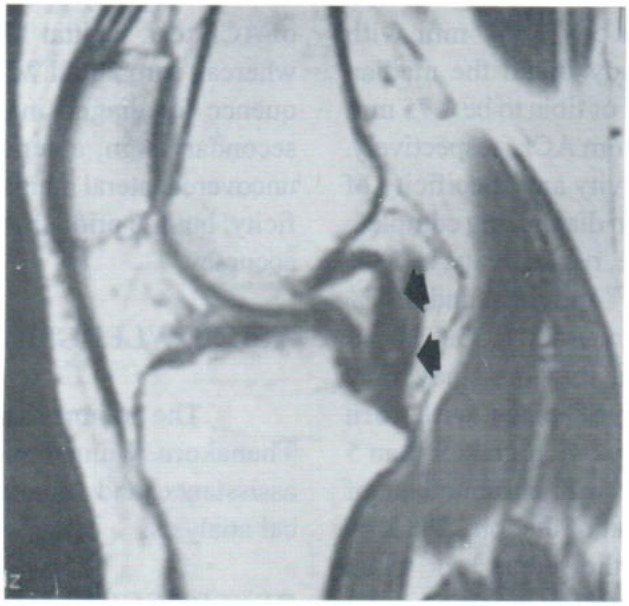

Fig. 4 Present buckling of PCL. Sagittal T1-weighted MR image reveals posterior angulation of the PCL. The PCL is outlined by the black arrows.

DISCUSSION

MR imaging has been reported to be accurate in showing the normal and injured anatomy of the ACL.[8,13-19] The distinction of complete tears from partial tears is clinically important because the presence of a partial tear is not an indication for surgical reconstruction.[20-23] Conversely, patients with complete ACL tear may have functional disability that can lead to meniscal injury and osteoarthritic changes.[20] Previous reports have emphasized the advantages of T2WI sagittal images in improving sensitivity, with overall accuracy rate of 95%.[3,24] In our study, the accuracy of T2W sagittal images for diagnosing complete ACL tear is 93.5%, corresponding to previous studies. We also found that sagittal T2W sequence was the most accurate sequence among those used in evaluating primary sign of ACL tear, whereas coronal T1WI showed the highest specificity (95%). However, diagnosing ACL tear can be difficult in certain situations. The whole length of an intact ACL may not be seen on one sagittal image in 5-10% of patients,[4,25] resulting misinterpretation as tear. Contrary, ACL may appear to be abnormal on sagittal MR image in the absence of ligamentous tear due to the presence of mucoid or eosinophilic degeneration within the ligament.[6,26] In addition, suboptimal selection of the sagittal imaging plane, volume averaging of the ligament with effusion in the intercondylar notch (or with the lateral femoral condyle or the periligamentous fat), as well as pulsation artifacts originating in the popliteal artery[7] may also cause diagnostic problems.[6-8] In these circumstances, other MR signs of ACL tear may have a role.

Secondary sign of ACL tear in MR imaging were investigated by many authors.[1,4,6,7,20,27,28] When the ACL is deficient, the tibia may become displaced anteriorly.[28] Vahey et al.[7] reported anterior translation of tibia at the level of midsagittal lateral femoral condyle to be 0.8 $\pm$

0.6 mm when the ACL was intact, 4.1 ± 1.0 mm with acute ACL tear, and 5.8 ± 0.7 mm with chronic ACL tear. Our study found the median value of anterior translation of tibia to be 0.75 mm and 7.8 mm with intact and torn ACL, respectively. Using 5 mm cut off, sensitivity and specificity of anterior translation of tibia in diagnosing complete ACL tear was reported to be, respectively, as 58% and 93%,[7] 86% and 99%,[20] and 78% and 100% by our study. The higher accuracy (93%) in our results compared with 69% in previous study[7] may be due to small number of cases with torn ligament in our study. Subluxation greater than 5 mm can be falsely negative with chronic tears of the ACL due to reattachment of the torn fibers by bridging fibrous tissue to the femur,[20] or when there is concomitantly displaced bucket-handle tear of the lateral meniscus blocks anterior subluxation of tibia.[20,29]

Relative posterior displacement of the lateral meniscus compared with the posterior cortical margin of the lateral tibial plateau has been described as a sign of increased anterior shift of tibia.[6,11,12] This "uncovered lateral meniscus sign" was reported to have respective sensitivity and specificity of 18% and 100%,[6] and 56% and 98.5%.[27] We reported the sensitivity, specificity, and accuracy of this sign to be 44%, 100%, and 83%, respectively. From many reports, this sign has been shown to have specificity approaching 100% in diagnosing complete ACL tear. However, its low sensitivity makes this sign of limited use.

Buckling of PCL occurs secondary to anterior subluxation of the tibia during positioning for imaging, resulting in an acute angulation of the normally smooth, convex posteriorly margin of PCL.[7] The assessment of PCL buckling is subjective, and was reported to have respective sensitivity, specificity, and accuracy of 17%, 100%, and 44%. Our study demonstrates higher sensitivity (87.5%) and accuracy (89%) but less specificity (90%) for this sign.

Our study concluded that, for primary sign of ACL tear, sagittal T2WI was the most accurate whereas coronal T1WI was the most specific sequence for diagnosing complete ACL tear. For secondary sign, anterior translation of tibia and uncovered lateral meniscus sign have 100% specificity, but the prior showed higher sensitivity and accuracy.

ACKNOWLEDGMENT

The authors thank Adun Kampangtip and Thanakorn Wongsinpiboon, for their technical assisstance; and Amarin Thakkinstian for statistical analysis.

REFERENCES

1. Brandser EA, Riley MA, Berbaum KS, El-Khoury GY, Bennett DL. MR imaging of anterior cruciate ligament injury: independent value of primary and secondary signs. AJR 1996;167:121-126
2. Glachow JL, Katz R, Schneider M, Scott D. Double-blind assessment of the value of magnetic resonance imaging in the diagnosis of anterior cruciate and meniscal lesions. J Bone joint Surg 1989;71-A:113-119
3. Mink JH, Levy T, Crues JV III. Tears of the anterior cruciate ligament and menisci of the knee: MR imaging evaluation. Radiology 1988; 167: 769-774
4. Robertson PL, Schweitzer ME, Bartolozzi AR, Ugoni A. Anterior cruciate ligament tears: evaluation of multiple signs with MR imaging. Radiology 1994;193:829-834
5. Remer EM, Fitzgerald SW, Friedman H, Rogers LF, Hendrix RW, Schafer MF. Anterior cruciate ligament injury: MR imaging diagnosis and patterns of injury. RadioGraphics 1992;12:901-915

6. Tung GA, Davis LM, Wiggins ME, Fadale PD. Tears of the anterior cruciate ligament: primary and secondary signs at MR imaging. Radiology 1993;188:661-667
7. Vahey TN, Hunt JE, Shelbourne KD. Anterior translocation of the tibia at MR imaging: A secondary sign of anterior cruciate ligament tear. Radiology 1993; 187:817-819
8. Fitzgerald SW, Remer EM, Friedman H, Rogers LF, Hendrix RW, Schafer MF. MR evaluation of the anterior cruciate ligament: value of supplementing sagittal images with coronal and axial images. AJR 1993;160:1233-1237.
9. Beltran J. The knee. In: Beltran J, ed. MRI of the musculoskeletal System. Philadelphia: Lippincott, 1991: 7.20-7.24
10. Buckwalter KA, Pennes DR. Anterior cruciate ligament: oblique sagittal MR imaging. Radiology 1990;175:276-277
11. Moses M, Kier R, McCauley T, Barton J, Lynch K, Jokl P. Anterior cruciate ligament injury: indirect signs at MR imaging (abstr). Radiology 1992;185(P): 146-147
12. Mink J. The cruciate and collateral ligaments. In: Mink J, Reicher M, Crues J, Deutsch A, eds. Magnetic Resonance Imaging of the Knee. 2nd ed. New York, NY: Raven, 1993; 141-188
13. Beltran J, Noto AM, Mosure JC, Weiss KL, Zuelzer W, Christoforidis AJ. The knee: surface coil imaging at 1.5 T. Radiology 1986;159:747-751
14. Hinson GW, Middleton WD. The knee. In: Middleton WD, Lawson TL, eds. Anatomy and MRI of the Joints. New York: Raven, 1989:205-250
15. Mesgarzadeh M, Schneck CD, Bonakdarpour A. Magnetic resonance imaging of the knee and correlation with normal anatomy. RadioGraphics 1988;8: 707-725
16. Polly DW, Callaghan JJ, Sikes RA, McCabe JM, McMahon K, Savory CG. The accuracy of selective magnetic resonance imaging compared with the findings of arthroscopy of the knee. J Bone Joint Surg 1988;70-A:192-197
17. Reicher MA, Rauschning W, Gold RH, Bassett LW, Lufkin RB, Glen W Jr. High -resolution magnetic resonance imaging of the knee joint: normal anatomy. AJR 1985; 145:895-902
18. Reicher MA, Hartzman S, Bassett LW, Mandelbaum B, Duckweiler G, Gold RH. MR imaging of the knee: Part 1. Traumatic disorders. Radiology 1987;162:547-551
19. Turner DA, Prodromos CC, Petasnick JP, Clark JW. Acute injury of the ligaments of the knee: magnetic resonance evaluation. Radiology 1985;154:717-722
20. Chan WP, Peterfy C, Fritz RC, Genant HK. MR diagnosis of complete tears of the anterior cruciate ligament of the knee: importance of anterior subluxation of the tibia. AJR 1994;162:355-360
21. Noyes FR, Cummings JF, Grood ES, Walz -Hasselfeld KA, Wroble RR. The diagnosing of knee motion limits, subloxations, and ligament injury. Am J Sports Med 1991;19:163-171
22. Odensten M, Lysholm J, Gillquist J. The course of partial anterior cruciate ligament ruptures. Am J Sports Med 1985;13: 1830186
23. Samberg R, Balkfors B. Partial rupture of anterior cruciate ligament: natural course. Clin Orthop 1987;220:176-178
24. Lee JK, Yao L, Phelps CT, Wirth CR, Czajka J, Lozman J. Anterior cruciate ligament tears: MR imaging compared with arthroscopy and clinical tests. Radiology 1988;166:861-864
25. Mink JH, Reicher MA, Crues JV III, Deutsch AL. MRI of the knee. 2nd ed. New York, NY: Raven , 1987;145-162

26. Hodler J, Haghighi P, Trudell D, Resnick D. The cruciate ligaments of the knee: correlation between MR appearance and gross and histologic findings in cadaveric specimens. AJR 1992;159:357-360

27. McCauley TR, Moses M, Kier R, Lynch JK, Barton JW, Jokl P. MR diagnosis of tears of anterior cruciate ligament of the knee: importance of ancillary findings. AJR 1994;162:115-119

28. Gentili A, Seeger LL, Yao L, Do HM. Anterior cruciate ligament tear: indirect signs at MR imaging. Radiology 1994; 193:835-840

29. Torg JS, Conrad W, Kalen V. Clinical diagnosis of anterior cruciate ligament instability in the athlete. Am J Sports Med 1976;4:84-93

ANGIOKERATOMA OF THE WRIST

Suphaneewan JAOVISIDHA MD.,[1] Wiwat VISUTHIKOSOL MD.[2]
Prawat NITIYANANT MD.[3] Pimjai SIRIWONGPAIRAT MD.,[1]
Charin EUAVILAIJITR MD.[1]

ABSTRACT

A case of angiokeratoma was presented. The patient had a red-to-purple soft tissue mass about 1 cm size at volar aspect of the right wrist that gradually enlarged with time to be 9x8x7 cm. Multi-modality imagings were performed and revealed a large, fat-containing mass with multifocal small soft-tissue densities within the fat. The presumptive diagnosis was hemangioma. Angiographic study revealed nearly complete occlusion of the interosseous (feeding) artery with collateral circulation filled its distal part subsequently. This pattern is not common in hemangioma. The histologic diagnosis was angiokeratoma which although being a benign vascular tumor of skin, need wide surgical excision margin to prevent local recurrence. Careful observation of uncommon imaging findings in the case presumptively diagnosed as hemangioma will help to raise the possibility of other entities.

INTRODUCTION

Angiokeratoma is a benign vascular tumor of skin which may be presenting in various characteristics in the body.[1,2] It usually arises as a soft, compressible, pink to red papules 1-3 mm in diameter. With the passage of time, many lesions develop keratotic changes, become darker, and present a warty appearance.[3] Because angiokeratoma is usually asymptomatic and small, with average size of 3 mm,[1,4] imaging investigation and surgical intervention are rarely performed. We presented a case of angiokeratoma of the wrist which was large and diagnosed as angiosarsoma by clinical findings and as hemangioma by imaging findings.

CASE REPORT

In January 1995, a 39-year-old Thai woman came to the Hand clinic because she had a right wrist mass. This mass has appeared since birth as a nodule of 1 cm size involving the skin of volar aspect of right wrist, showing dark red coloration with lobulated contour. At that time surrounding skin was normal. This lesion slowly enlarged with time, and multiple small red-black dots lately developed in the surrounding skin. In some instances, she had associated pain and low-grade fever. She had normal range of motion of the right wrist and fingers. She did not have any relatives with this disease. Physical examination revealed a married, female agriculturer with normal consciousness. She was not pale, and did not have icteric sclera. Heart, lungs, and abdominal examinations were normal. Extremity examination disclosed a lobulated mass of 9x8x7 cm in size, soft consistency, with red-purple coloration involving the volar aspect of the right wrist. Multiple small red-black nodules are observed on

[1] Department of Radiology, Ramathibodi hospital, Mahidol University, Rama 6 street, Bangkok 10400, Thailand
[2] Department of Surgery, Division of Plastic surgery, Ramathibodi hospital, BKK.
[3] Department of Pathology, Ramathibodi hospital, BKK.

the surrounding skin (Fig. 1). The radial and ulna pulses could not be palpated. The motor and sensory functions were intact. The circumferences of the right wrist was 21 cm whereas of the left was 15 cm. The presumptive diagnosis was hemangioma with suggested malignant transformation (angiosarcoma). Plain radiograph revealed soft tissue swelling at the volar aspect of right distal forearm all through the wrist and palm. Large area of fat density was seen in the lesion. No bone involvement was demonstrated (Fig. 2). Incisional biopsy was performed, yielding a result of angiokeratoma. Computerized tomography (CT scan) (Fig. 3) and magnetic resonance imaging (MRI) (Fig. 4) revealed that this lesion was fat-containing, with multiple small soft tissue densities distributing within the fat. Multifoci of skin thickening were observed. Bony structure appeared normal. Contrast-enhanced CT scan showed minimal enhancement of the soft-tissue component of the lesion. Right brachial angiography was subsequently performed (Fig. 5). In arterial phase; there was nearly complete occlusion of the interosseous (feeding) artery at the level of mid forearm with collateral circulation filling its distal part. The distal part of radial artery was displaced laterally by the mass. No significant arterial abnormality was seen at level of the wrist. In capillary phase; there were diffuse, multiple small contrast medium retentions which remained opacified late into the venous phase. The angiographic diagnosis was hemangioma involving soft tissue of the right wrist. Surgical exploration revealed that the mass could be easily removed from underlying muscles and tendons except at the wrist where a part of the mass involved the flexor retinaculum resulting in this structure having to be resected. The wound defect was covered with split thickness skin graft (STSG) harvested from left thigh. Post operative conditions were satisfactory. Follow-up at 1, 2, and 3 months revealed normal functions and range of motion of the right wrist and fingers. No evidence of local recurrence is detected.

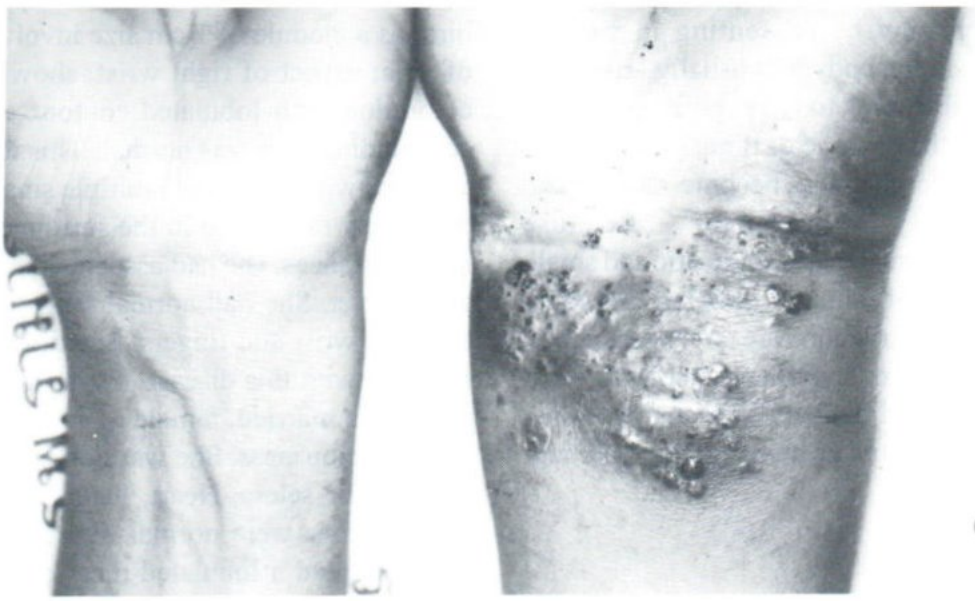

Left **Right**

Fig.1 Preoperative photograph of the lesion shows an ill-defined mass with red-purple coloration involving the volar aspect of the right wrist. Multiple small red-black nodules are observed in the surrounding skin.

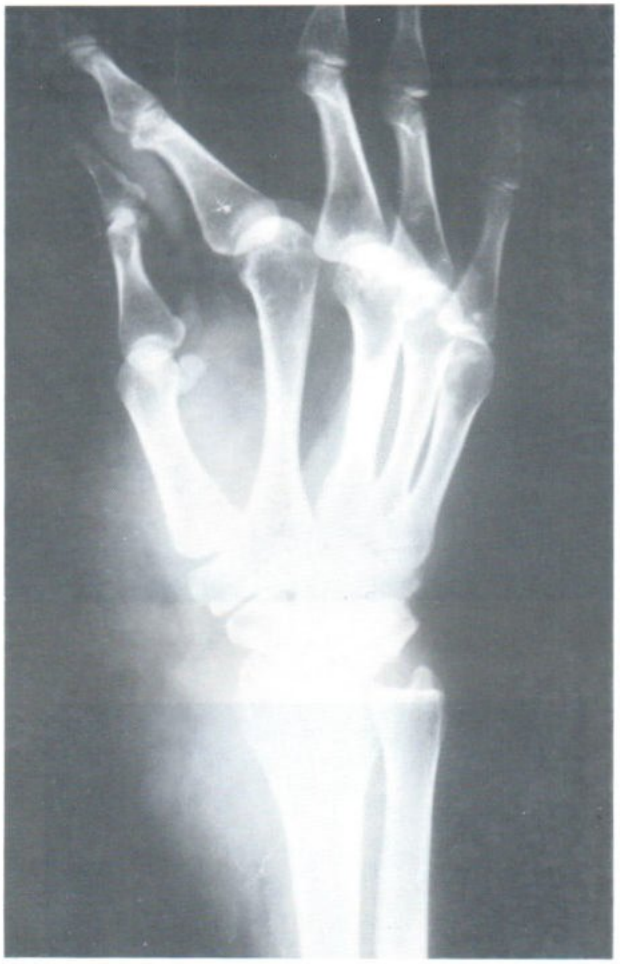

Fig. 2 Oblique plain radiograph of right distal forearm including hand reveals soft tissue swelling in the volar aspect of the wrist with fat density distributing throughout. No bone destruction is observed.

Fig. 3 Axial CT scan demonstrates that the lesion has a large amount of fat, with multiple small soft tissue densities distributing within the fat. Skin thickening is noted.

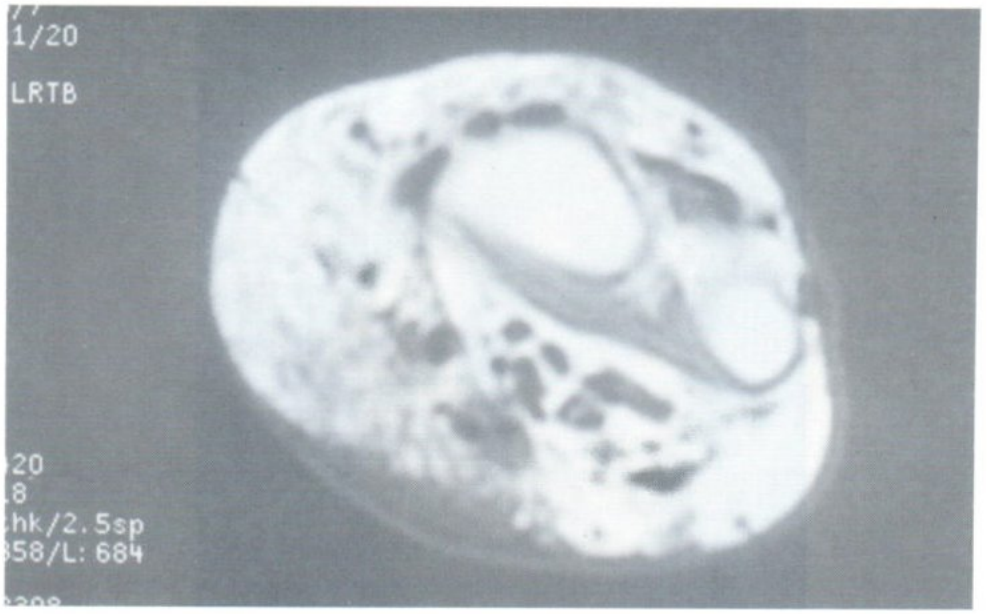

4A

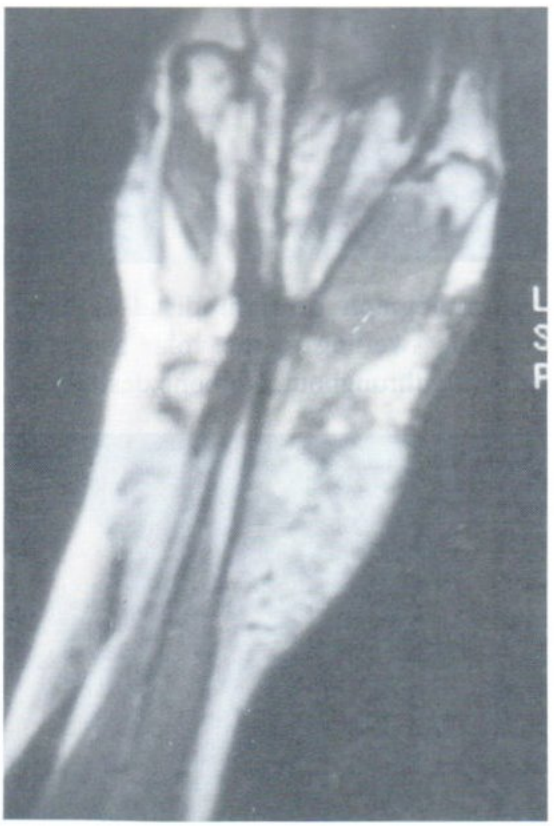

4B

Fig. 4 a) Axial and b) coronal T1-weighted MR images exhibit the fat to insinuate between the normal-appearing tendons. Some small hypointensities are seen within the fat.

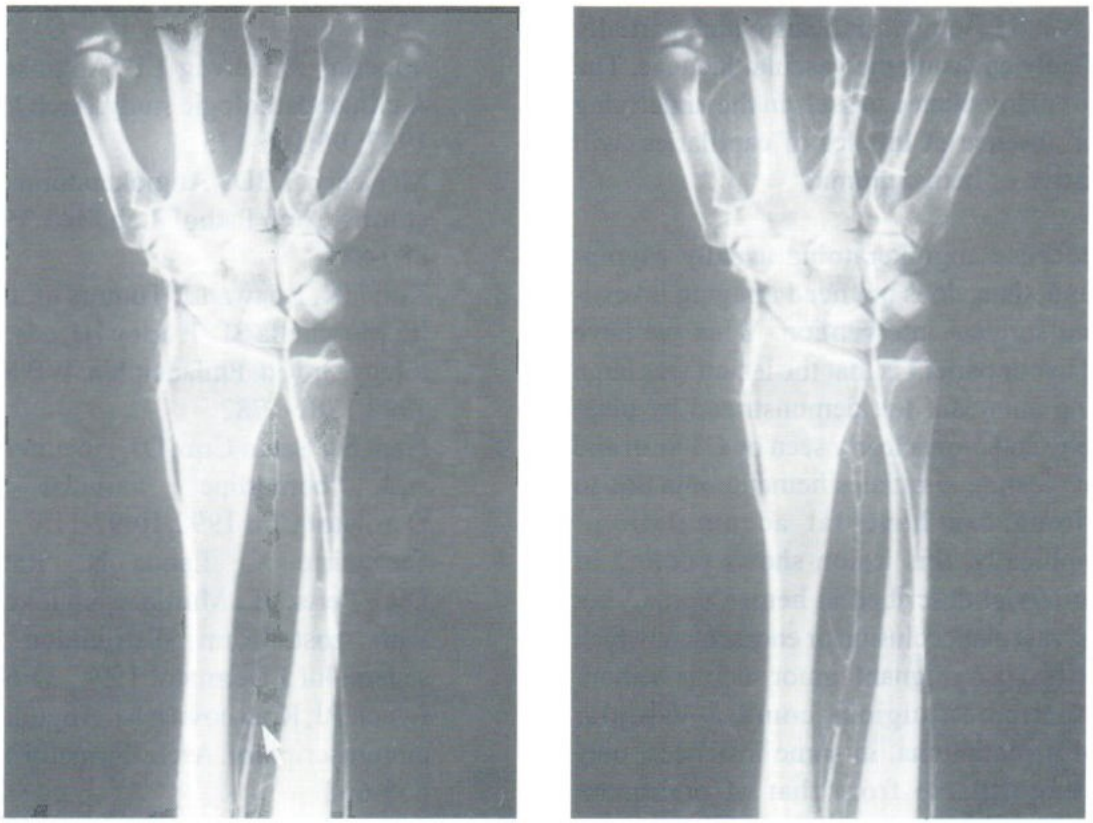

5A 5B

Fig. 5 Angiographic study discloses nearly complete occlusion of the interosseous artery (arrow in Fig. 5 a) which was filled subsequently by the collateral vessels (Fig. 5 b)

DISCUSSION

Five clinical forms of angiokeratoma are generally recognized:[1,3-5] 1) the Mibelli type, occurring as hyperkeratotic lesions on the hand and feet,[4] particularly on the dorsum of fingers and toes,[5] 2) the Fordyce type, involving the scrotum and vulva, 3) angiokeratoma corporis diffusum, associated typically with Fabry's disease, and also with fucosidosis,[4] 4) angiokeratoma circum-scriptum, is present at birth or early childhood, and females are affected three times more commonly than males. The process is almost always unilateral.[3] On histopathologic examination, it is a true hemangioma,[5,6] 5) solitary or multiple papular angiokeratomas which may locate in any part of the body[5] but favors the lower extremity.[1,3,4] Histopathologically, it has the criteria of a true angiokeratoma.[5]

Because angiokeratoma appears as variably hyperkeratotic lesions with coloration ranging from pink-red to purple, brown, or black; differential diagnosis can include hemangioma, nevus, verruca, and melanoma.[1,4] Although usually asymptomatic, angiokeratoma may become irritated and bleed, perhaps as the result of local trauma.[4]

Histopathologic features suggesting the diagnosis of angiokeratoma are combination of marked vascular dilatation of the papillary

vessels, forming large lacunae in the papillary area of dermis; and having acanthosis which partially or completely encasing the vascular lacunae. The absence of many dilated vessels in the underlying dermis or absence of lobules of capillaries, will be suggestive of hemangioma.[1]

Because angiokeratoma usually asymptomatic and, thus, does not need imaging investigation and surgical intervention. What we have observed in our patient is that the lesion was large and having abundant fat, demonstrated by plain radiography and more clearly seen by CT scan and MRI. This feature simulates hemangioma due to hamangioma can have fat accumulation.[7] Angiographically, this lesion shows pooling of contrast material described in hemangioma,[8] but exhibiting vascular occlusion or encasement which was described in malignant tumor such as hemangioendothelioma (angiosarcoma).[9] Vascular pattern of hemangioma, in some instances, may be indistinguishable from that of malignant tumor.[8,10] The diagnosis can be made only by histology as in this case. Differentiation of angiokeratoma from hemangioma is important because angiokeratoma needs wider excision margin to prevent recurrence whereas hemangioma can be treated by local excision.[10] In our case, nearly complete occlusion of the feeding artery demonstrated angiographically is uncommon in hemangioma, and raise the possibility of other disease.

In summary, from this present case, angiokeratoma is a benign vascular lesion of skin that may enlarge with time, and may simulate hemangioma in multi-modality imaging findings. Careful observation of uncommon imaging findings in the case presumptively diagnosed as hemangioma may help to raise the possibility of other entities. Correct diagnosis obtained by histologic examination is of importance for proper surgical treatment.

REFERENCES

1. Imperial R, Helwig EB. Angiokeratoma: A clinicopathologic study. Arch Dermatol 1967; 95:166-175
2. McNeely TBD. Angiokeratoma of the clitoris. Arch Pathol Lab Med 1992;116: 880-881
3. Koh HK, Bhawan J. Tumors of the skin. In: Moschella SL, Hurley HJ, eds. Dermatology. 3rd ed. Philadelphia, WB Saunders 1992,1781-1782
4. Hunt SJ, Santa Cruz DJ. Acquired benign and "borderline" vascular lesions. Dermatol Clin 1992;10:97-115
5. Eizaguirre X, Landa N, Raton JA, Diaz-Perez JL. Multiple angiokeratomas with zosteriform distribution in two sisters. Int J Dermatol 1994; 33:641-642
6. Lynch PJ, Kosanovich M. Angiokeratoma circumscriptum. Arch Dermatol 1967;96: 665-668
7. Resnick D, Kyriakos M, Greenway G. Tumors and tumor-like lesions of bone: Imaging and pathology of specific lesions. In: Resnick D, ed. Diagnosis of Bone and Joint Disorders. 3rd ed. Philadelphia, WB Saunders 1995,3821-3828
8. Levin DC, Gordon DH, McSweeney J. Arteriography of peripheral hemangiomas. Radiology 1976;121:625-628
9. Tegtmeyer CJ. Angiography of bones, joints, and soft tissues. In: Abrams HL, ed. Abrams Angiography: Vascular and Interventional Radiology. 3rd ed. Boston, Little, Brown and Company 1983,1937-1977
10. Madewell JE, Sweet DE. Tumors and tumor-like lesions in or about joints. In: Resnick D, ed. Diagnosis of Bone and Joint Disorders. 3rd ed. Philadelphia, WB Saunders 1995,3950-3953

ROLE OF TC-99M DISIDA SCINTIGRAPHY IN INFANTS WITH SUSPECTED OF BILIARY ATRESIA: A 6-YEAR EXPERIENCE

Molrudee EKMAHACHAI, M.D., Nonglak VILASDECHANON, M.Sc.
Sombut BOONYAPRAPA, M.D.

ABSTRACT

Hepatobiliary scintigraphy using Technetium-99m diisopropyl iminodiacetic acid(Tc-99m DISIDA scintigraphy) performed in 105 infants with predominantly conjugated hyperbilirubinemia and suspected of biliary atresia(BA) were reviewed. Radionuclide hepatobiliary scintigraphy is well recognized as the only noninvasive diagnostic method to demonstrate the patency of biliary system. All patients had the Tc-99m DISIDA scintigraphy performed after 5 days of phenobarbital therapy. Of the 55 infants with no evidence of radiotracer excretion into the biliary and/or gastrointestinal(GI) tract up to 24 hours after injection, 47 had a final diagnosis as BA proven by surgery. Whereas the remaining 8 patients, 2 were diagnosed as biliary hypoplasia, 2 were diagnosed as bile-plug syndrome, and 4 had a diagnosis as infectious neonatal hepatitis(NH). All of these were proven by laparotomy with intraoperative cholangiography and follow up clinical course. The remaining 50 patients demonstrated definite excretion of the radiotracer into the GI tract, thus entirely excluded the diagnosis of BA. Of these, 22 had a final diagnosis as idiopathic NH, 19 were diagnosed as infectious NH, and 9 had a diagnosis as having cholestatic jaundice of unknown cause. In our series, we found that the sensitivity, specificity and accuracy of Tc-99m DISIDA scintigraphy for the diagnosis of BA were 100%, 86% and 92%, respectively. The positive and negative predictive value were 85% and 100%. The results of our study indicate that Tc-99m DISIDA scintigraphy is a sensitive and highly accurate method in the diagnosis of BA. Therefore, it is highly recommended as a routine screening investigation of choice in evaluating infants with suspected of BA.

INTRODUCTION

While there are several causes of conjugated hyperbilirubinemia in the neonatal period, the major differential diagnosis of these infants is between biliary atresia(BA) and neonatal hepatitis(NH), since majority of the non-surgical cholestasis are due to NH.[1,2] BA is one of the most common diseases of the biliary tree in infants. It is also a very important disease, due to its serious and potentially fatal if not treated.[3] Thus, an accurate and noninvasive investigation for diagnosis of BA is essential. It is extremely important to distinguish between these two entities for proper treatment. The treatment of BA requires prompt surgical intervention, whereas NH needs only medical or conservative treatment.[1,3,4]

Early diagnosis of BA by a sensitive diagnostic test is essential, since the success of surgical treatment is primarily dependent on early intervention, and it is most successful when

Department of Radiology, Faculty of Medicine, Chiang Mai University, Chiang Mai 50200, THAILAND.

performed before the age of 2 months.[3,4] The distinction between BA and NH by the clinical evidence, biochemical tests and histological features is very difficult and unreliable.[5-7] Therefore, many diagnostic techniques have been developed for the differential diagnosis of BA including ultrasonography,[8] duodenal fluid collection,[9,10] percutaneous transhepatic cholangiography,[11] endoscopic retrograde cholangiopancreatography,[12] laparoscopy,[13] laparotomy with intrahepatic cholangiography,[14] percutaneous liver biopsy[15] and radionuclide hepatobiliary scintigraphy.[5-8, 16-19] Among these modalities, radionuclide hepatobiliary imaging using Technetium-99m iminodiacetic acid (IDA) derivatives is well recognized as the only simple, safe and noninvasive investigation, which can demonstrate the hepatocyte function and the patency of biliary system.

The typical scintigraphic finding in BA is prompt hepatic uptake with no evidence of tracer excretion into the GI tract up to 24 hours after injection. Therefore, definite excretion of the radioactivity into the intestine excludes the diagnosis of BA, and avoids unnecessary laparotomy in these groups of patients.

The purpose of our study was to verify the reliability of the hepatobiliary scintigraphy using Technetium-99m diisopropyl iminodiacetic acid (Tc-99m DISIDA scintigraphy) in the differential diagnosis of patients with suspected of BA.

MATERIALS AND METHODS

Tc-99m DISIDA hepatobiliary scintigraphy in 105 consecutive infants with predominantly conjugated hyperbilirubinemia and suspected of BA obtained between January 1992 and December 1997, were reviewed retrospectively. The patients included 54 male and 51 female infants, who ranged in age from 17 days to 7 months. The average direct and total bilirubin levels of the patients were 7.71 ± 3.91 mg/dl (range, 2.88 to 23.62), and 14.26 ± 6.95 mg/dl (range, 5.3 to 34.3) respectively. The patients presented with either persistent jaundice with predominantly conjugated hyperbilirubinemia, acholic stools, hepatomegaly and/or splenomegaly. All patients had their Tc-99m DISIDA scintigraphy performed after phenobarbital premedication in a dose of 5 mg/kg/day orally, divided into two equal doses for 5 days.

The infants were fast for at least 2 hours before, and until 2 hours after injection of the radiopharmaceutical to prevent possible dilution of the excreted radiotracer in the bowel, and to minimize contraction of the gallbladder(GB). Tc-99m DISIDA scintigraphy was performed by intravenous injection of the Tc-99m labeled DISIDA with a dose of 100-200 microCi/Kg (3.7-7.4 MBq/Kg) of body weight, with a total dose of at least 1 mCi (37 MBq). The patients were placed in the supine position under a large-field-of-view gamma camera, equipped with a low-energy all-purpose collimator, using either ZLC Siemens or APEX SP-4 Elscint gamma camera. Sequential anterior abdominal imaging was obtained at 5, 15, 30, 45 minutes, and at 1, 2, 4 and 6 hours after injection. Each image was acquired for 300 Kcounts in 256 x 256 matrix. Other views, especially the right lateral view of the abdomen was also obtained in order to differentiate the right renal activity from the biliary and/or intestinal activity. The studies were terminated earlier if the images showed definite radiotracer excretion into the intestine. If no evidence of tracer excretion into the GI tract occurred at 6 hours, 24 hour image on the following day was routinely performed.

RESULTS

Of the 105 infants evaluated with Tc-99m DISIDA scintigraphy, 55 patients (52.4%) revealed no evidence of tracer excretion into the biliary system and/or the GI tract up to 24 hours after injection. Of these, 47 patients had a final

diagnosis as BA proven by surgery. Whereas the remaining 8 patients, 2 were diagnosed as biliary hypoplasia, 2 were diagnosed as bile-plug syndrome, and 4 had a diagnosis as having infectious NH from cytomegalovirus. Therefore, we have overall 47 true positive scans (85.5%), and 8 false positive scans (14.5%) in our study. All of these patients were proven by laparotomy with/without intraoperative cholangiography, and followed up the clinical course.

Regarding the hepatic uptake in these 8 patients with false positive scans for BA, 2 patients with biliary hypoplasia showed moderately decreased hepatic uptake. Two patients with bile-plug syndrome, one showed good hepatic uptake, and another one showed slightly decreased hepatic uptake. The remainder 4 patients with infectious NH, 2 revealed good hepatic uptake, one showed slightly decreased hepatic uptake, and the last one demonstrated markedly decreased hepatic uptake.

The remaining 50 patients (47.6%) demonstrated definite excretion of the radiotracer into the intestinal tract, which indicated the patency of biliary system. Thus, a diagnosis of BA was entirely excluded in these patients. Therefore, we can avoid unnecessary laparotomy in these groups of patients. Of these, 22 had a final diagnosis as idiopathic NH, 19 were diagnosed as infectious NH (cytomegalovirus 15, rubella virus 2, syphilis 1, and human immunodeficiency virus 1), and 9 had a diagnosis as having cholestatic jaundice of unknown cause.

Moreover, of the 50 patients who did show tracer excretion into the intestine, 22 (44%) demonstrated bowel activity within 1 hour, 27 (54%) showed tracer excretion during 1-4 hours, and the remaining one patient (2%) revealed intestinal activity at 6 hours after injection.

In our study, we found that the sensitivity, specificity and accuracy of Tc-99m DISIDA scintigraphy for the diagnosis of BA were 100%, 86% and 92%, respectively. The positive and negative predictive value were 85% and 100%.

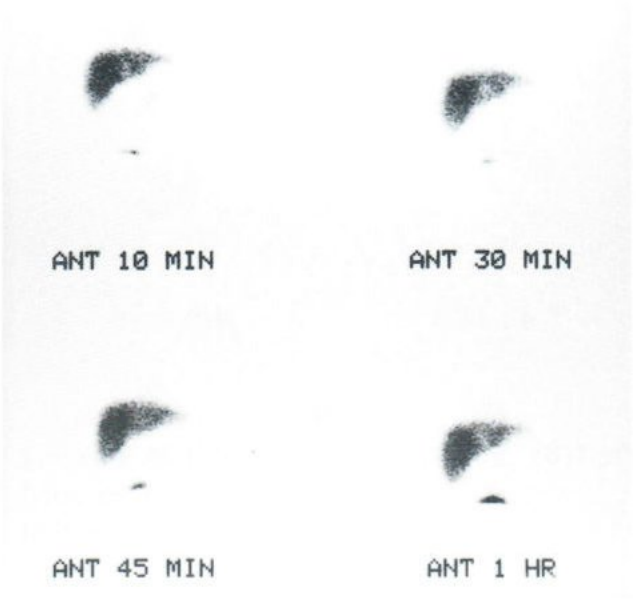

1A

Fig.1(A) Biliary atresia. A 2-month-old infant presented with persistent conjugated hyperbilirubinemia and acholic stools. The Tc-99m DISIDA hepatobiliary scintigraphy reveals prompt hepatic uptake with no evidence of tracer excretion into the biliary and/or GI tract up to 6 hours after injection. The 24 hour image (not shown) also fails to demonstrate the GI activity. The patient had a final diagnosis as BA proven by surgery.

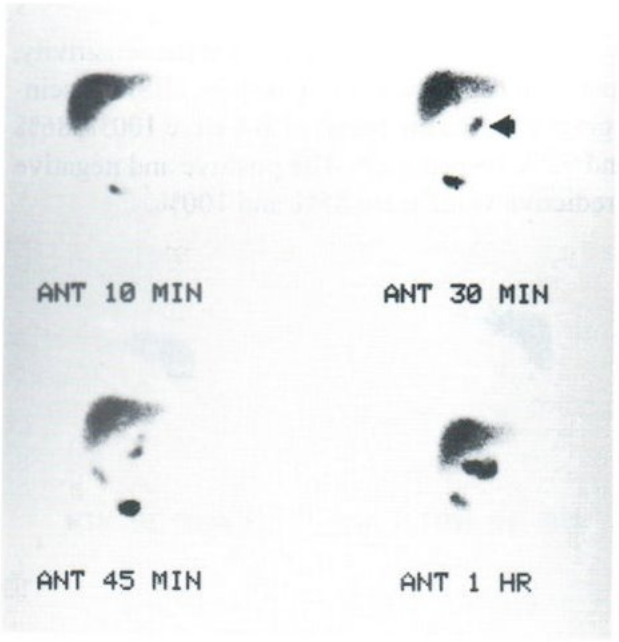

1B

Fig.1(B) Follow up Tc-99m DISIDA imaging after Kasai's operation reveals good hepatic uptake with biliary excretion of the radiotracer into the intestine (arrow).

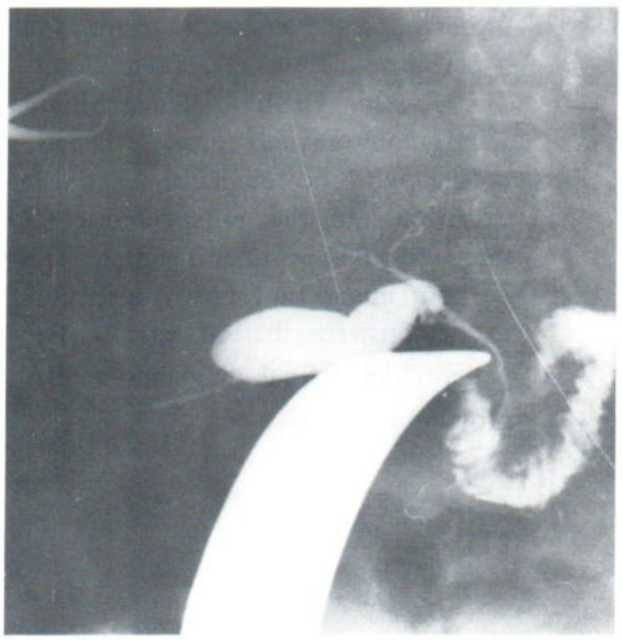

2B

Fig.2(B) Intraoperative cholangiography demonstrates the patency of biliary system.

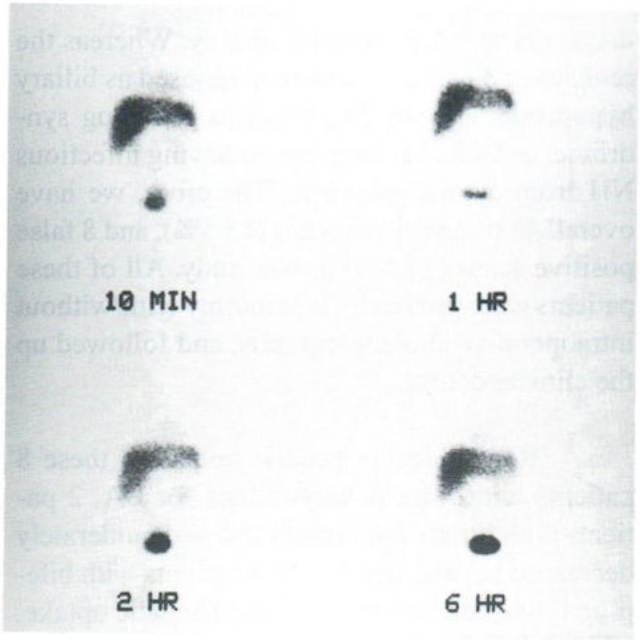

2A

Fig.2 (A) **Bile-plug syndrome.** A 3-month-old infant with persistent jaundice and conjugated hyperbilirubinemia. Sequential anterior abdominal imaging with Tc-99m DISIDA shows rather good hepatic uptake with no definite tracer excretion into the intestine up to 24 hours after injection. The patient was diagnosed as bile-plug syndrome proven by laparotomy with intraoperative cholangiography.

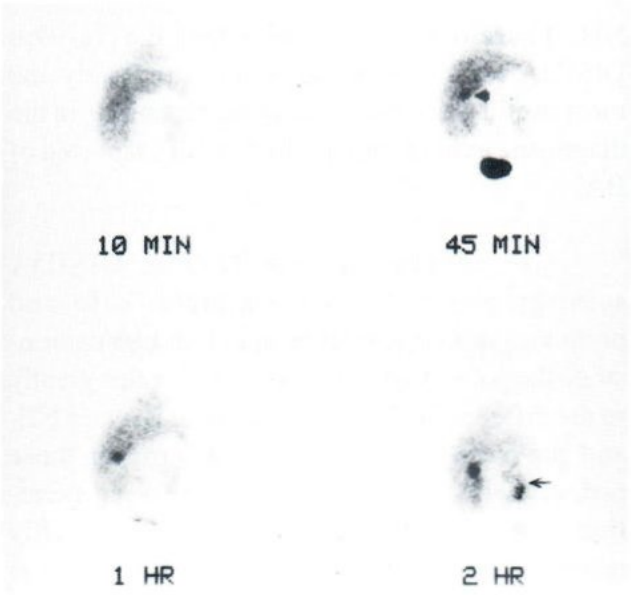

Fig.3 Neonatal hepatitis. A 2-month-old infant with positive cytomegalovirus titers and conjugated hyperbilirubinemia. The hepatobiliary scan reveals moderately decreased hepatic uptake with evidence of tracer excretion into the gallbladder since 45 minutes after injection (arrow head). Decreased and delayed tracer excretion into the intestine is observed (thin arrow). There is still persistent cardiac blood-pool activity.

DISCUSSION

In infants with conjugated hyperbilirubinemia, the main clinical problem usually arises in distinguishing BA from NH.[1,2,7] Hepatobiliary imaging using Tc-99m IDA derivatives is a useful imaging technique in the diagnostic evaluation of these groups of patients.[16-19]

The IDA derivatives undergo the same metabolism as bilirubin and organic anions. After hepatocyte uptake, it is excreted into the biliary tree and eliminated in the intestine.[20] Hepatobiliary scintigraphy with Tc-99m IDA derivatives is well recognized as the only noninvasive diagnostic method to demonstrate the patency of biliary system, and it is the only technique which provides the real-time assessment of bile flow from the liver to the intestine.[20,21] Moreover, it is useful not only in the diagnosis of BA, but also plays role in the postoperative assessment after surgical treatment as well.[7]

Among a variety of Tc-99m IDA derivatives, Tc-99m DISIDA is most commonly used in hepatobiliary scintigraphy.[22,23] It has rather high hepatic extraction, and low urinary excretion. Tc-99m DISIDA scintigraphy can be successfully performed even though in patients with high bilirubin levels up to 20-30 mg/dl.[21,22] Normally the radiotracer is accumulated in the liver within 5 minutes, and the tracer excretion should be seen in the biliary tract within 10-15 minutes, with maximum activity at 40-45 minutes after injection. The small bowel activity should be seen within 30-60 minutes, and the GB should be seen within 1 hour after injection.[20,21] Therefore, it is most useful when definite tracer excretion into the GI tract occurs, which indicates evidence of biliary patency, and excludes the diagnosis of BA. In our series, we could avoid unnecessary laparotomy in 50 patients who revealed definite tracer excretion into the GI tract.

The classical scintigraphic finding in BA is good hepatic uptake with no definite tracer excretion into the intestine up to 24 hours.[1,20,21] When this finding occurs, the diagnosis of BA can be made with an extremely high degree of accuracy. However, nonvisualization of the tracer in the bowel does not always indicate BA, since other causes of neonatal jaundice such as NH and bile-plug syndrome may reveal no biliary excretion throughout the study as well.[5,6,18,23] In our study, we also found that 4 patients with infectious NH, 2 patients with biliary hypoplasia, and 2 patients with bile-plug syndrome, revealed no definite tracer excretion into the intestine up to 24 hours.

It is of interest that we found 6 NH patients (idiopathic NH 5, NH from cytomegalovirus 1) with serum bilirubin levels more than 30 mg/dl, who still demonstrated evidence of tracer excretion into the intestine. The average direct and total bilirubin levels of these patients were 15.13 ± 6.44 mg/dl (range, 9.08 to 23.62), and 32.91 ± 1.27 mg/dl (range, 31.02 to 34.3) respectively. This finding confirms that Tc-99m DISIDA scintigraphy is a reliable and useful imaging in differentiating BA from other causes of neonatal cholestasis, even in patients with serum bilirubin levels as high as 30 mg/dl.

Concerning the patients with positive GI activity, we found that 49 out of 50 patients (98%) demonstrated intestinal activity within 4 hours, and all (100%) showed bowel activity within 6 hours after injection. Whereas the 55 patients with no definite biliary excretion, all showed no evidence of tracer excretion at 6 hours, and at 24 hours after injection. Therefore, we wonder whether if no evidence of tracer excretion into the GI tract occurs at 6 hours, the 24 hour images should still be routinely performed or not.

Majd et al demonstrated that the specificity and accuracy of Tc-99m IDA scintigraphy in differentiating BA from NH increased significantly when performed after phenobarbital treatment.[1] Phenobarbital will enhance the biliary excretion of Tc-99m IDA agents by inducing the hepatic microsomal enzymes.[1,23] So, we routinely performed our study after 5 days of phenobarbital therapy. In our series, the Tc-99m DISIDA scintigraphy had a 100% sensitivity, 86% specificity and 92% accuracy for the diagnosis of BA. The positive and negative predictive value were 85%, and 100% respectively. The predictive accuracy of a negative imaging is therefore high enough to clinically exclude the diagnosis of BA. The results of our study indicate that the Tc-99m DISIDA scintigraphy is a sensitive and highly accurate method for the differentiation of BA from NH. Therefore, we consider that the Tc-99m DISIDA hepatobiliary imaging is probably the most useful noninvasive imaging technique in the diagnostic evaluation of infants with suspected of BA.

In conclusion, the Tc-99m DISIDA scintigraphy is the only simple, safe and noninvasive imaging technique that can demonstrate the patency of biliary system. It helps greatly in the differential diagnosis between BA and NH, and prevents unnecessary laparotomy in those patients who demonstrate definite tracer excretion into the intestine. Therefore, it is highly recommended as a routine screening investigation of choice in infants with suspected of BA.

REFERENCES

1. Majd M, Reba RC, Altman RP. Effect of phenobarbital on Tc-99m IDA scintigraphy in the evaluation of neonatal jaundice. Sem Nucl Med 1981; 11: 194-204.
2. Sty JR, Wells RG. Physiologic and pharmacologic interventions in pediatric nuclear medicine. In: Freeman LM, eds. Nuclear Medicine Annual. New York: Raven Press; 1992:105-21.
3. Adelman S. Prognosis of uncorrected biliary atresia: An update. J Pediatr Surg 1978;13: 389-91.
4. Kasai M, Suzuki H, Ohashi E, et al. Technique and results of operative management of biliary atresia. World J Surg 1978;2:571-80.
5. Wynchank S, Guillet J, Leccia F, et al. Biliary atresia and neonatal hepatobiliary scintigraphy. Clin Nucl Med 1984;9:121-4.
6. Gerhold JP, Klingensmith WC, Kuni CC, et al. Diagnosis of biliary atresia with radionuclide hepatobiliary imaging. Radiology 1983;146:499-504.

7. Treves ST, Jones A. Hepatobiliary scintigraphy. In: Treves ST, eds. Pediatric Nuclear Medicine. New York: Springer-Verlag; 1985:157-70.
8. Abramson SJ, Treves S, Teele RE. The infant with possible biliary atresia: Evaluation by ultrasound and nuclear medicine. Pediatr Radiol 1982;12:1-5.
9. Greene HL, Helinek GL, Moran R, et al. Adiagnostic approach to prolonged obstructive jaundice by 24-hour collection of duodenal fluid. J Pediatr 1979;95:412-4.
10. Hung WT, Su CT. Diagnosis of atretic obstructive jaundice; Technetium-99m hepatolite excretion study. J Pediatr Surg 1990;25:797-800.
11. Hashimoto T, Yura J. Percutaneous transhepatic cholangiography (PTC) in biliary atresia with special reference to the structure of the intrahepatic bile ducts. J Pediatr Surg 1981;16:22-25.
12. Guelrud M, Jaen D, Mendoza S, et al. E RCP in the diagnosis of extrahepatic biliary atresia. Gastrointest Endosc 1991; 37:522-6.
13. Hirsig J, Rickham PP. Early differential diagnosis between neonatal hepatitis and biliary atresia. J Pediatr Surg 1980;15:13-15.
14. Schwartz MZ. An alternate method for intraoperative cholangiography in infants with severe obstructive jaundice. J Pediatr Surg 1985;20:440-2.
15. Ferry GD, Selby ML, Udall J, et al. Guide to early diagnosis of biliary obstruction in infancy: review of 143 cases. Clin Pediatr 1985;24:305-11.
16. Hitch DC, Leonard JC, Pysher TJ, et al. Differentiation of cholestatic jaundice in infants: Utility of diethyl-IDA. Amer J Surg 1981; 142: 671-7.
17. Ben-Haim S, Seabold JE, Kao SCS, et al. Utility of Tc-99m mebrofenin scintigraphy in the assessment of infantile jaundice. Clin Nucl med 1995;20:153-63.
18. Majd M, Reba RC, Altman RP. Hepatobiliary scintigraphy with Tc-99m PIPIDA in the evaluation of neonatal jaundice. Pediatrics 1981; 67:140-5.
19. Kirks DR, Coleman RE, Filston HC, et al. An imaging approach to persistent neonatal jaundice. AJR 1984;142:461-5.
20. Williams AG, Mettler FA, Christie JH. Hepatobiliary and pancreatic imaging. In: Mettler FA, eds. Radionuclide imaging of the GI tract. New York, Edinburgh, London, Melbourne: Churchill Livingstone; 1986:183-215.
21. Weissmann HS, Sugarman LA, Freeman LM. The clinical role of Tc-99m iminodiacetic acid cholescintigraphy. In: Freeman LM, Weissmann HS,eds. Nuclear Medicine Annual. New York: Raven Press; 1981:35-89.
22. Weissmann HS, Badia JD, Hall T, et al. Tc-99m Diisoporpyl iminodiacetic acid (DISIDA) : The best overall cholescintigraphic radionuclide for the evaluation of hepatobiliary disorders [Abstract]. J Nucl Med 1980;21:18P.
23. Howman-Giles R, Uren R, Bernard E, et al. Hepatobiliary scintigraphy in infancy. J Nucl Med 1998; 39: 311-9.

THE APPEARANCE OF NEUROBLASTOMA IN CT

Pannee VISRUTARATNA, MD., Parichad CHANPONG, MD.

ABSTRACT

CT scans were reviewed of 22 children diagnosed with neuroblastoma but not yet treated. Most of the children had abdominal mass or bone pain. 63.6% (14/22) of the tumors originated in the adrenal glands, 13.6% (3/22) were in the paravertebral region, 9.1% (2/22) in the pelvic cavity, and 13.6% (3/22) in the chest. According to Evan's system, 50% (11/22) of the patients were stage III, 40.9% (9/22) stage IV, and 9.1% (2/22) stage IV-S. Most of the tumors were poorly defined. One half of the tumors contained calcifications. 22.7% (5/22) had invaded the spinal canal. Metastases (bone, liver, or pulmonary) were seen in CT scans in 72.7% (8/11) of the patients at stage IV or IV-S. Most of the patients only sought help when the neuroblastomas had already reached late stages. CT scans of the neuroblastomas not only demonstrated the extent of the primary tumor, but also helped to detect metastases.

INTRODUCTION

Neuroblastoma is the most common extracranial solid malignant tumor in children; it is the third most common malignancy of childhood, surpassed in incidence only by acute leukemia and primary brain tumor.[1] The patient's age, site of tumor, and stage of disease at initial diagnosis are the main factors in the prognosis of this disease. Patients under one year of age have a more favorable prognosis. Thoracic neuroblastomas have a better prognosis than abdominal or pelvic neuroblastomas.

CT and bone scintigraphy in conjunction with pertinent clinical data and bone marrow aspiration will accurately stage at least 95% of patients using Evan's classification.[2] CT is essential for the confirmation, localization, and staging of neuroblastoma.

MATERIALS AND METHODS

We reviewed CT scans performed from October 1991 to December 1997 on 22 children ranging in age from 2 months to 15 years with neuroblastoma not yet treated. The average age was about 4 years. There were 9 girls and 13 boys. The presenting symptoms were abdominal mass (10/22), bone pain (6/22), prolonged fever (2/22), neck mass (1/22), paraplegia (1/22), and periorbital ecchymosis (1/22). One child had an incidental posterior mediastinal mass.

The diagnoses were made from bone marrow aspiration biopsy, fine needle aspiration biopsy of the tumor, cervical lymph node biopsy, or histological examination after surgical removal of the tumor. Twenty-one tumors were neuroblastomas histologically. One thoracic tumor was ganglioneuroma with neuroblastoma foci.

According to Evan's system,[3] 50% (11/22) of the patients were stage III, 40.9% (9/22) stage IV, and 9.1% (2/22) stage IV-S.

Department of Radiology, Faculty of Medicine, Chiang Mai University, Chiang Mai 50200, Thailand.

The CT scans were performed using contiguous axial 10 mm slices. Scans were performed both before and after administration of bolus intravenous contrast medium. Oral contrast medium was also given to patients with abdominal neuroblastoma. The CT scans were examined for

1. site of the main tumor mass;
2. extension of the tumor mass;
3. encasement of the great vessels (aorta and its branches, IVC, or SVC);
4. tumor characteristics (margins, calcifications, and areas of necrosis);
5. intraspinal extension; and
6. liver, bone, or pulmonary metastases.

RESULTS

It was found that of the 22 neuroblastomas, 14 (63.6%) originated in the adrenal glands (Fig. 1), 3 (13.6%) were in the paravertebral region (Fig. 2), 2 (9.1%) in the pelvic cavity (Fig. 3), and 3 (13.6%) in the chest (Fig. 4).

Most of the tumors (19/22) were poorly defined. The remaining three were well defined; two of these were stage IV-S (Fig. 5) and one was stage III (Fig. 6). Encasement of the great vessels was seen in 14 children. One half of the tumors contained calcifications. All of the tumors had areas of necrosis. 22.7% (5/22) had invaded the spinal canal; only 1 child had symptoms of cord compression. On CT scans of the primary tumor, bone metastases were seen in 4 children (Fig. 7), liver metastases in 2 children, and pulmonary metastases in 1 child.

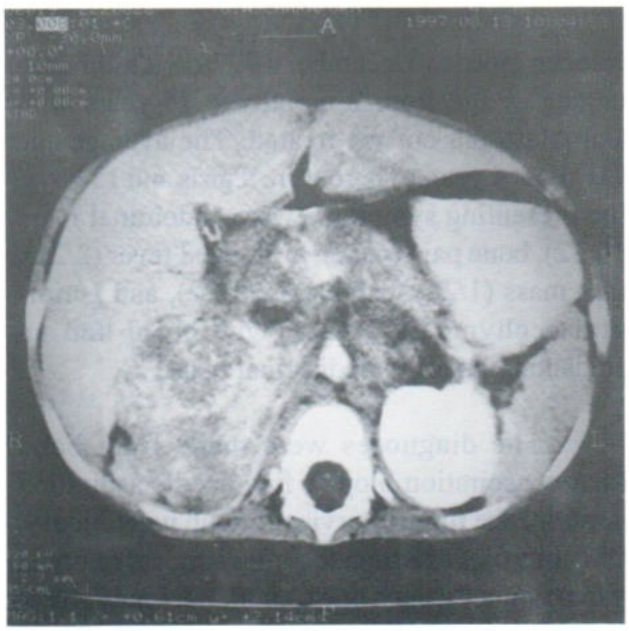

Fig. 1 Contrast CT scan shows an ill-defined inhomogeneous soft tissue mass in the right suprarenal region. The mass encases the great vessels and extends across the midline.

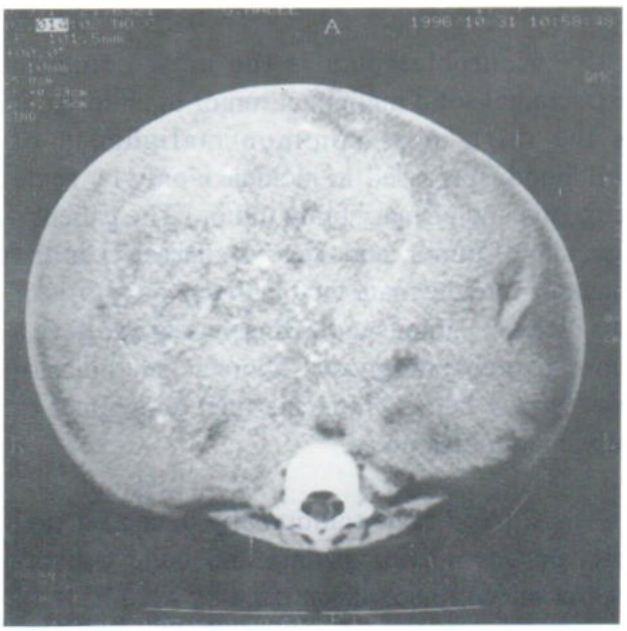

Fig. 2 Contrast CT scan shows a huge inhomogeneous soft tissue mass with multiple stippled calcifications in the paravertebral region.

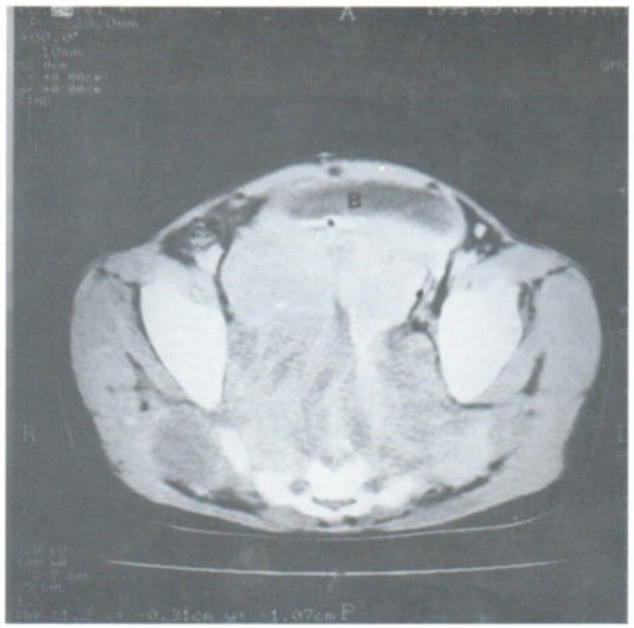

Fig. 3 Contrast CT scan shows an ill-defined inhomogeneous soft tissue mass in the pelvic cavity. The mass has extended through the pelvic side walls and destroyed the sacrum. (B= urinary bladder)

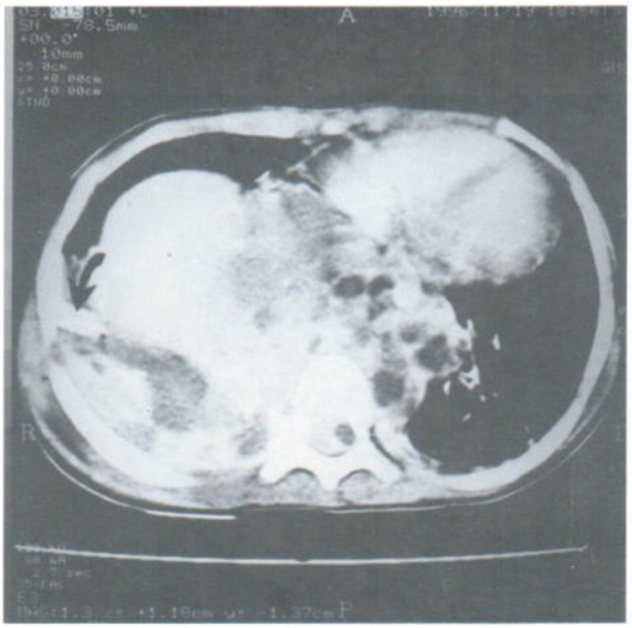

Fig. 4 Contrast CT scan shows an ill-defined inhomogeneous soft tissue mass in the mediastinum. Note the extension of the mass to the right chest wall and epidural space. (arrow = thoracostomy tube)

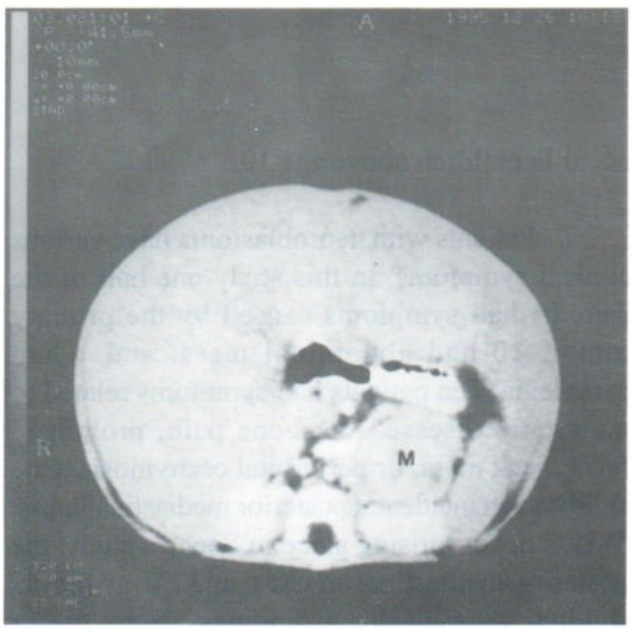

Fig. 5 Contrast CT scan shows a well-defined left suprarenal mass (M) and diffuse inhomogeneous density of the liver caused by metastases.

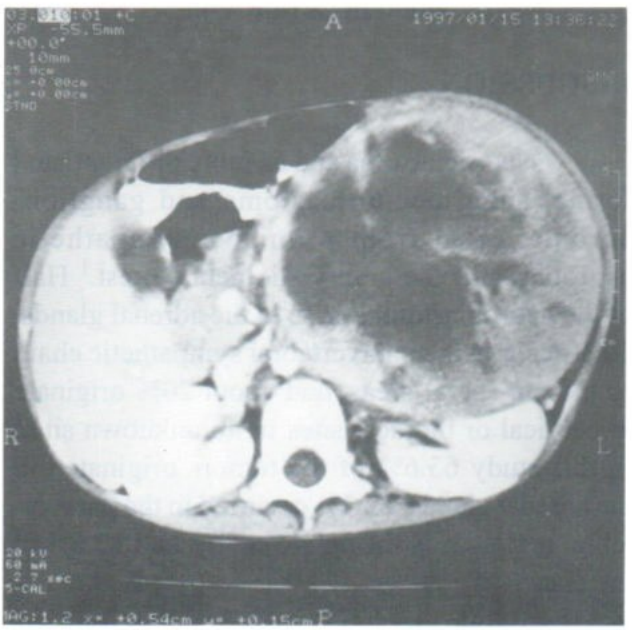

Fig. 6 Contrast CT scan shows a well-defined inhomogeneous soft tissue mass which is pressing the anterior aspect of the left kidney. It extends across the midline but does not encase the great vessels.

Fig. 7 Neuroblastoma with bone metastases

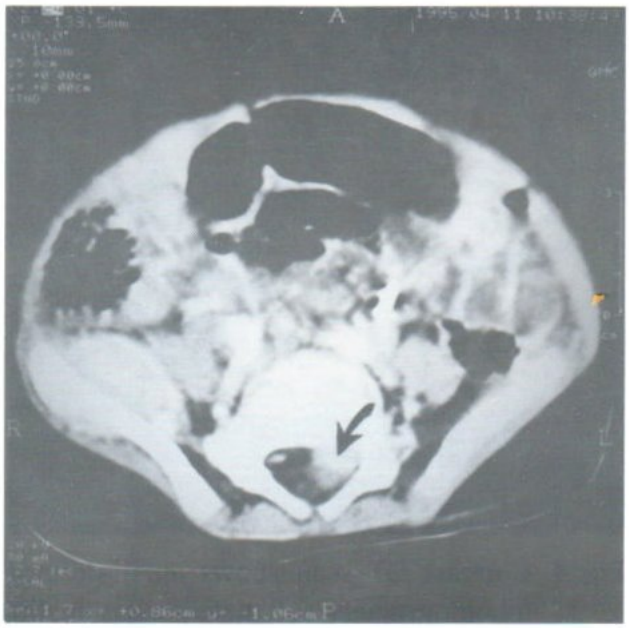

Fig. 7A Contrast CT scan shows soft tissue masses on both sides of the right iliac bone. Note the extradural mass (arrow).

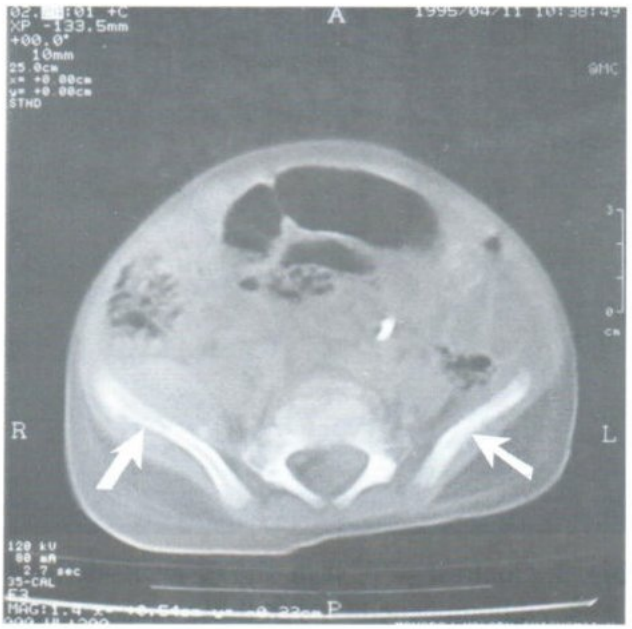

Fig. 7B CT scan (bone window display) shows destruction of the right and left iliac bones.

DISCUSSION

Neuroblastoma and its more differentiated forms, ganglioneuroblastoma and ganglioneuroma, arise from primitive sympathetic neuroblasts of the embryonic neural crest.[1] Half of the neuroblastomas arise in the adrenal glands, 30% occur in the paravertebral sympathetic chain or the pre-sacral areas, and about 20% originate in cervical or thoracic sites or an unknown site.[4] In this study 63.6% of the tumors originated in the adrenal glands, 22.7% occurred in the paravertebral region or in the pelvic cavity, and 13.6% in the chest.

The tumor is more common in boys than in girls; the male/female ratio is 1.2:1 in most large studies.[4] 75% of patients are less than 4 years of age, and fewer than 10% of neuroblastomas occur in children above age 10.[1]

Patients with neuroblastoma have various clinical symptoms. In this study one half of the patients had symptoms caused by the primary tumor, 10 had abdominal mass, and 1 had paraplegia. Ten patients had symptoms related to metastatic disease, i.e., bone pain, prolonged fever, neck mass, or periorbital ecchymosis. One child had an incidental posterior mediastinal mass. This is not surprising since in Saenz's study, the posterior mediastinal masses in 32% of the 63 children were incidental findings.[5] None of our patients had paraneoplastic syndromes, i.e. myoclonic encephalopathy of infancy;[6] syndrome of intractable watery diarrhea, hypokalemia, and achlorhydria;[1] and excessive catecholamine

syndrome (hypertension, headache, flushing).[4]

Neuroblastoma is characterized by a calcified suprarenal mass or pararenal mass.[2,7] In Peretz and Lam's experience the most reliable sign of abdominal neuroblastoma is the displacement of the IVC and aorta, particularly when they are separated from the vertebral bodies.[8] In their study calcifications were found in CT scans in 76% of patients with abdominal neuroblastoma. Golding, et al. found that 24/33 (72.7%) of thoracic and abdominal neuroblastomas contained minor or heavy calcifications.[9] We found fewer calcifications than previously reported. Only one half of our patients had calcifications in CT scans.

As most abdominal neuroblastomas arise in the adrenal gland near the aorta, celiac axis, and/or superior mesenteric artery, it is not surprising that tumors crossing the midline tend to involve vital vessels. Since surgery currently plays a major role in the treatment, the relation of the tumor to the great vessels is a more reliable and important factor in predicting the outcome of these children than the extension and location of the tumor with reference to the midline.[10] CT after intravenous contrast enhancement is helpful in assessing the great vessels. One of our stage III patients had a well defined tumor crossing the midline but not encasing the aorta or great vessels. It was able to be totally resected.

A small number of children with neuroblastoma present with symptoms of cord compression.[11] Golding et al found that a significant number of children had clinically unsuspected extensions of tumor into the spinal canal[9]; four of our patients with such extensions had no clinical signs.

Common sites of metastases for neuroblastomas are skeleton, bone marrow, liver, lymph nodes, and skin. The pattern of metastases varies greatly with age. Bone metastases are extremely common in children over one year of age, usually involving the long bones and orbits. In newborn liver and skin metastases are more common than bone metastases.[1] Pulmonary parenchymal metastases are considered extremely rare in patients with neuroblastomas. Pulmonary metastases occur in patients with widespread disseminated disease. It is a grave prognostic sign and considered a pre-terminal event.[1]

Ultrasonography is usually the initial imaging modality for a child with a palpable abdominal mass. It has limited value in detecting retroperitoneal and retrocrural lymph node metastases. It is unable to detect extradural extension of tumor into the vertebral canal.

CT is extremely valuable for determining the extent of neuroblastomas. It is able to detect prevertebral extension of tumor across the midline, encasement of the great vessels, renal invasion, nodal metastases, intraspinal extension, liver metastases, response to therapy, and tumor recurrence. It is excellent for demonstrating retrocrural extension to the chest, which commonly occurs in abdominal neuroblastoma.

MR imaging plays an important role in defining tumor resectability; it is better than CT in defining vascular encasement, hepatic metastases, bone marrow metastases, and intraspinal extension.[12-14] The disadvantage of MRI is that bone erosion and pulmonary metastases are less well visualized than they are with CT.[5]

CONCLUSIONS

Most of our patients only sought help when the neuroblastomas had already reached late stages. CT scans of most of our stage IV and IV-S tumors not only demonstrated the extent of the primary tumor, but they also helped to detect metastases (bone, liver, or pulmonary).

REFERENCES

1. Bousvaros A, Kirks DR, Grossman H. Imaging of neuroblastoma: an overview. Pediatr Radiol 1986;16:89-106.
2. Stark DD, Moss AA, Brasch RC, et al. Neuroblastoma: diagnostic imaging and staging. Radiology 1983;148:101-5.
3. Evans AE, D'Angio GJ, Randolph J. A proposed staging system for children with neuroblastoma. Cancer 1971;27:374-8.
4. Brodeur GM. Neuroblastoma and other peripheral neuroectodermal tumors. In: Fernbach DJ, Vietti TJ, eds. Clinical pediatric oncology, 4th ed. St. Louis: Mosby Year Book, 1991:437-64.
5. Saenz NC, Schnitzer JJ, Eraklis AE, et al. Posterior mediastinal masses. J Pediatr Surg 1993;28(2):172-6.
6. Baker ME, Kirks DR, Korobkin M, Bowie JD, Filston HC. The association of neuroblastoma and myoclonic encephalopathy: an imaging approach. Pediatr Radiol 1985;15:184-90.
7. Siegel MJ, Sagel SS. Computed tomography as a supplement to urography in the evaluation of suspected neuroblastoma. Radiology 1982;142:435-8
8. Peretz GS, Lam AH. Distinguishing neuroblastoma from Wilms tumor by computed tomography. J Comput Assist Tomogr 1985;9(5):889-93.
9. Golding SJ, McElwain TJ, Husband JE. The role of computed tomography in the management of children with advanced neuroblastoma. Br J Radiol 1984;57:661-6.
10. Boechat MI, Ortega J, Hoffman AD, Cleveland RH, Kangarloo H, Gilsanz V. Computed tomography in stage III neuroblastoma. AJR 1985;145:1283-7.
11. Punt J, Pritchard J, Pincott JR, Till K. Neuroblastoma: a review of 21 cases presenting with spinal cord compression. Cancer 1980;45:3095-101.
12. Dietrich RB, Kangarloo H, Lenarsky C, Feig SA. Neuroblastoma: the role of MR imaging. AJR 1987;148:937-42.
13. Siegel MJ. Jamroz GA, Galzer HS, Abramson CL. MR imaging of intraspinal extension of neuroblastoma. J Comput Assist Tomogr 1986;10:593-5.
14. Slovis TL, Meza MP, Cushing B. Thoracic neuroblastoma: what is the best imaging modality for evaluating extent of disease? Pediatr Radiol 1997;27:273-5.

MAMMOGRAPHIC AND SONOGRAPHIC APPEARANCES OF NON-HODGKIN'S LYMPHOMA OF THE BREAST

***POJCHAMARNWIPUTH Suwalee, M.D., *MUTTARAK Malai,M.D., *EUATHRONGCHIT Juntima, M.D., **CHAIWUN Benjaporn, M.D. **SIRIANGKUL Sumalee, M.D.**

ABSTRACT

PURPOSE ;

Secondary non-Hodgkin's lymphoma is uncommonly encountered in the breast. This paper aims to demonstrate mammographic and sonographic findings of non -Hodgkin's lymphoma of the breast.

MATERIALS AND METHODS :

From August 1996 to July 1997, three patients (mean age 42.3 years, range 19-78 years) with NHL of the breast were diagnosed. Two patients had both mammography and sonography while one patient had sonography alone. Histologic confirmation was obtained in all cases.

RESULTS :

All three patients had secondary NHL of the breast. One of them had AIDS-related lymphoma. Mammography revealed multiple, circumscribed uncalcified masses in one patient and diffuse increased parenchymal density with skin thickening in the other. Sonography showed multiple hypoechoic masses in two patients and diffuse inhomogeneous echoes in one patient. Histologic examination showed diffuse NHL in all patients.

CONCLUSION :

In patient with a history of NHL, the diagnosis of secondary breast NHL should be considered when multiple masses or diffuse lesions are observed.

NHL = Non-Hodgkin's lymphoma

INTRODUCTION

Non-Hodgkin's lymphoma (NHL) of the breast is rare. It can originate as a primary breast tumor, but most often it occurs in conjunction with extramammary disease with the breast involved secondarily as part of a disseminated process[1]. We reviewed our experience with NHL of the breast

* Department of Radiology,
** Department of Pathology, Faculty of Medicine, Chiang Mai University, Chiang Mai 50200, Thailand.

in three women with the aim of determining the imaging characteristics.

MATERIALS AND METHODS

From August 1996 to July 1997, three patients (mean age 42.3 years, range 19-78 years) were diagnosed with NHL of the breast. Two patients had both mammography and sonography while one patient had sonography alone. Histologic confirmation was obtained in all cases.

RESULTS

CASE 1 : A 78-year-old woman had multiple palpable masses in the left breast, left axilla and left side of the anterior abdominal wall that continued to enlarge for 3 months after they had been identified. Mammography showed multiple, well-circumscribed masses without calcification in the left breast associated with enlarged left axillary lymph nodes (Fig. 1). The right breast was normal. Ultrasound revealed multiple well-defined hypoechoic masses in the left breast (Fig. 2), a large solid mass in the left anterior abdominal wall and three hypoechoic masses in the liver.

Histologic examination of the left breast mass and anterior abdominal wall mass revealed diffuse NHL of predominantly mixed large and small cell types. Chemotherapy was given without clinical improvement.

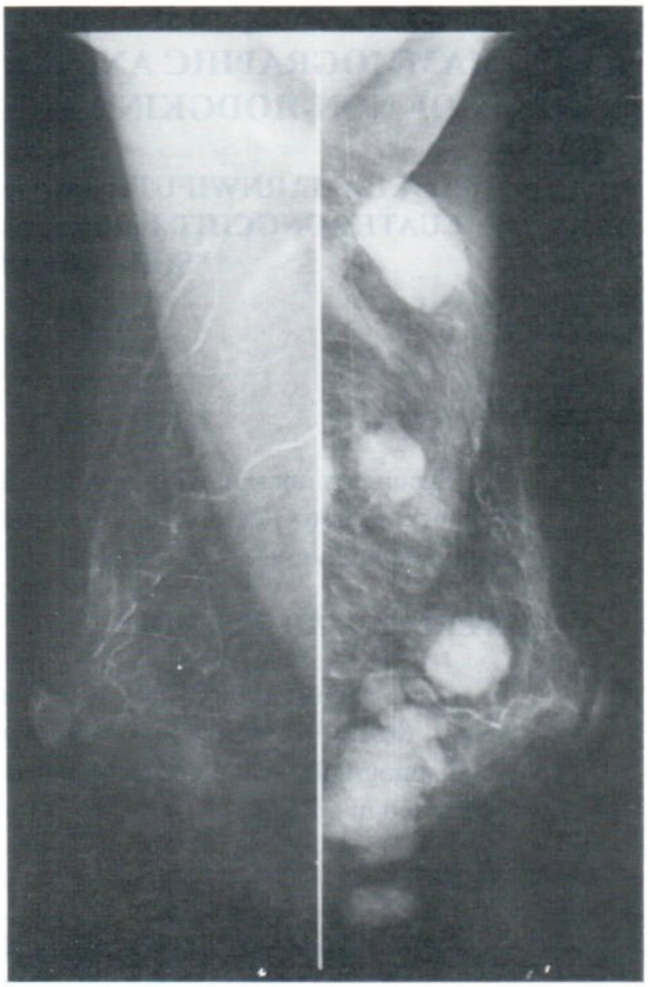

Fig. 1 Case 1 Mediolateral oblique mammogram of the breasts reveals multiple well-circumscribed noncalcified masses in the left breast and enlar ged left axillary lymph node. The right breast appears normal.

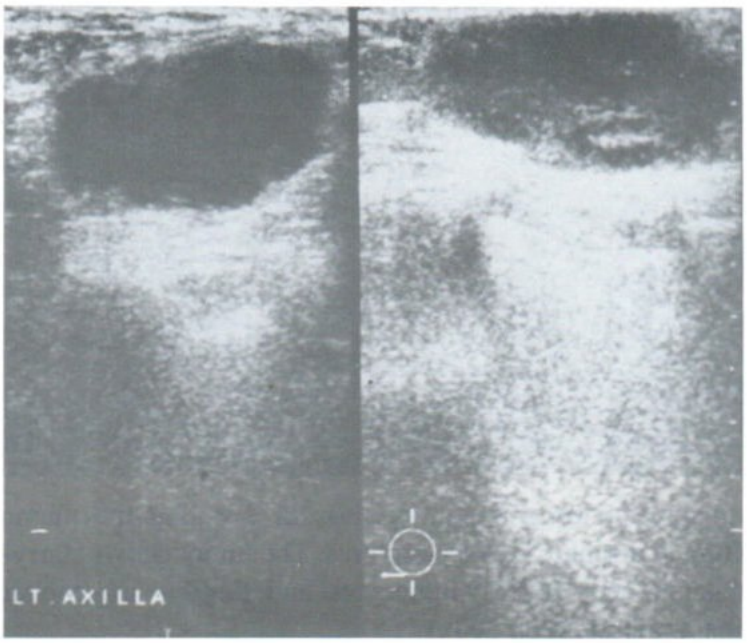

Fig. 2 US scan shows a hypoechoic mass in the left axilla which was thought to be an enlarged axillary lymph node (left). In the left breast, there was a well - defined solid mass with heterogeneity of internal echoes and marked posterior acoustic enhancement (right).

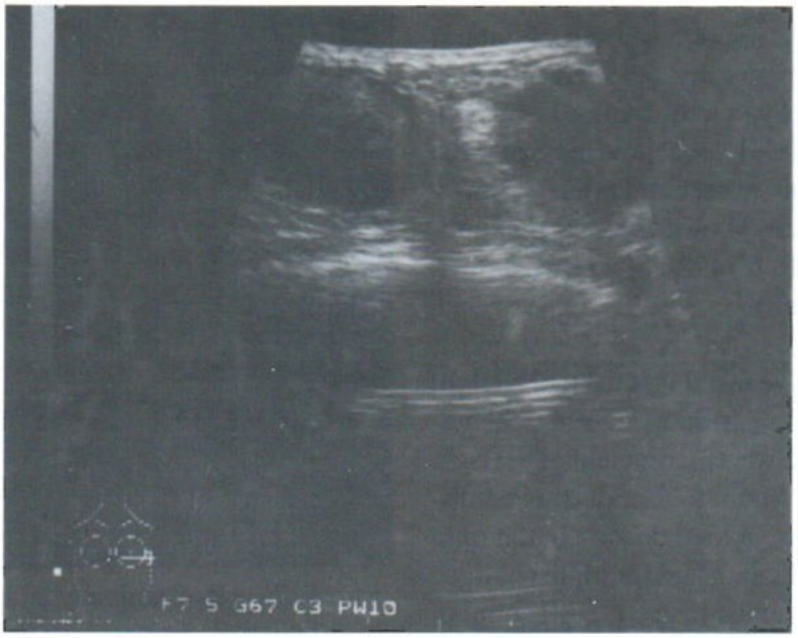

Fig. 3 Case 2 US scan of the left breast reveals multiple well-defined hypoechoic masses with no posterior acoustic enhancement.

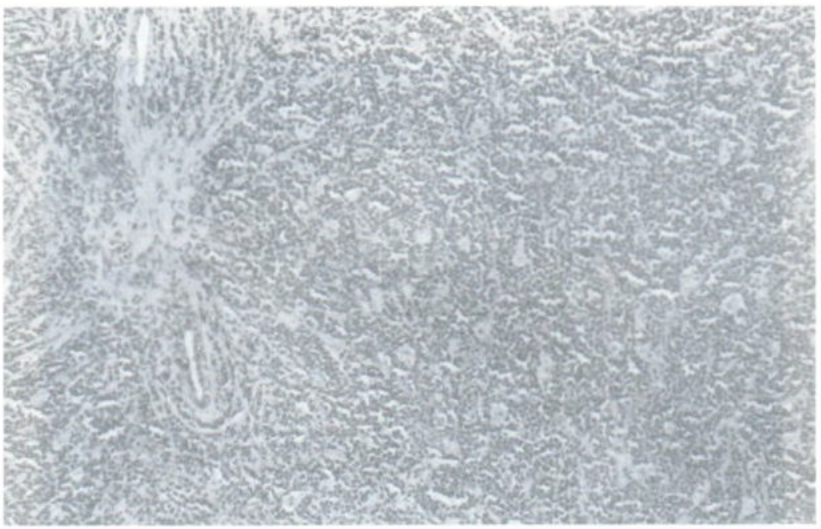

Fig. 4 Low magnification of the tumor mass in filtrating the mammary tissue resulting in atrophic ductal structures. The tumor shows starry-sky pattern with small neoplastic lymphocytes and tingible macrophages. (H&E, original magnification 100x)

CASE 2 : A 19-year-old woman with AIDS-related lymphoma presented with multiple palpable masses in both breasts for 2 months and dyspnea for a week. Physical examination revealed hepatomegaly, bilateral multiple breast masses and ascites.

The chest radiograph showed bilateral pleural effusion. Sonography revealed multiple, well-circumscribed hypoechoic masses in both breasts (Fig.3), multiple hypoechoic masses in the liver, bilateral ovarian masses and ascites. Biopsy of the right breast mass showed diffuse predominantly small cell NHL (Fig. 4). She refused treatment and went home.

CASE 3 : A 30-year-old woman had NHL of the lymph nodes for 11 months. During chemotherapy, there was diffuse enlargement of the right breast over 1 week. Mammography showed diffusely increased parenchymal density in the right breast with skin thickening and multiple enlarged right axially lymph nodes (Fig 5). Diffuse inhomogeneous echoes in the right breast with skin thickening were present on ultrasound (Fig. 6).

Biopsy of the right breast showed diffuse NHL. The disease progressed despite a new regimen of chemotherapy.

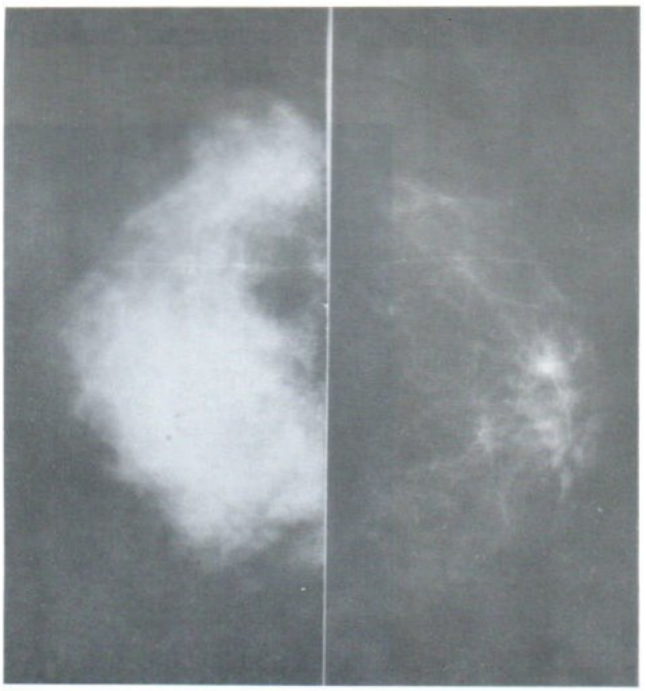

Fig. 5 Case 3 Craniocaudal mammogram of the breasts reveals diffusely increased parenchymal density associated with skin thickening in the right breast. The left breast is normal.

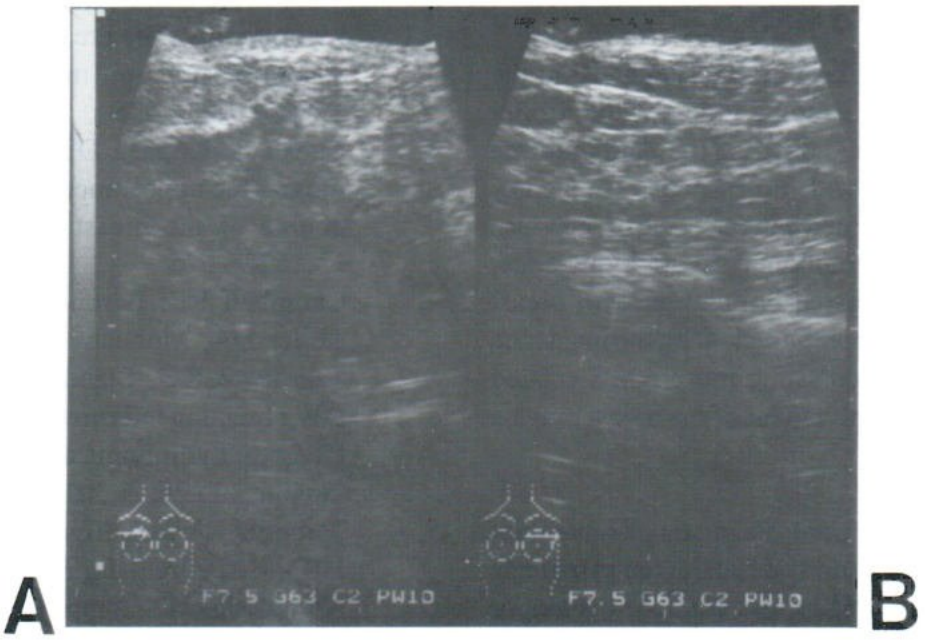

Fig.6 (A, B) US scan of the breasts demonstrate diffuse inhomogeneous echoes with skin thickening in the right breast (A) in comparison with normal echoes in the left breast (B).

DISCUSSION

Primary breast lymphoma accounts for 0.05-0.53% of all breast malignancies.[1,2] Lymphoma of the breast usually occur as secondary disease. Most of these malignancies are non-Hodgkin type. The frequency of primary versus secondary breast lymphoma varies in the literature.[1,3,4] The tumor architecture can be classified as either follicular (nodular) or diffuse, with the cell type predominantly large cell (histocytic) predominantly small cell (lymphocytic) , or mixed large and small cell.

Breast lymphoma most often occurs in women aged 50-60 years. The radiological features of breast lymphoma are nonspecific. The typical mammographic findings of primary or secondary non-Hodgkin lymphoma, consist of one or more, discrete round or oval uncalcified masses with well-circumscribed, lobulated or ill-defined borders that may mimic benign tumors such as fibroadenoma. Enlarged axillary lymph nodes may be seen. Less commonly, breast lymphoma may present as diffusely increased parenchymal density in conbination with skin thickening.[1-5] This occurred in only one case in our study. Spiculated masses and miliary densities have been reported.[2,3,5] Calcifications, which often occur in breast carcinoma, are rarely seen. Localized desmoplastic or scirrhous reaction with architectural distortion is typically not identified on mammography.[4] Most authors report unilateral involvement, but bilateral disease has been observed.[5]

Reports of the sonographic appearances of breast NHL are even more limited than those of the mammographic appearances. Jackson and Lalani[6] reported a wide spectrum of sonographic appearances ranging from well-defined to poorly-defined, hypo- to hyperechoic lesions, and focal to diffuse involvement, with variable posterior attenuation.

In our series, the mammographic and sonographic appearances were similar to those

described in previous reports.

Prognosis of breast NHL depends on the clinical stage and histologic grade of the lesion. All our three cases had diffuse NHL and multiple organ involvement with no response to chemotherapy in the two treated patients. One of our cases had AIDS-related lymphoma. To our knowledge, no case of AIDS-related lymphoma with breast involvement has been reported. With the incidence of HIV infection increasing, more AIDS-related lymphoma with involvement of the breast may be encountered.

In conclusion, the diagnosis of secondary NHL of the breast should be considered in patients with a history of NHL when multiple masses or diffuse lesions are observed in the breast.

REFERENCES

1. Liberman L, Giess CS, Dershaw DD, Louie DC, Deutch BM.: Non-Hodgkin Lymphoma of the breast: Imaging characteristics and correlation with histopathologic findings. Radiology 1994;192:157-160.
2. Slanetz PJ, Whitman GJ.: Non-Hodgkin's Lymphoma of the breast causing multiple vague densities on mammography. AJR 1996;167:537-538.
3. Meyer JE, Kopans DB, Long JC.: Mammographic appearance of malignant lymphoma of the breast. Radiology 1980;-135:623 - 626.
4. Campbell RE, Barone CA, Makris AN, Miller DA, Mohuchy T, Putnam SG 3rd, Schroeder KG, Standiford KN, Stewart DW.: Imaging interpretation session; Non-Hodgkin Lymphoma of the breast. Radio Graphics 1994;14:201-203.
5. Pameijer FA, Beijerinck D, Hoogenboom HHVM, Deurenberg JJM, Nortier JWR.: Non-Hodgkin's Lymphoma of the breast causing miliary densities on mammography. AJR 1995;164:609-610.
6. Jackson FI, Lalani ZH.: Breast lymphoma: Radiologic imaging and clinical appearances. Can Assoc. Radiol J 1991;42:48-54.

BRAIN SWELLING FACTOR : A FAVORABLE PROGNOSTIC FACTOR OF COMPUTED TOMOGRAPHIC APPEARANCE OF POST-TRAUMATIC ACUTE SUBDURAL HEMATOMA

Khomdao BOONCHIT [1], Chatchawuan THANAPURA[2]

ABSTRACT

Computed tomography (CT scan) used in diagnosis and management of 102 cases of post-traumatic acute subdural hematoma during January 1996 to December 1997 were analyzed. By measurement and calculating, the Brain Swelling Factor or difference between the midline shift and the hematoma thickness seems to be important prognostic factor. The midline structures are displaced not only by the space occupying subdural hematoma but also by the edematous processes on the injured side. When the midline shift exceeded the hematoma thickness, the survival rate was 31% (16/51) and when the hematoma thickness was greater than the midline shift, the survival rate was 65% (24/37).

INTRODUCTION

The prognosis of post-traumatic acute subdural hematoma is poor. Mortality rate is very high, ranging from 50% to 90% in published series.[1-5] A number of factors are thought to be prognostically favorable in surgical treatment of acute subdural hematoma, such as early surgery,[6,7] young age patient, [1] a Glasgow Coma Scale score of more than 5,[7, 8] and the presence of lucid interval.[9-11]

Computed tomography (CT scan) was used for diagnosis and management of head injury and acute subdural hematoma. [12-14]

OBJECTIVE

The patients suffering from acute subdural hematoma who cannot be examined neurologically because they have undergone intubation and sedation, the Brain Swelling Factor calculated from CT scans will be a favorable prognostic factor.

Computed tomographic data from 102 cases of post-traumatic acute subdural hematoma in Udornthani Hospital were reviewed retrospectively by the fact that the patients admitted usually had be treated with intubation, sedation, artificial ventilation with neurological examination not performable

PATIENTS AND METHOD

In a retrospective study 102 patients with isolated head injury and unilateral acute subdural hematoma were investigated during January 1996 to December 1997. Before CT scanning, patients with insufficient respiration underwent intubation and ventilation. CT scans were performed at the time of admission and immediate surgical treatment were given if the patient still survived.

From the CT data, cases with acute subdural hematoma less than 2 mm. or with cerebral contusion on the contralateral side were excluded

[1] Department of Radiology, Udornthani Hospital, Meung, Udornthani, 41000 THAILAND.
[2] Department of Neurosurgery, Udornthani Hospital, Meung, Udornthani, 41000 THAILAND

from this study. Two parameters, the thickness of hematoma and the midline shift were determined. The hematoma thickness was measured as the largest perpendicular distance between the cortex and the inner table of cranial vault (Fig.1). The midline shift is the largest perpendicular distance between an imaginary reference line joining the frontal crest and internal occipital protuberance, and the most shifted point of the septum pellucidum (Fig.2). The data was given in millimeters. Brain Swelling Factor was calculated as the difference between the midline shift and the hematoma thickness.

On admission, the patients were categorized according to age, sex, Glasgow Coma Scale, pupillary light response, and outcome on 7 days, 6 weeks, 6 months as good recovery, moderate, severe disabilities, vegetative state and death.

The Brain Swelling Factor or relationship of the midline shift and the hematoma thickness seems to be important measurement for predicting the prognosis than the hematoma alone. If the difference is positive, not only the hematoma but also brain swelling is contributing to an additional midline shift of the brain into the side originally not affected.

RESULTS

The patients consisted of 85 (83%) male and 17 (12%) female. Their ages ranged from 11 to 75 years (mean = 33 years). Glasgow Coma Scale on admission ranged from 2 to 14. GCS less than or equal to 5 was 62% and more than 5 was 38%. (Fig.3)

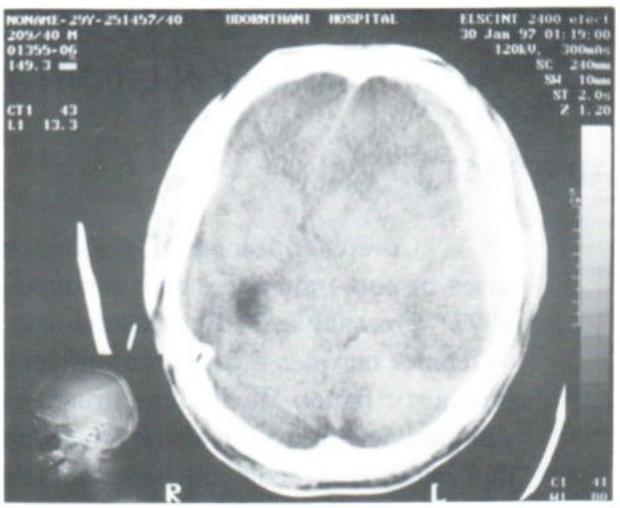

Fig. 1 The hematoma thickness measurement

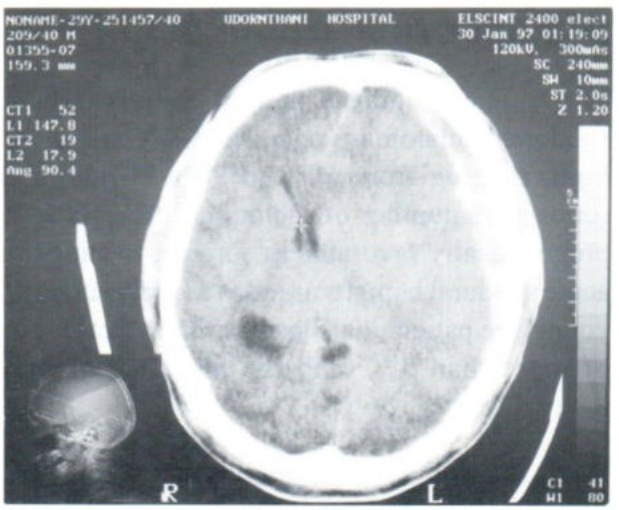

Fig. 2 The midline shift thickness measurement.

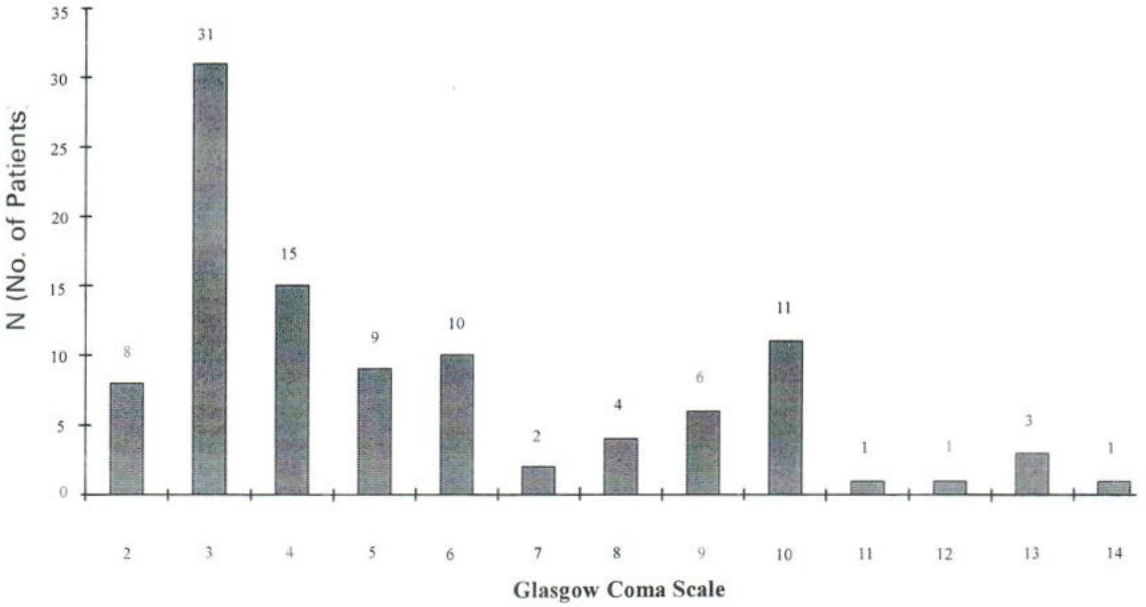

Fig. 3 Distribution of coma scores (Glasgow Coma Scale) at admission (n = 102)

CT FINDINGS

In 102 patients, the hematoma thickness ranged from 2 to 38 mm. and the midline shift were 0 to 28 mm. The midline shift exceeded the hematoma thickness in 51 patients (50%), the hematoma thickness equaled to the midline shift in 14 patients (14%) and the hematoma thickness was greater than the midline shift in 37 patients (36%). 52 patients (51%) were dead on first day to tenth day after admission. 50 patients (49%) had good recovery, moderate or severe disabilities. In summary, when the midline shift exceeded the hematoma thickness 1-5 mm. the survival rate is 36.6%(15/41) and drops to 10% (1/10) when the midline shift exceeded the hematoma thickness more than 5 mm. (table 1, Fig.4). The midline shift exceeded the hematoma thickness, the survival rate was 31%(16/51) and when the hematoma thickness was greater than the midline shift, the survival rate was 65% (24/37) (table 2).

Table 1 Difference of the MLS and the HT related to survival rate.

Difference of the MLS	survived		died	
and the HT(mm.)	No.	%	No.	%
<-5	8	66.7	4	33.3
(-5) - (-1)	16	64.0	9	36.0
0	10	71.4	4	28.6
1 - 5	15	36.6	26	63.4
>5	1	10.0	9	90

Difference significant: $p < 0.001$

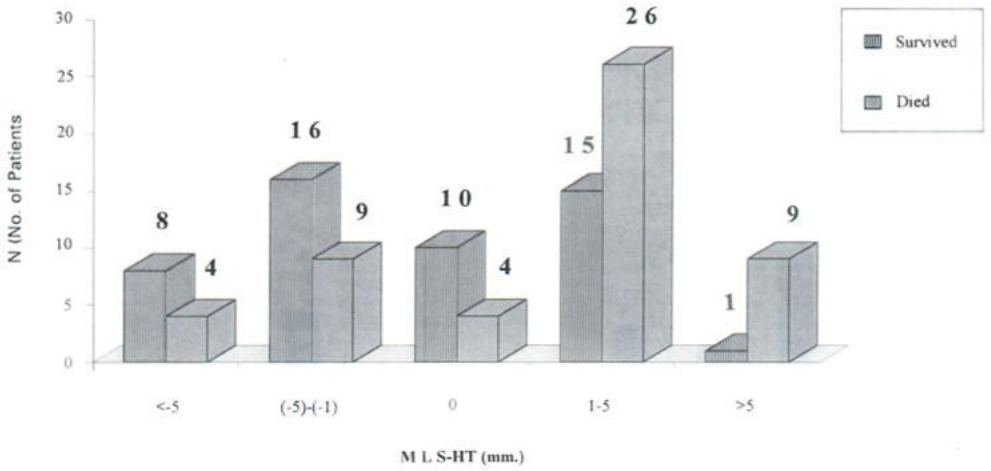

Fig. 4 Relationship of difference between midline shift (MLS) & hematoma thickness (HT) and outcome in 7 days.

Table 2 Survival rate related to relationship of the MLS and the HT.

	MLS<HT		MLS=HT		MLS>HT	
	No.	%	No.	%	No.	%
Survived	24	64.9	10	71.4	16	31.4
Died	13	35.1	4	28.6	35	68.6
Total	37	100	14	100	51	100

Difference significant: $p < 0.001$

DISCUSSION

The midline shift signifies compression of the neuronal structures, so the midline shift and prognosis behave reciprocally.[4,15-17] Review of three reports considering the midline shift and survival rate was compared to our data (table 3). When the midline shift equals to the hematoma thickness (difference is 0 mm.), the volume reserved provided by the subarachnoid space is completely exhausted by the development of the hematoma. Difference become positive (the midline shift more than the hematoma thickness) when the volume reserved capacity is exhausted and brain swelling develops on the injured side. This state characterized by a concomittent decrease in survival rate.

Table 3 Results of Surgical Treatment Considering Midline Shift and Survival Rate.

Series (Ref. No.)	Midline Shift (mm)	Survival Rate (%)
Marshall et al. (17)	<5	64
	5-15	53
	>15	13
Kotwica and Jakubowski(18)	<15	60
	5-30	48
	>30	24
Lobato et al.(16)	<6	86
	6-15	77
	>15	69
Present study	<10	82
	10-15	33
	>15	14

By calculating, the "Brain Swelling Factor" as the difference between the midline shift and the hematoma thickness, we quantify brain swelling and thus the grade and extent of the induced brain damage. The midline structures are displaced not only by the space occupying subdural hematoma but also by the edematous processes on the same side of subdural hematoma. The edema is an additional space occupying lesion and should be taken into consideration when estimating prognosis.

Zumkeller and et al.[19] recomended that if the hematoma thickness exceeded 18 mm., the survival rate drops below 50%. 50% survival rate is reached when the midline shift is 20 mm. and drops to zero at 28 mm. If the midline is shifted by 3 mm. more than the hematoma thickness, the survival rate is 50%.

REFERENCES

1. Alberico AM, Ward JD, Choi SC, Marmarou A, Young HF: Outcome after severe head injury: Relationship to mass lesion, diffuse injury and ICP course in pediatric and adult patients. J Neurosurg 67:648-656, 1987.
2. Gennarelli TA, Spielman GM, Langfitt TW, Gildenberg PL, Harrington T, Jane JA, Marshall JD, Pitts LH: Influence of the type of intracranial lesion on outcome from severe head injury. J Neurosurg 56: 26-32, 1982.
3. Klun B, Fettich M: Factors determining prognosis in acute subdural haematoma. Acta Neurochir (Wien) 28(Suppl): 134-136, 1979.
4. Kotwica Z, Brzezinski J: Acute subdural hematoma in adults : An analysis of outcome in comatose patients. Acta Neurochir (Wien) 121:95-99, 1993.
5. McKissock W, Richardson A, Bloom WH: Subdural haematoma: A review of 389 cases. Lancet 1:1365-1369, 1960.
6. Haselsberger K, Pucher R, Auer LM: Prognosis after acute subdural or epidural haemorrhage. Acta Neurochir (Wien) 90: 111-116, 1988.
7. Seelig JM, Becker DP, Miller JD, Greenberg PR, Ward JD, Choi SC: Traumatic acute subdural hematoma: Major mortality reduction in comatose patients treated within four hours. N Engl J Med 304:1511-1518, 1981.

8. Greenberg J, Wendy JD, Cohen A,Cooper PR: The "hyperacute" extraaxial intracranial hematoma: Computed tomographic findings and clinical significance. J Neurosurg 17:48-56, 1985.
9. Gardner WJ: Traumatic subdural hematoma with particular reference to the latent interval. Arch Neurol Psychiatry 27: 847-858, 1932.
10. Stone JL, Rifai MHS, Sugar O, Lang RGR, Oldershaw JB, Moody RA: Acute subdural hematoma: Part I-Progress in definition, clinical pathology, and therapy. Surg Neurol 19:216-231, 1983.
11. Wilberger JE, Harris M, Diamond DL: Acute subdural hematoma: Morbidity, mortality, and operative timing. J Neurosurg 74:212-218, 1991.
12. Forbes GS, Sheedy PF, Piepgras DG, Houser OW: Computed tomography in the evaluation of subdural hematomas. Radiology 126:143-148, 1978.
13. Zimmerman RA, Bilaniuk LT, Gennarelli T, Bruce D, Dolinskas C, Uzzell B: Cranial computed tomography in diagnosis and management of acute head trauma. Am J Roentgenology 131:27-34, 1978.
14. Marshall LF, Marshall SB, B.S.N., Klauber MR, Clark MVB: A new classification of head injury based on computerized tomography. J Neurosurg 75:S14-S20, 1991
15. Kuchiwaki H, Inao S, Furuse M, Hirai N, Misu N: Computerized tomography in the assessment of brain shifts in acute subdural hematoma. Zentralbl Neurochir 56: 5-11, 1995.
16. Lobato RO, Rivas JJ, Gomez PA, Castaneda M, Canizal JM, Sarabia R, Cabrera A, Munoz MJ: Head-injured patients who talk and deteriorate into coma. J Neurosurg 75:256-261, 1991.
17. Marshall LF, Toole BM, Bowers SA: The National Traumatic Coma Data Bank: Part 2-Patients who talk and deteriorate: Implications for treatment. J Neurosurg 59: 285-288, 1983.
18. Kotwica Z, Jakubowski JK: Acute head injuries in the elderly: An analysis of 136 consecutive patients. Acta Neurochir (Wein) 118:98-102, 1992.
19. Zumkeller M, Behrmann R, Heissler HE, Dietz H: Computed tomographic criteria and survival rate for patients with acute subdural hematoma. J Neurosurg 39:708-713, 1996.

SMALL BOWEL LEIOMYOMA ; CASE REPORT

Porntip SUPAWONGSE MD.[1] Kosin TRIRUTVIRAPONG MD.[2]

ABSTRACT

Tumour of small bowel, both benign and malignant, are relatively uncommon and often present a diagnostic challenge as their symptoms are often vague and mimic with other diseases of the digestive tract. Here is a case which was suffering from nonspecific chronic abdominal pain for a long time, about 10 months, before operation indicated by gut obstruction. Radiographic studies, UGI, SBFT, BE and CT were performed. Dilatation of proximal jejunum with mucosal edema were demonstrated. No definite cause of obstruction is detected and the contrast media passing through the colon was observed. Intussusception of small bowel with self release was diagnosed.

UGI = Upper G.I.
SBFT = Small Bowel Follow Through Study
BE = Barium Enaema

CASE REPORT

A thai female, 48, first came to the hospital with a chief complaint of melena and abdominal pain. Physical examination revealed good built, 62.5 kg., and stable vital signs but markedly pale was noted. CBC showed Hb 4.7%, Hct 15% with normal morphology and differential count. Blood chemistry and electrolytes were within normal limits. Gastroscopy revealed two hemorrhagic spots at roof of the bulb. Telangiectasia or vascular ectasia was suspected. Double contrast BE and UGI studies were normal. She was treated as peptic ulcer disease and received blood replacement. Bleeding ceased and the patient noticed some improvement.

However she still had abdominal pain, on and off, and noticed that it was aggrevated after get up in the morning until evening but relieved at night. Sometime nausea, vomitting, refered pain to the back and constipation occur. Seven months after the first admission, marked abdominal distension with pain and constipation brought her to the second admission and gut obstruction was diagnosed.

BE study was again normal. UGI with small bowel follow through (SBFT) showed dilatation of the proximal part of small bowel, prominently at jejunum and lessly at duodenum, with edematous wall. Distal small bowel was unremarkable. Transitional zone was visualized without mass, pressure effect or definite cause of obstruction. (Fig. Ia, Ib, Ic) CT study showed normal solid organ and confirmed the finding in SBFT. (Fig. IIa, IIb, IIc) No mass or ascites was detected. Small bowel obstruction with self release was concluded.

Exploratory laparotomy was performed and revealed a well circumscribed small bowel

[1] Division of Radiology , Pranangkloa Hospital , Nonthaburi , Thailand
[2] Division of Surgery , Pranangkloa Hospital , Nonthaburi , Thailand

tumour 1 cm. in diameter, at 1.5 feet from ligament of Treiz. The mass involved through mucosa. The proximal jejunum and the jejunum 2 feet distal from the mass were dilated. The rest of small bowel and colon were normal .

The bowel including tumour and adjacent lymph nodes were resected and end to end anastomosis was performed. Histopathological study of the resected mass was reported as leiomyoma with free margin and lymph node hyperplasia. The patient got well since then.

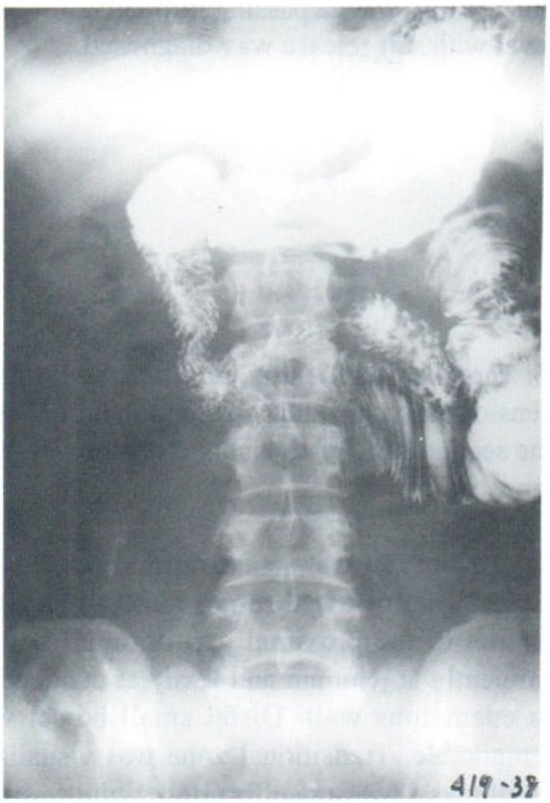

1A

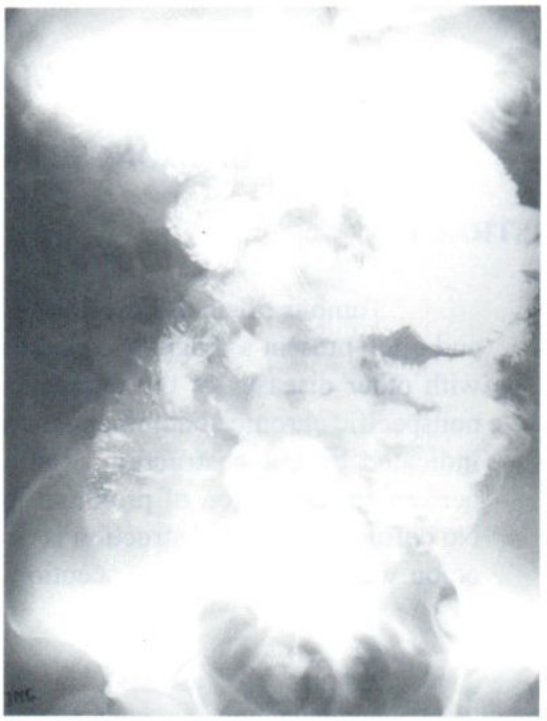

1B

FIG. 1 Small bowel follow through study

1A. 15 min. After intake, slightly dilated C-loop with dilated proximal jejunum

1B. 30 min. Continuous dilated proximal jejunum with mucosal edema, transitional zone noted at midline of lower part of the film, no intraluminal mass or extrinsic pressure effect visualized

1C. 45 min. Normal ileum and colon visualized

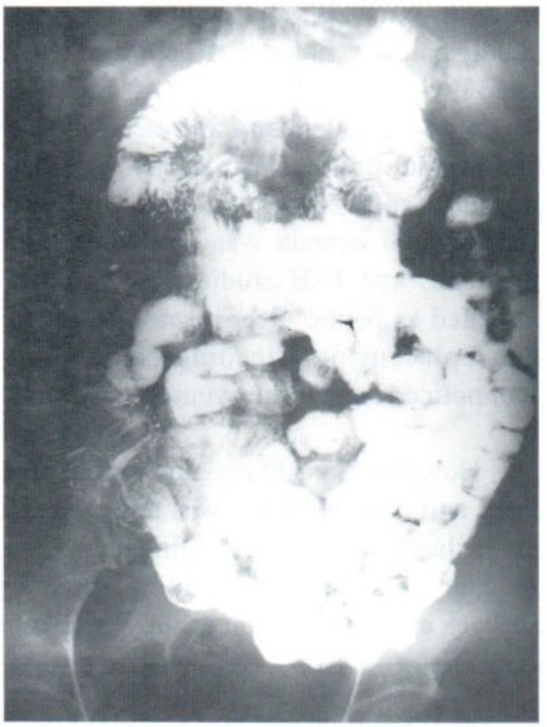

1C

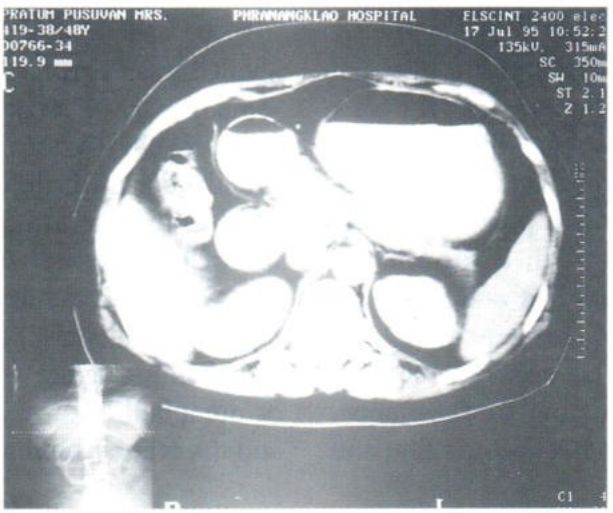

2A

FIG. 2 CT study

2A. Dilated C-loop at pancreatic head level, cross section view

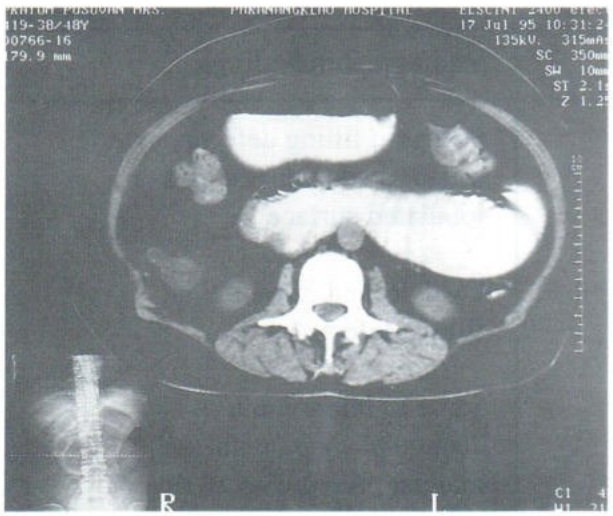

2B

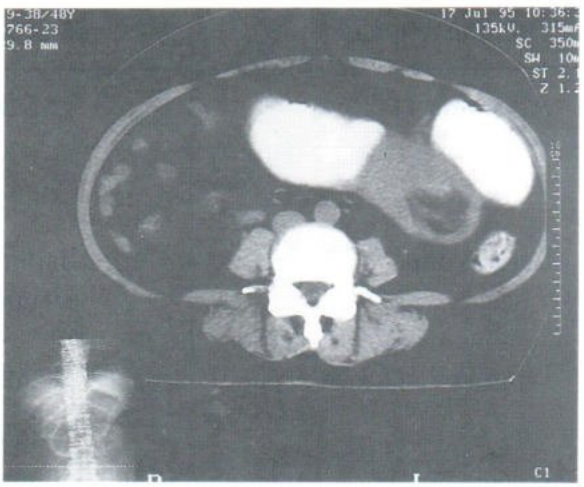

2C

2B. Continuous dilated loop of jejunum with slight mucosal edema

2C. Dilated jejunal loop and nondilated distal small bowel with contrasted filled

DISCUSSION

Neoplasms of small bowel are rare and comprising only 2-5 % of tumours of GI tract[1,3] and much less than that of colon which is said to be about 1: 40[4]. Benign group is found slightly more than the malignant one. It presents to both clinician and radiologist with a formidable diagnostic challenge. Symptoms and signs are often absent, sometime intermittent and nonspecific. There may be poorly localized abdominal pain, vague feeling of flatulence, chronic occult blood loss, bowel obstruction and palpable mass.

Of the benign group, about 90% are adenoma, leiomyoma, lipoma and hemangioma in order of frequency.[5] Adenoma and leiomyoma are about the same frequency in some series.[4] Leiomy -oma is in the first rank when included with those of stomach.[6] Within small bowel, leiomyoma oftenly occurs in jejunum, lessly in ileum and duodenum. The tumour mass oftenly grows out through the serosal layer and causing extrinsic mass effect. Sometimes it occurs in submucosal layer (as in our case) and causing smooth oval or round filling defect. It may pedunculated, bilobed or dumpbell shaped with one part in the lumen and the other protuding out of the serosal.

The tissue histology, frequency, locations and radiographic findings of the common small bowel tumours are shown on table 1 .

Table I ; Differences in locations and radiographic findings of common small bowel benign tumours[3,5]

Tumour/frequency	Locations	Radiographic findings
Adenoma 17-25 %	Duodenum	Polypoid filling defects , usually pedunculated and lobulated surface
Leiomyoma 17 %	Jejunum Ileum	Oval , round intraluminal filling defect
Lipoma 14 %	Ileum	Same as leiomyoma . change of shape with manual pressure on abdomen
Hemangioma 10 %	Jejunum	Intramural or intraluminal round polypoid mass

Accepted clinical indications for small bowel radiography include 1) unexplained GI bleeding, 2) possible small bowel tumour,, 3) small bowel obstruction, 4) Crohn's disease, and 5) malabsorption. Because of the inherent difficulty of visualizing numerous loops of an actively peristaltic bowel a reliable imaging method is needed not only for detection of small or early structural abnormality but also for accurately documented normalcy.The yield of information provided by enterocyclis and its high negative predictive value suggested that it should be a primary method for small bowel examination.[1] However, many radiologist prefer overhead -based conventional small bowel follow through as it is easier to perform and causing less discomfort to the patient particularly in the presence of bowel obstruction. The study may reveal only secondary changes of obstruction such as bowel dilatation and wall edema as in this case. Small mass effect, filling defect or transitional zone may be masked by overlapping loops. Sometime transitional zone shows nothing if intussusception is the cause of obstruction and the tumour is the leading point, as the mass should be localized in the dilated part

CT can be a useful test for evaluation of small bowel obstruction and can reveal both the diagnosis of obstruction and its differentiation from other conditions resulting in small bowel dilatation. Some specific criteria were proposed to indicate obstruction i.e. 1) the presence of continuous bowel dilatation, 2) the presence of prestenotic dilatation, and 3) the identification of transitional zone between normal and abnormal dilated part. Intermittent dilatation of small bowel, dilatation of large bowel, mucosal edema and bowel fluid more than 50 %, are nonspecific and could be found in nonobstructive group as well.[2]

Angiography is sometime helpful in demonstrating small intestinal leiomyomas, even if performed at a time when the patient is not in active bleeding. These tumours are often hypervascular and show intense opacification during the capillary phase of the injection, and there may be early opacification of large mesenteric veins draining the tumour.[5]

In this case, continuous bowel dilatation and mucosal edema were demonstrated in both SBFT and CT studies without definite identification of tumour mass. Furthermore flow to colon was shown in SBFT study. So only one specific criteria by Gaselle,[2] continuous bowel dilatation, was fitted to indicate obstruction. As correlate to clinical symptoms, the patient was likely suffered from intermittent intestinal intussusception with self release. As we know, small bowel tumour is a common cause of intestinal intussusception in adult and elderly .

CONCLUSION

Leiomyoma of small bowel is a rare disease, occuring in late adult or elderly and often undiagnosed because there are usually symptomless or only vague nonspecific abdominal symptoms. Sometime it would take a long time before we can make a diagnosis. With prolonged abdominal pain, GI bleeding or bowel obstruction the condition should be kept in mind and investigation should be performed. Enterocyclis is proposed to be the primary test to be obtained. SBFT should be an alternative study if enterocyclis is not possible. CT should follow as a complimentary study and for evaluation of situations of other organs. Sometime definite diagnosis of tumour cannot be concluded before operation and histologic study .

REFERENCE

1. Maglinte DDT, Kelvin PM, O'Conner K., Lappas LC, Chernish SM ; Current status of small bowel radiography (Review), Abdominal imaging (3) : 247-257,1996 May-Jun.
2. G-Scotte Gaselle, Mark A. Goldberg, Jack Wittenberg, Elkan F. Halpern, Lynne Pinkney, Peter R. Mueller : Efficacy of CT in distinguishing small-bowel obstruction from other cause of small bowel dilatation AJR 1994;162;43-47.
3. Shearman David JG : Disease of gastrointestinal tract and liver 1989;439-440
4. Courtney M. Townsend, Jr. , Jame C. Thompson ; Schwartz Principle of surgery; 6th edition; 1994,1170-1178
5. Robert E. Kochler, Alexander R. Margulis; Alimentary tract radiology 3rd edition; 1979 , 962-965
6. Mendes da Costa P., Beernaert SA, Benign tumour of upper gastrointestinal tract (stomach, duodenum, small bowel) ; a review of 178 surgical cases ; Belgian multicentric study Acta Chirurgica Belgica; 1993 , Mar.- Apr. , 93(2):39-42

COMPUTED TOMOGRAPHY IN RETINOBLASTOMA : CT AND HISTOPATHOLOGICAL CORRELATION

Pipat CHIEWVIT, M.D., Sa-nga PATTHAMARUEDEE, M.D., Orasa CHAWALPARIT, M.D., Anchalee CHUROJ, M.D., Suthisak SUTHIPONGCHAI, M.D.

ABSTRACT

Computed Tomography (CT) scan is a valuable adjunct in the differential diagnosis and management of retinoblastoma. Retrospective study of the known retinoblastoma patients with CT scans performed prior to therapy between January 1994 - December 1996 are studied.

18 of 24 Retinoblastoma patients study with CT scan had intraocular calcification demonstrated in at least one eye. 100% of tumors in this study showed evidence of calcification that help much in the diagnosis of retinoblastoma especially in patients under three years old who account for 87.5% of patients. In addition, orbital and brain CT scan performed in all patients are useful in the diagnosis of retrobulbar extension, intracranial seedling, including brain metastasis. Intraparotid gland metastasis in one case, which has no report in any literature, is also found in this study.

INTRODUCTION

Retinoblastoma is the most common intraocular malignant tumor in children. The tumor usually arises from the inner retinal layers and extends as a fleshy nodular mass in the vitreous cavity. The most common route of extraocular extension is along optic nerve, and extension into retrobulbar space or into subarachnoid space. Detection when the disease is confined to the globe is of utmost importance for local control.[1] It is sometimes difficult to diagnose due to a variety of simulating lesions such as coat's disease, primary hyperplastic primary vitreous (PHPV), toxocariasis. Retinal detachment associated with retrolental fibrosis, retinopathy of prematurity must be excluded. To serve this purpose, knowing that the DNA released from necrotic cells in retinoblastoma having a propensity to form a DNA - Calcium complex is usually detected in approximately 95% of histologically examined retinoblastoma.[2] Among the diagnostic tools, CT scan is one of the diagnostic tools that is sensitive in the detection of calcification. Therefore, role of CT in the detection of intraocular calcification and diagnosis is obvious. Not only for detecting the intraocular calcification but also for delineating the retroorbital extent of the tumor and determining if the optic nerve is involved or if there is an intracranial extension when the CT scan is indicated.

MATERIALS AND METHODS

- Twenty four patients (13 males and 11 females) with histopathologically proven to be retinoblastoma with thin section CT scan performed prior to therapy between 1994 and 1996

Department of Radiology, Siriraj Hospital, 2 Prannok Road, Bangkok 10700.

were studied. In these cases, 2 mm. contiguous axial scans are obtained through orbits, with thicker sections through the rest of the head.

- Eighteen of the 24 patients had unilateral involvement and 6 had bilateral tumors. The patients' ages ranged from 2 months to 5 years, with a mean of 2.1 years. All patients with unilateral retinoblastoma had their affected eyes enucleated as well as patients with bilateral retinoblastoma had both eyes enucleated. All enucleated eyes were examined histologically.

- By correlative study of the histopathological findings and the image findings from CT scan, we tried to determine the accuracy of CT scan in the detection of intraocular calcification, uveal-scleral tissue involvement, optic nerve involvement, and extraocular extension. In addition, benefits of CT scan in the detection of intracranial metastasis is also documented.

RESULTS

Among 24 patients, 6 patients enucleated from other hospital with no available preoperative CT scan were excluded from this study. Therefore, 18 patients (21 eyes of retinoblastoma) had been studied.

All 18 patients (21 eyes) showed intraocular calcification from CT scan. The patterns of calcification are varied as single and small (Fig. 1A), single and large (Fig. 1B) or multiple and punctate (Fig. 1C). (Table 1)

The choroidal invasion were studied by using the criteria of irregularity, thickness of the uveal - scleral tissue more than 2 mm. (Fig. 2). However, the accuracy in the detection is quite low about 52% accuracy. (Table 2)

Table 1 Intraocular calcification

		Pathological findings	
		positive	negative
CT findings	positive	21	0
	negative	0	0

Table 2 Uveal - scleral involvement

		Pathological findings	
		positive	negative
CT findings	positive	9	8
	negative	2	2

Table 3 Retrobulbar involvement

		Pathological findings	
		positive	negative
CT findings	positive	2	0
	negative	0	19

Table 4 Optic nerve involvement

		Pathological findings	
		positive	negative
CT findings	positive	7	0
	negative	4	10

In contrary to the choroidal invasion, the detection of retrobulbar involvement is easily detectable from the evidence of mass that replaced normal retrobulbar fat space (Fig. 3). In our study the accuracy is 100% (Table 3). The optic nerve involvement is demonstrated by CT scan by observing of the enlargement of the optic nerve and/or perioptic enhancement (Fig. 4). Those findings are 83% accuracy (Table 4). Four patients had microscopical evidence of tumor spread past through the lamina cribosa of optic nerve and not reaching the transsection line. This was not detected by CT scan. There were five patients (22%) who had intracranial spreading of tumor. They presented in a normal pattern of CSF spreading with or without hydrocephalus in four cases and an unusual pattern as intraparenchymal mass in one patient (Fig 5, 6). In addition, two patients of those intracranial spread had MRI spines work up for the evaluation of intraspinal metastases. Both of them are positive for intraspinal metastases by the MRI findings which are clearly demonstrated in sagittal post gadolinium contrast study (Fig 7, 8). Moreover, there was a patient who had bilateral retinoblastoma with a subsequent right parotid gland metastasis (Fig. 9). No patient had an evidence of pulmonary metastasis. Only one patient had bony metastasis that involved long bone of lower extremity (Fig. 10).

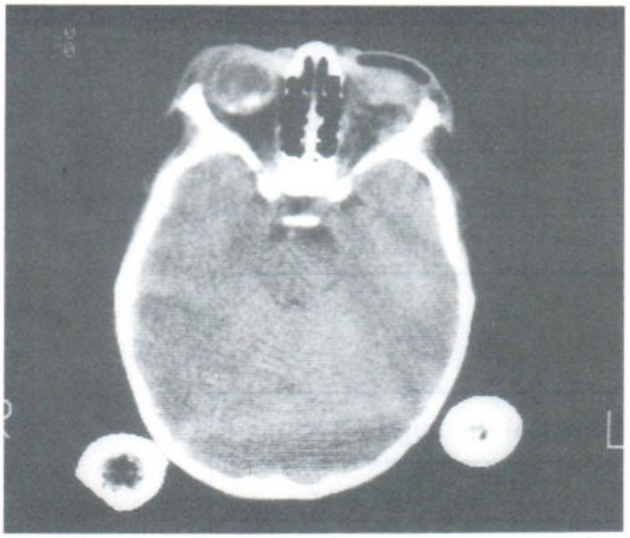

1A

Fig. 1A. This is a case of bilateral retinoblastoma scanning post enucleation of the left eye. The tumor calcification in the right eye is small in size.

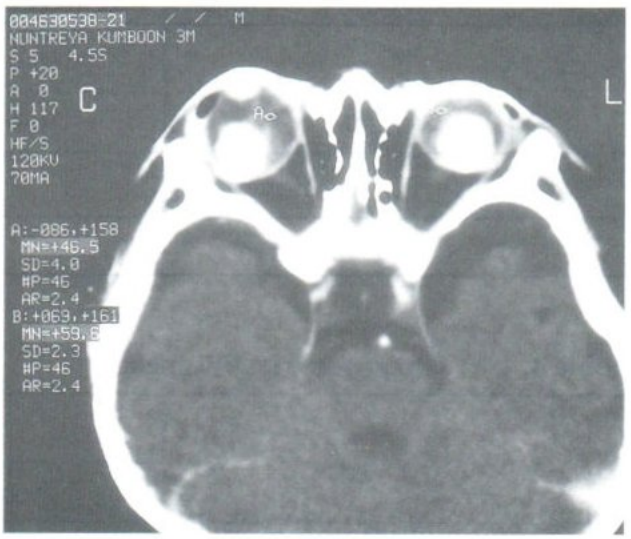

1B

Fig. 1B. This is a bilateral retinoblastoma patient which has a large single tumor calcification pattern.

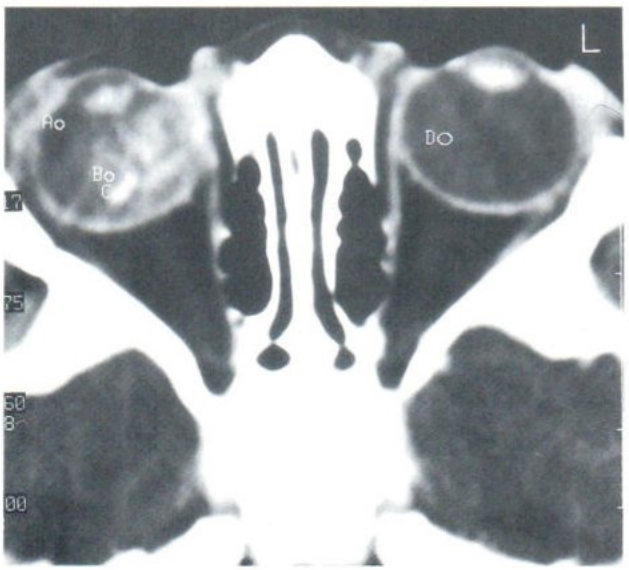

1C

Fig. 1C Multiple punctate intraocular tumor calcification is a pattern of calcification in retinoblastoma.

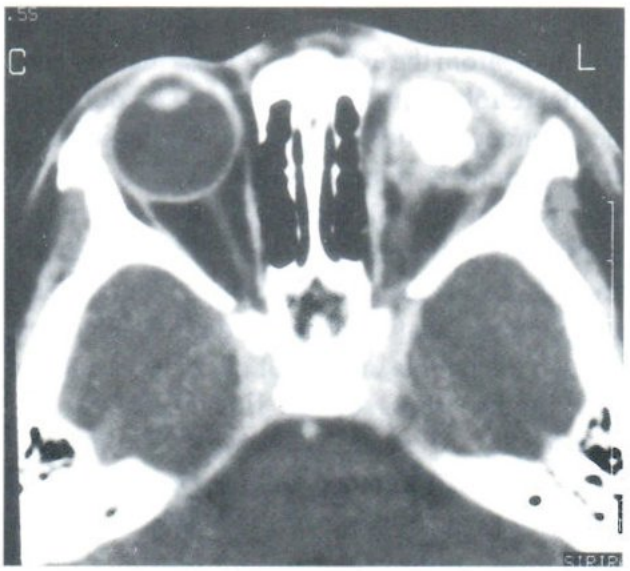

Fig. 2 This is a unilateral retinoblastoma with uveal-scleral tissue invasion. CT depicted as irregular, nonuniform thickening of ocular wall of left eye.

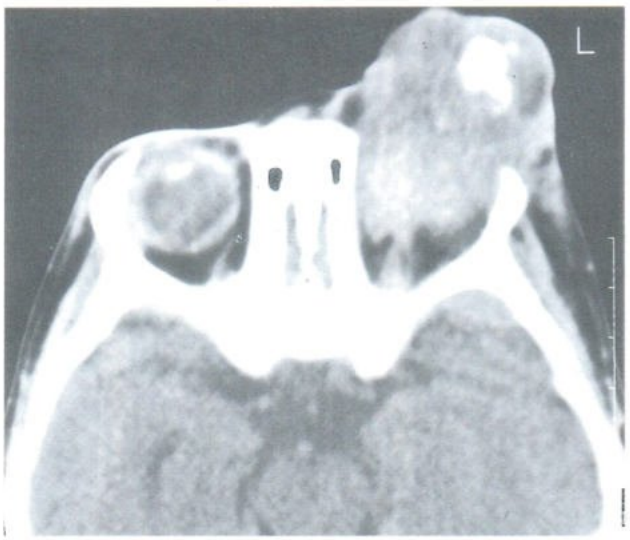

Fig. 3 Unilateral retinoblastoma in left eye with extraocular extension especially retro-bulbar spread

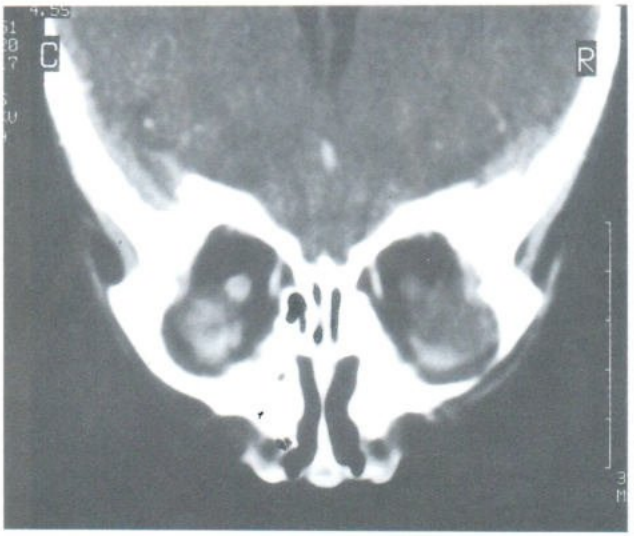

Fig. 4 Contrast enhanced CT brain study in coronal plane reveals asymmetrical enlargement, enhancement of the left optic nerve in a case of retinoblastoma left eye which is suggestive of tumor extension along the optic nerve.

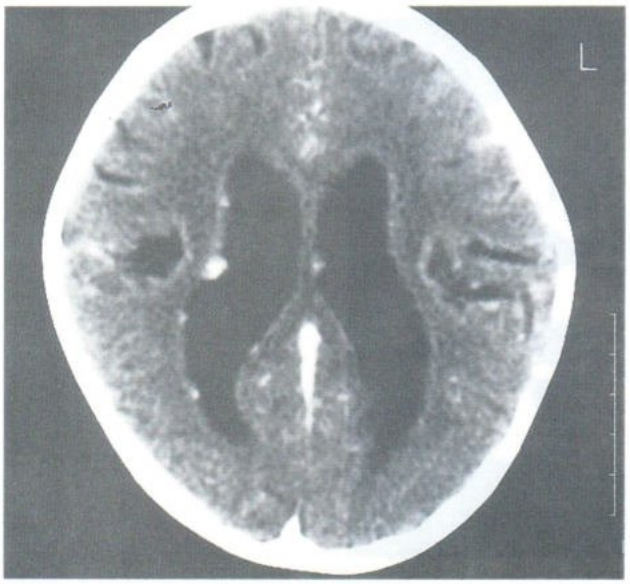

Fig. 5 Contrast enhanced CT brain scan shows multiple ependymal nodules seedling with increase enhancement along the venticular wall and leptomeninges linining of the brain (an example of CSF seedling).

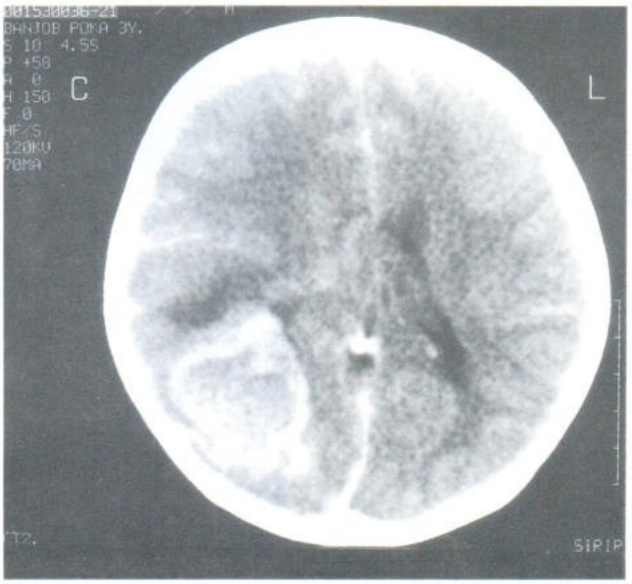

Fig. 6 Contrast enhanced CT brain scan in a known bilateral retinoblastoma, reveals intrapa-renchyma brain metastasis in the right temporo-occipital lobe.

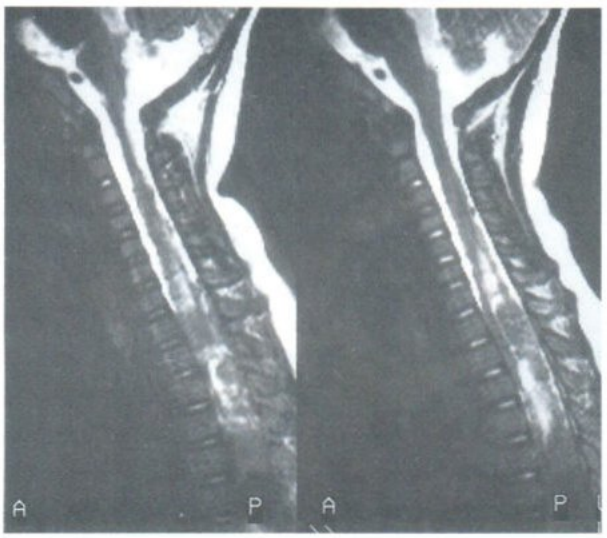

Fig. 7 MRI of cervical spines in bilateral retinoblastoma shows intramedullary metastais of cervical cord.

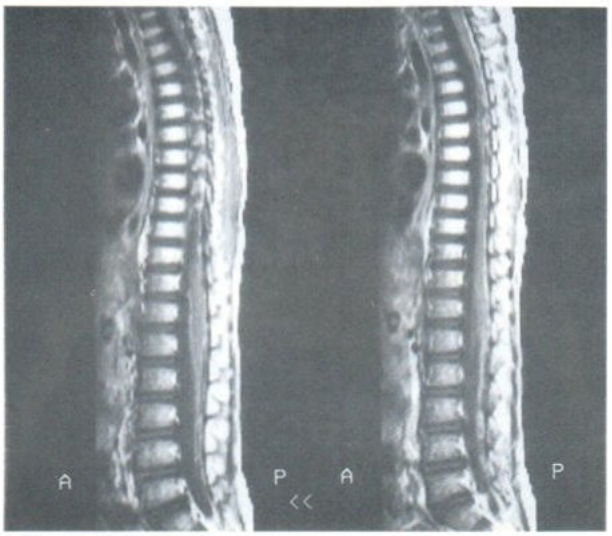

Fig. 8 Gadolinium enhanced MRI of lumbosacral spines showed an abnormal increase enhancement of the dural lining of spinal cord suggestive of tumor seedling along CSF space.

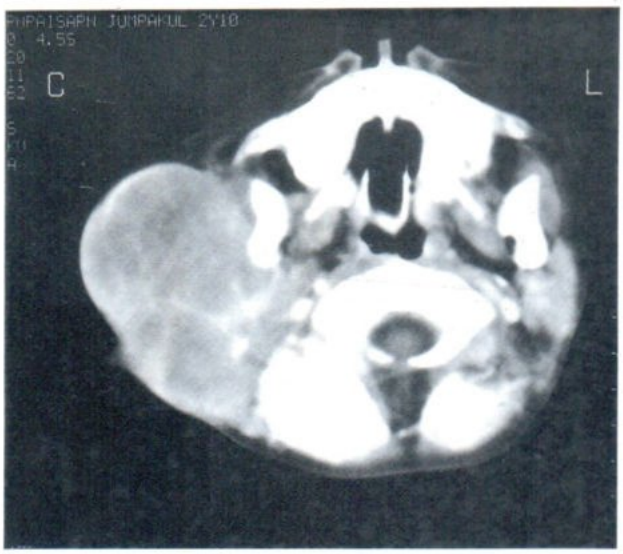

Fig. 9 Contrast enhanced CT study reveals asymmetrical enlargement of the right parotid gland, biopsy proven to be retinoblastoma metastasis.

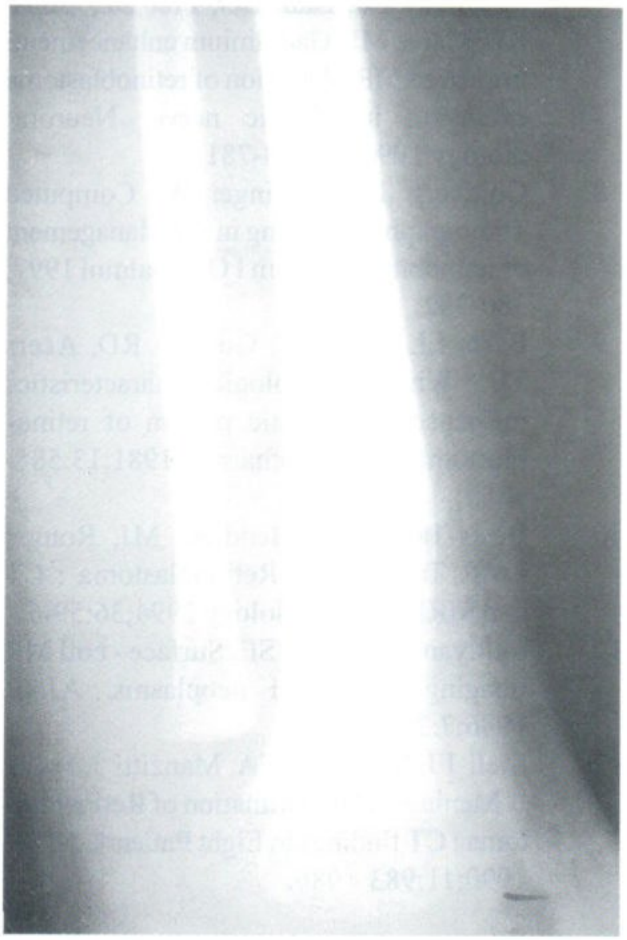

Fig. 10 Plain radiography of the leg in retinoblastoma patient reveals metastatic bone destruction involving anterior aspect of proximal tibia with overlying soft tissue swelling.

DISCUSSION

Computed Tomography can detect calcification within retinoblastomas with a high degree of accuracy. The presence o absence of calcification on the CT examination of the eyes of a patient less than three years of age is an important finding in the diagnosis and the differentiation from other simulating lesions. None of the simulating lesions including optic nerve head drusen, retinal astrocytoma, choroidal hemangioma with previous hemorrhage, choroidal osteoma, toxocariasis, persistent hyperplastic primary vitreous, Coat's disease, retinal dysplasia or trauma tend to contain calcification in the age group (0-3 years) in which retinoblastoma is usually diagnosed.[3-6] Our study confirms the usefulness of the computed tomography in the detection of intraocular calcification with high accuracy as well as the retrobullar extension. The accuracy of optic nerve involvement is quite satisfactory. However, to improve accuracy, MRI (Magnetic Resonance Imaging) with Gadolinium enhancement may be helpful.[7] In term of choroidal invasion, it is very difficult for CT scan to evaluate whether choroidal invasion is present in case of no extraocular extension. It is a fact that the posterior ocular wall composed of retinal, choroidal and scleral layer from inner to outer wall respectively. These structures are not more than 2 mm. in thickness. We attempt to evaluate the tumor invasion by a criteria of asymmetry and/or focal thickening of ocular wall. However, the accuracy is not satisfactory. This could be a limitation of the CT. The other advantages from CT study in the evaluation of the intracranial metastasis are reported.[8,9,12] Our study confirms previous studies,[8,9] in this issue. There are four cases of intracranial metastases, some of these show intraparenchymal metastases. Two of them have intraspinal spreading. In addition, our study shows a patient with bilateral retinoblastoma after enucleation of both eyes coming with right parotid gland metastasis. This was proven by histological section and was an example of lymphatic metastasis. In this decade, eventhough MRI (Magnetic Resonance Imaging) also plays role in the diagnosis of intraocular lesions. We agree with other authors[10,11] suggesting that MRI was not as specific as CT for the diagnosis of retinoblastoma. The superiority of the MRI to CT scan is the ability in the differentiation of Coat's disease from retinoblastoma and subretinal fluid from tumor.[10] We believe that CT is still the method of choice in the diagnosis of retinoblastoma, but when equivocal arises, MRI should be performed for a better differentiation from other

lesions such as Coat's disease[10] and for the improvement of the detection of optic nerve extension.[7]

REFERENCES

1. Donaldson SS, Smith LM. Retinoblastoma : Biology, presentation and current management. Oncology 1989;3:45-52.
2. Bullock JD, Campbell RJ, Waller RR. Calcification in retinoblastoma. Invest Ophthalmol Visul Sci 1977;16:252-255.
3. Hedges TR III, Pozzi - Mucelli R, Char DM, Newton TH. Computed tomographic demonstration of ocular calcification ; correlation with clinical and pathological findings. Neuroradiology 1982;23:15-21.
4. Brant - Zawadzki M, Engmann DR. Orbital computed tomography : Calcific densities of the posterior globe. J Comput Assist Tomogr 1979;3:503-5.
5. Goldberg MF, Mafee M. Computed tomography for diagnosis of persistent hyperplastic primary vitreous (PHPV) Opthalmology 1983;90:442-51.
6. Char DH, Hedges TR, Norman D. Retinoblastoma : CT diagnosis. Ophthalmology 1984;91:1347-1349.
7. Ainbinder DJ, Haik BG, Frei DF, Gupta KL, Mafee MF. Gadolinium enhancement: Improved MRI detection of retinoblastoma extension into optic nerve. Neuroradiology 1996;38:778-781.
8. Goldberg L, Danzinger A. Computed Tomographic scanning in the Management of retinoblastoma. Am I Ophthalmol 1997; 380-382.
9. Basta LL, Israel W, Gourley RD, Acers TE. Which pathologic characteristics influence echographic pattern of retinoblastoma. Ann Ophthalmol 1981;13:585-588.
10. Beets-Tan RGH, Hendriks MJ, Romos LMP, Tan KEWP. Retinoblastoma : CT and MRI. Neuroradiology 1994;36:59-62.
11. Sullivan JA, Harms SE. Surface - coil MR imaging of orbital neoplasms. AJNR 1986;7:29-34.
12. Meli FJ, Boccaleri CA, Manzitti J, Lylyk P. Meningeal Dissemination of Retinoblastoma : CT findings in Eight Patients. AJNR 1990;11:983 - 986.

TREATMENT OF HEPATOCELLULAR CARCINOMA BY INJECTION OF IODINE*131 LABELLED LIPIODOL INTO HEPATIC ARTERY.

PRABHASAVAT Krisdee, KRUATRACHUE C., CHAITEERASUWET S., DANPUKDEE K., VANAPRUKS S., TONGDEE T., PLEEHACHINDA R., PUSUWAN P., BURANAPONG P., CHAUDAKSHETRIN P., MANATHATHIT S.*, SOMCHITPRASERT P.,

ABSTRACT

Purpose: To study therapeutic efficacy of iodine*131 labelled Lipiodol in the treatment of hepatocellular carcinoma (HCC). The results of the treatment were evaluated in 4 aspects, 1 size of the tumor, 2 serum alphafetoprotein level 3. the quality of patient's life, and 4 the survival rate.

Materials and methods. The hepatocellular carcinoma was diagnosed by evidence of mass in the liver by computed tomography or ultrasonography with tissue biopsy and/or high level of alphafetoprotein more than 500 U. 20 patients were randomized into 2 groups for comparison. The patients in group A were treated by intrahepatic injection of iodine*131 labeled Lipiodol 60 miliCuries (mCi). The patients in group B were treated by intrahepatic injection of mixture of Lipiodol and chemotherapeutic agents, mitomicin c 20 mg., and 5-fluouracil 500 mg. and followed by selective hepatic artery embolization of small pieces of gelatin sponge (gelfoam). Both groups were evaluated by computed tomography (CT) and possible repeating treatment protocol in 2 months.

Results. There was no serious side-effect or major complication in both groups of patients. The patients' conditions got worse by 40% in both groups. The tumors' sizes remained unchanged by 50% in both groups. The serum alphafetoprotein levels had increased by 40% in group A, and remained unchanged by 50% in group B.The survival rate at 1 and 2 years in group A were 20%, 20%, and in group B were 30%, 0%, respectively.

Conclusion Satisfactory results were obtained in the treatment of a small HCC, size less than 5 cm. with intrahepatic artery injection of iodine*131 labeled Lipiodol. In the large HCC (>10cm) there was no response of the tumor in both groups. This was the first study performed in Thailand.

Introduction Hepatocellular carcinoma (HCC) is one of the most common malignant tumor in the Thai population, especially in the male patients. The incidence in Thailand are 36 cases/100,000/year in male, and 14 cases/100,000/year in the female

Department of Radiology and Nuclear medicine
Department of Medicine* Faculty of Medicine, Siriraj Hospital Mahidol University, Bangkok, Thailand.

population. There are several risk factors for the Thai people; hepatitis B and C, represented 10% of the population or around 6 millions people. Cirrhosis, food additives, toxins, parasitic infestation, etc. are included in the causative agents of the tumor. Today, HCC can be found in the younger age group, 20-40 years, who are active working - people. Furthermore, most of the patients came to see the doctor, when they had already been in advanced and late stages. This was because there were no symptoms yet when the sizes of the HCC in the liver were small. So the sizes of the HCC in the patients were often larger than 10 cm and/or there were vascular invasion, and they were unresectable. Although the tumor was small, surgical resection was often not indicated because the liver had already got advanced cirrhosis, multiple focalities, or vascular portal vein invasion.

For the treatment of the unresectable HCC, systemic chemotherapy, ligation of hepatic artery, and now - a -day, trans-catherized arterial oily chemoembolization (TOCE) were used. Nakakuma found that an oily contrast medium, Lipiodol used for contrast lymphagiograms injected through hepatic artery was selectively retained in HCC. The computed tomography (CT) performed after TOCE showed that the small droplets of lipiodol remained in the tumor vascular bed for months. Furthermore, Lipiodol has been used as a carrier for therapeutic agents in chemotheurapy for HCC. Lipiodol is an ethyl ester of poppy seed oil fatty acid that contains 38% stable iodine127 by weight. By exchange method, labeling of Lipiodol with radioactive iodine 131(I*131) can be achieved. Intrahepatic artery injection of Lipiodol-I*131 showed a high tumor to nontumor ratio and longer effective half life in the vascular HCC than the normal hepatic parenchyma. One reason is that HCC was mainly supplied by hepatic artery. There were many reports of therapeutic trial of internal radiation therapy for HCC with this Lipiodol-I*131.

The purpose of this study is to evaluate and compare the therapeutic efficicacy between Lipiodol-I*131 and TOCE, in the treatment of HCC in 4 aspects, 1. the size of the tumor, 2. serum alphafetoprotein level, 3. quality of life and 4. survival rate.

Our project study was approved by the ethical committee of Faculty of medicine, Siriraj hospital, Mahidol University and research fund from Faculty of Medicine Siriraj Hospital.

MATERIALS AND METHODS

Patients: There were 20 patients,19 were male, and only 1 was female. The patients were 28 to 72 years old, average 46 years old. All of them had evidences of mass in the liver, by computed tomography (CT), or ultrasonography (US). The diagnosis of HCC was confirmed by tissue biopsy, with pathological diagnosis and/or serum alphafetoprotein was greater than 500 units. The patients were randomized and divided symmetrically into 2 groups, A and B.

MATERIALS

Lipiodol is an oily contrast medium used

in lymphangiography. It is a lipid compound derived from or ethylester of poppy seed oil. It contains stable iodine 127, 38% by weight. One dose of Lipiodol is 10-15 ml depending on the volume of HCC. When injected into the hepatic artery, it is selectively retained in the HCC for more than 2 months.

Lipiodol-I*131, its trade name is "Lipiocis". It was manufactured by CIS biointernational company in France. One dose of Lipiodol-I*131 contains radioactive I*131,60 miliCurie (mCi) or 2220 MBq. The radioactive I*131 emits 2 kinds of radiation , A. electron emission or beta rays, with the main energy of 0.61 Mev, B. photon emission or gamma rays, with the main energy of 0.36 Mev. The physical half life of I*131 is 8 days. So after Lipiodol-I*131 was manufactured, it was sent directly and immediately by airplane to the hospital. After injection into the hepatic artery, the biological half life is 5 days.

METHODS

Treatment protocol

Enrolled patients
↓
confirm diagnosis by tissue pathology or alphafetoprotein>500 u.
↓
interviewing and consent
↓
randomized grouping
↓

group A	group B
Rx Lipiodol I*131	Rx TOCE
↓	↓
Evaluation by clinical examination, CT, and blood exam.	
↓	↓
repeat Rx (2 months interval)	repeat Rx

↓
follow up, and medical supportive Rx

IN GROUP A,LIPIODOL-I*131

The hepatic angiography was performed, by Seldinger's technique via femoral artery approach. The cobra 4 or 5 French size catheter was selected inserting into the subsegmental branch of hepatic artery that supply to the HCC, then the patient was moved from angiographic room to cancer ward ,for radiation protection reason. The Lipiodol-I*131 2ml,or radioactivity 60 mCi ,in the leaded protected glass syringe was slowly injected by radiologist into the HCC via catheter. After injection, the patient was on his bed, where there were lead-shield blocks around the patient's bed, for 24 hours, and was in an isolated radiation protective room for 6 days (figure 1a,1b). There was monitoring for radiation exposure recorded during, and after injection procedure.

Fig. 1A. **1A**
Showing the lead shield syringe.

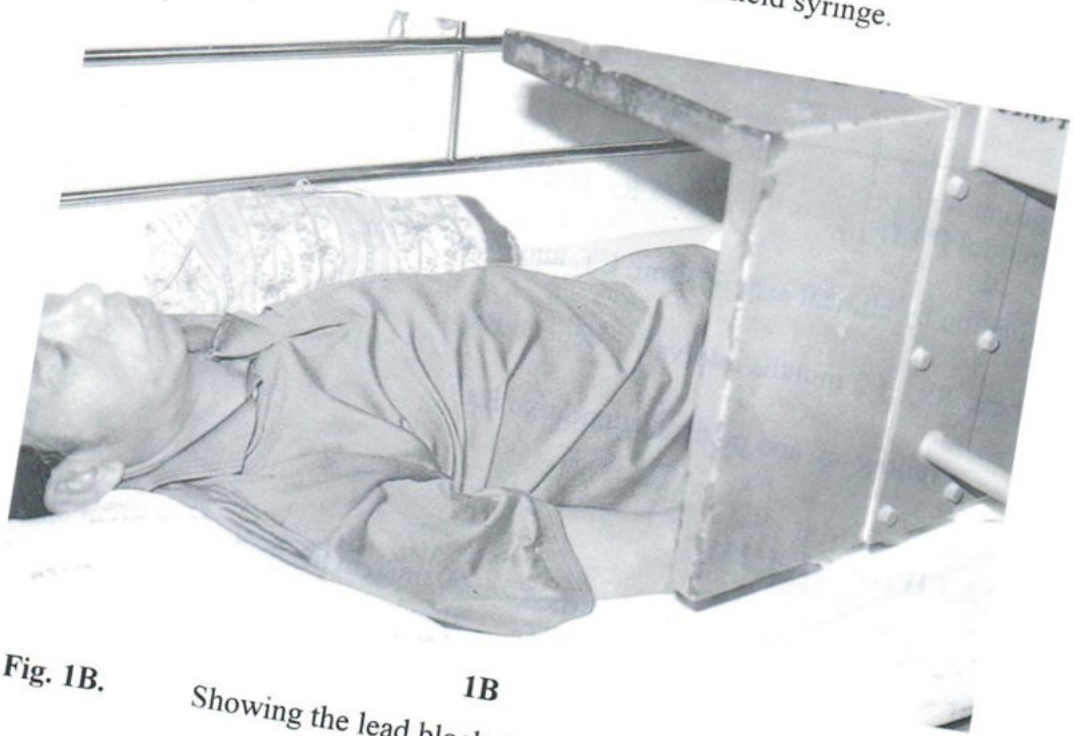

Fig. 1B. **1B**
Showing the lead block around the abdomen of the patient.

IN GROUP B,TOCE

The hepatic angiography was performed, by Seldinger's technique. The 3 to 5 French size catheter was selected inserting into the sub segmental branch of hepatic artery that supply to HCC. We mixed 5 ml of Lipiodol and mitomycin C 20 mg solution, and another 5 ml of Lipiodol and 5 fluorouracil 500 mg solution. The suspension were pushed to and fro between 2 syringes and 3 ways stop cock so as to turn the two suspensions into a fine droplets of oil suspension. Then we injected the oil mixtures into the sub segmental branch of hepatic artery feeding HCC via catheter. After that, if the patient had normal portal vein, we embolized the branch of hepatic artery with small pieces of gelfoam(size 0.5 mm.), or gelatin sponge.

Evaluation. The patients in both groups were evaluated by complete clinical examination, every 2-4 weeks, with computed tomography of abdomen, chest film, complete blood examination, complete blood count, liver function test,and alphafetoprotein level, in every 2 months. All of the patients also had medical supportive treatment. And in the Lipiodol-I*131 group, gamma camera scintigraphy of the whole body was performed, in the first 1-2 weeks ,after injection of Lipiodol -I*131.

RESULTS

The data of both groups were as the followings **(table 1).**

	A,Lipiodol-I*131	B,TOCE
1. patients	9 male,1 female	10 male
2. ages	32-59 ,mean=47	28-72, mean=45 years.
3. virus hepatitis B	2	6 cases
4. Okuda*classification stage 1: 2 : 3	6 : 4 : 0	4 : 6 : 0 cases
5. tumor sizes <5 : 5-10 : >10 cm.	1 : 4 : 5	2 : 4 : 4 masses
6. location of tumors both lobes: right : left lobes	3 : 7 : 0	2 : 8 : 0 lobes
7. alphafetoprotein levels	3.2-204800	6.2-1050 units
8. portal vein thrombosis	3	3 cases
9. number of treatment injections	1 injection for 6 2 injections for 1 3 injections for 3	1 injection for 4 cases 2 injections for 2 cases 3 injections for 1 cases 4 injections for 1 case 5 injections for 1 case 6 injections for 1 case

* Okuda's classification for cirrhosis :
Signs
a. serum albumin <3 gm.%
b. total bilirubin >3 mg.%
c. ascites
d. tumor size is greater than 50% of the liver volume.
Stage 1 have none of these signs.
Stage 2 have one, or two signs.
Stage 3 have more than two signs.

After the patients were treated by injection of Lipiodol-I*131,and TOCE ,as in the protocol, the results were

1. Immediate results

1.1 For the group of Lipiodol-I*131 treatment. The patients were observed for possible side effect, but neither symptoms nor change of vital signs developed after injection of radioactive Lipiodol-I*131.Patients'compliant of slight abdominal pain in the area of the liver, and mild fever developed within few days after injection. There were 3 cases of low grade fever, and 4 cases of mild abdominal pain, no evidence of leukopenia or gastro-intestinal complication.

1.2 For the TOCE treatment group ,there were 2 cases of low grade fever, 4 cases of mild abdominal pain, and two cases of nausea, vomiting, but no evidence of leukopenia was noted.

2. As for the patient condition , a period after the treatment in the Lipiodol-I*131 group, there were improvement in 3 cases, no changes in 3 cases and getting worse in 4 cases. In the TOCE group, there were improvement in 3 cases, no changes in 3 cases and getting worse in 4 cases.

3. For the tumor sizes, in the Lipiodol-I*131 group, there were decreasing size in 3 cases, unchanging size in 5 cases and increasing size in 2 cases.

In the TOCE group, the tumor sizes a showed a decreasing size in 2 cases, unchanging in 4 cases and increasing in 3 cases.

4. About the portal vein thrombosis, the patients in both Lipiodol-I*131 and TOCE groups showed no change of portal vein thrombosis, after treatment.

5.The alphafetoprotein level, in the Lipiodol-I*131 group, the ratio of increasing : unchanging :decreasing was 4:3:3,while the TOCE group was 3:4:3.

6.The survival rates :In Lipiodol-I*131 group there was 20% survival rate in 12 months and 20% in 24 months.

In the TOCE group there was 30% survival rate in 12 months, and 0% in 24 months. The results of treatment of both groups were summarized as shown in the table 2.

Table 2.

The results after treatment	Lipiodol-I*131	TOCE	
Patient conditions			
improve:no change:worse	3:3:4	3:3:4	cases
Tumor size			
decrease:no change:increase	3:5:2	3:4:3	cases
Portal vein thrombosis			
no change	3	3	cases
AFP level			
increase:no change:decrease	4:3:3	3:4:3	cases
survival rate at			
1 year	20%	30%	
2 year	20%	0%	

Table 3. survival rate curves.

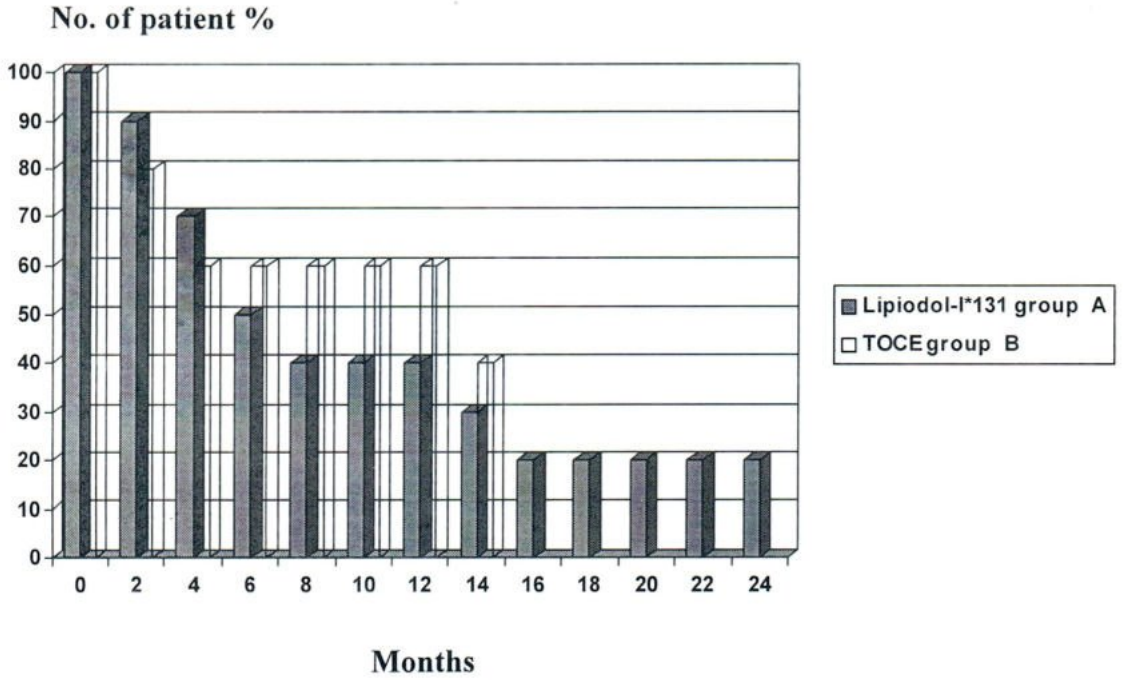

CASE REPORT

Lipiodol-I*131 treatment group

Case 1.This was the first case in Thailand who was treated by this drug. The patient was a Thai male, aged 50 years old. He had abdominal pain and weight loss for 2 months. The physical examination showed mild hepatomegaly, without ascites. The computed tomography of abdomen showed that there was a mass, sized 5x6x5 cu.cm. in the right lobe of the liver. The portal vein was patent.(figure 2a).The laboratory findings showed serum albumin at 4.7 mg%, total bili- rubin 1.3 mg% and alphafetoprotein was 63.9 ng/ml. The pathology of liver biopsy was hepatocellular carcinoma(Okuda class 1).He was admitted in Siriraj hospital for the treatment by injection of Lipiodol-I*131 into hepatic artery. The celiac angiography showed to have hypervascular mass about 5 cm. in size, with tumoral staining in the right lobe of the liver. The portal vein was normal.(figure 2b). Then, a subsegmental branch of right hepatic artery was selected to be inserted with 5 French catheter, and 1 dose of Lipiodol-I*131(2 ml,60 mCi) was injected into the HCC via right hepatic artery. After that he was admitted in the radioprotection ward for 1 week. The injection of Lipiodol-I*131 was performed, within 2 months interval for 3 times. After the first Lipiodol I*131 injection ,6 months later the HCC size had reduced to 2x3 cm. or about 75% reduction by volume (figure 3a-b).The patient's general condition was also improved, and he gained weight for 5 kgs. At that time, he was still alive for 24 months after treatment, the size of primary tumor was smaller and the primary tumor HCC was well controlled. But there was an evidence of right adrenal metastasis, after 2 years.

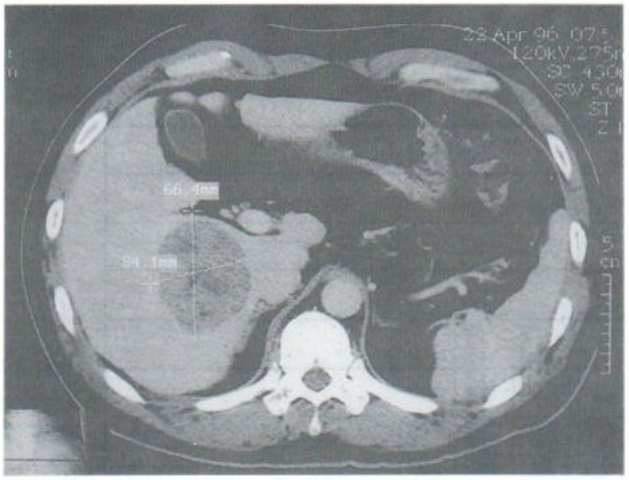

2A

Fig. 2A. The computed tomography of abdomen showed low density heterogenous mass, or HCC, size 5 cm. in the right lobe of the liver.

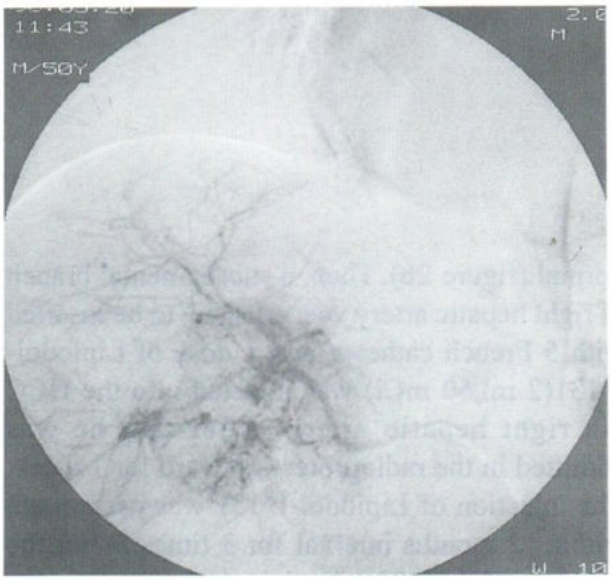

2B

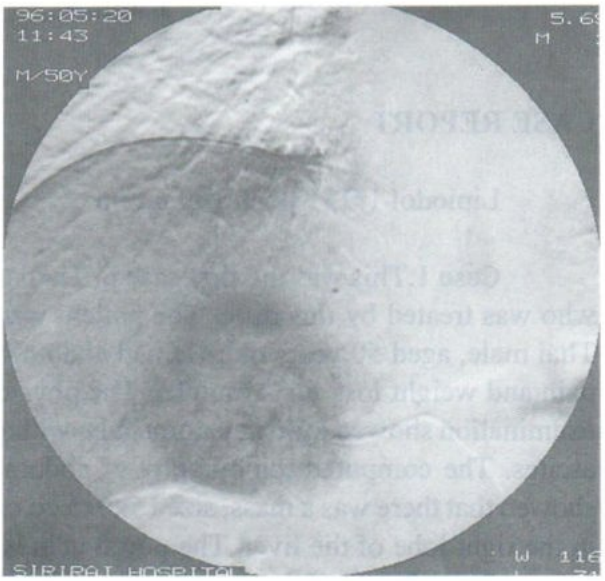

2C

Fig. 2B-C. The celiac angiography of the liver showed hypervascular mass, with staining in the right lobe of the liver

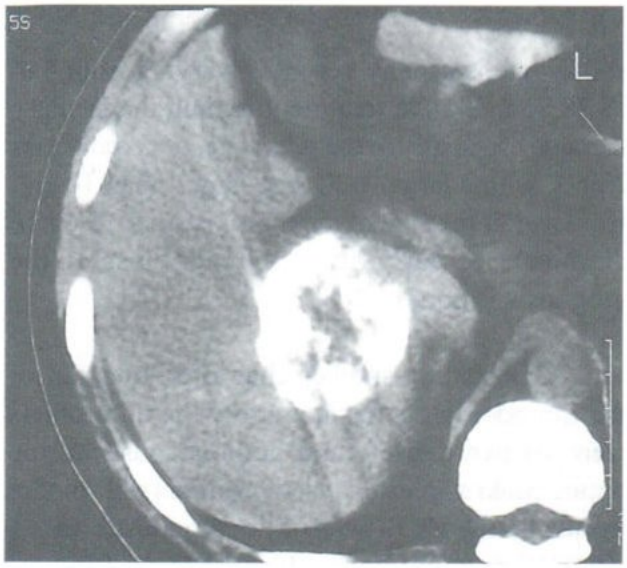

3A

Fig. 3A. The computed tomography of abdomen, after injection of Lipiodol-I*131, showed dense Lipiodol I*131 in the periphery of the HCC.

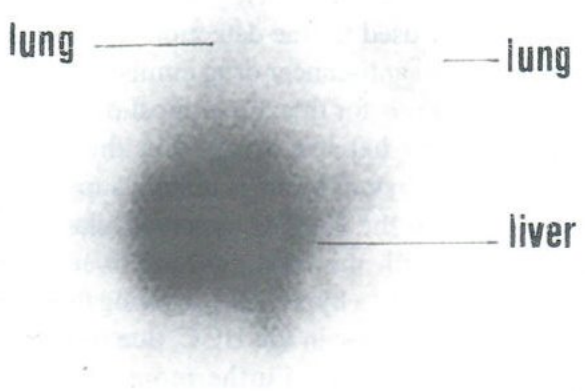

3B

Fig. 3B. The total body radionuclide scan showed hot spot of radioactivity in the tumor in the liver.

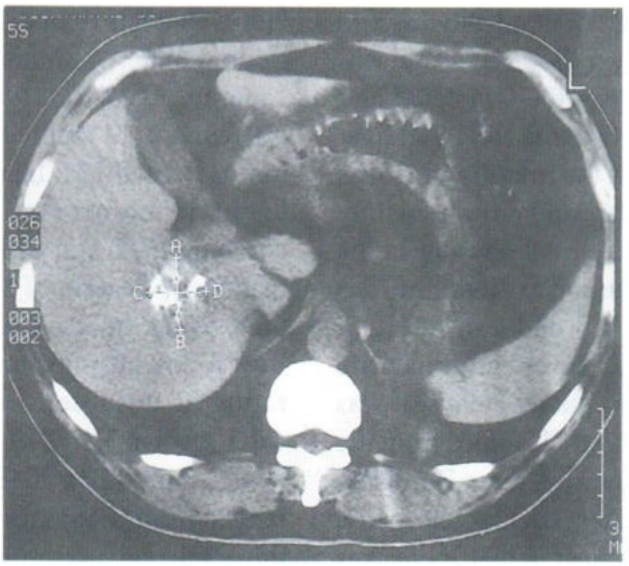

Fig. 4. Six months after the first injection of Lipiodol I*131, the computed tomography study of the abdomen showed the HCC was smaller than 2x3 cm.

DISCUSSION

Today ,we know that after injection of Lipiodol into the hepatic artery, the Lipiodol is selectively deposited in HCC, remains for a long time, and it is used for the detection for HCC and treatment with anti-cancer drug emulsions. There are many reasons for this. First ,most of the HCC is supplied by hepatic artery, but the normal hepatic parenchymal tissue is mainly supplied by portal vein. So the HCC is hypervascularized in comparison with the nontumorous liver tissue. Secondly, there is a hypothesis showing that there is a slow blood flow in the HCC, due to neovascularity in the tumor. Furthermore ,the architecture of the neovessels seems to account for an importance trapping of macromolecules into the extra capillary spaces, in HCC. Thirdly, the reduction or even absence of lymphatic vessel has also been suggested as a cause. And there is a poor reticuloendothelial system in HCC ,but not in a normal liver. The lipid droplets are captured by Kuffer cells, transferred to the hepatocytes, and then eliminated. J.Raoul studied the biodistribution of the I*131 labeled Lipiodol injected into the hepatic artery in the patient with HCC and liver metastasis, and showed that the investigation was extremely well tolerated. The Lipiodol was mainly in the liver, and there was a small amount in the lung. There was a high tumor to nontumorous activity ratio greater than 4.3 and 2.4, in HCC, and metastasis respectively. The effective half life of I*131 Lipiodol was more than 4.3 days. It was eliminated mainly in the urine. Clearance from the tumor was slower than the normal liver. Biodistribution did not change in the patients who had a second injection, which indicates that there was no saturation phenomenon. The study showed that the Lipiodol was a potential carrier vehicle for therapeutic agent, and for internal radiation of the tumor.

The prognosis of the patients with unresectable HCC is very poor. And the resectability rate is usually very low, varying from 4 to 18 %.So palliative treatment remain the primary therapy, especially in the late stage, or Okuda class 2 or 3, with a large HCC size larger than 10 cm. However, if the size of the tumor is small (5 cm in diameter) or early stage, Okuda class 1, the prognosis is good.

Our study showed that after injection of the Lipiodol in the hepatic artery the oil droplets were stained densely and homogenously in the tumor. Maki suggested that the amount of Lipiodol uptake by the HCC, was of the prognostic value. If the HCC was larger than 10 cm. and the Lipiodol droplets were distributed heterogenously in the tumor, it needed an increasing amount of Lipiodol to cover the entire tumor volume. Furthermore, in the late stage, there was usually hepatoportal or hepatohepatic AV shunting. The Lipiodol passed through the AV shunting to the systemic circulation and was trapped by lungs. So it was a need to embolize AV shunting before the injection of Lipiodol. Radiation dosimetry, A. The patients S.Perring et al studied dosimetric assessment of radioactive I*131 label Lipiodol as a potential agent in colorectal liver metastases using combined CT and SPECT. Their report showed that quantification of SPEC images indicated that 86% of the injected activity was retained in the liver following injection, and the tumor to the liver ratios of dose delivered ranged from 1.2:1 to 4.7:1,median 3.1:1 .Tumor doses ranged from 11.8 to 43.3 mGy/MBq of I*131 injected. Dose to lungs ranged from 0-46%,median 16%.And in our study the total body scintigraphy images showed the main radioactivity was in the tumor. (very hot spot in the liver, figure 3b) There was minimal activity in the lungs. And there was no measurable uptake of I*131 in the thyroid .It was possible that the release of stable iodine 127 from the injected contrast medium used in angiography and Lipiodol effectively blocked the thyroid.

Radiolabeled I*131 Lipiodol has been observed to have a whole body retention of approximately 5 days. Considerations of radioprotection would therefore necessitate an extended periods of hospitalization with isolation following administration. One patient was still alive longer than 2 years after the initial treatment. He did not have complications related to radioactive iodine such as hypothyroidism and bone marrow suppression.

B.The mean radiation exposure to the radiologist who injected lipiodol-I*131 measured by TLD method were as the followings :

at right hand	0.9 mSV.
at left hand	0.4 mSV
at thorax	0.1 mSV

The maxinum permissible dose are as the followings :

in the period of	3 months	1 year
for extremities	400	750 mSV
for gonad	30	50 mSV

So we conclude that the procedure was safe for the patients and radiologists.

The indications for injection of Lipiodol-I*131 into hepatic artery are :

1.unrectable/untransplantable HCC.

2 HCC with portal vein thrombosis.

And contraindications are :

1. HCC with cirrhosis Okuda class 3 ,
2. extrahepatic metastasis
3. severe pulmonary, or renal insufficiency.
4. Leukopenia/thrombocytopenina
5. pregnancy/lactation.

In our study, there were problems to be solved.

1. The lipiodol-I*131 must be imported directly from France by the hospital. Sometimes there is a delay in transportation. So the study must be well planned.

2.Problem concerning the isolation ward for radioprotection : There is limitations in number of these special beds in the hospital, and it is mainly occupied for treatment of carcinoma of thyroid by I*131.

3.Problem due to radiation exposure to paramedic personal : Some persons are afraid of radiation.

4.The cost of Lipiodol I*131 is high(about 1500 US$/dose.) However, we are thankful to the CIS ,and Biogenetect company who supply the lipiodol I*131 free of charge for our project in some patients.

However, the fact is that this project study is a complex procedure requiring a certain good cooperation between the departments of nuclear medicine, radiology, and medicine. And the important thing is that we have got a very good cooperation from everybody, that make the project successful .

CONCLUSION

Treatment of HCC by injection of Lipiodol I*131 was well tolerated, and associated with a good tumoral response in the small tumor group, (figure 4) and the patient was in good health for 2 years after treatment. In the large HCC group, the results were the same as treated by TOCE.

REFERENCES

1. J. Raoul, P.Bourguet ,J.Bretagne Hepatic artery injection of I-131-labeled Lipiodol, Part 1 Biodistribution study results in patients with hepatocellular carcinoma and liver metastases.,Radiology 1988;168:541-545.
2. J.Raoul, P. Bourguet, J, Bretagbe, Hepatic artery injection of I-131-labeled Lipiodol, Part 2 Preliminary results of therapeutic use in patients with hepatocellular carcinoma and liver metastases, Radiology 1988;168:547-550.

3. H. S. Yoo, J. T. Lee, K. W. Kim , Nodular hepatocellular carcinoma Treatment with subsegmental intraarterial injection of iodine-131-labeled iodized oil.Cancer Nov 1991 ;68:1878-1884.
4. J.I. Raoul, J.F. Bretagne, J.P. Caucanas, Internal Radiation Therapy for hepatocellular carcinoma , Cancer Jan 1992,69: 346-352.
5. S.Perring, R.Hind, J.Fleming, Dosimetric assessment of radiolabelled lipiodol as a potential therapeutuic agent in colorectal liver metastases using combined CT and SPECT , Nuclear mecidine communications 1994,15:34-38.
6. GM. Dusheiko, KE Dick, AK Burroughs. Treatment of small hepatocellular carcinoma. Lancet 1992;340:285-288.
7. S.I watsuki, TE Starzl, DG Sheahan. Hepatic resection versus transplantation for hepatocellular carcinoma. Ann Surg 1991;214:221-229.
8. T. Livaghi, D. festi, F Monti. US-guided percutaneous alcohol injection of small hepatic and abdominal tumors. Radiology 1986;161:309-312.
9. K. Takayasu, Y. Shima, Y Muramatsu. Hepatocellular carcinoma-treament with arterial iodized oil with and without chemotherapeutic agents. Radiology 1987; 162:345-351.
10. H. Nakamura , T Hashimoto , H Oi. Transcatheter oily chemoembolization of hepatocellular carcinoma. Radiology 1989;170:783-786.
11. K. Okuda, T. Ohtsuki , H. Obata . Natural history of hepatocellular carcinoma and prognosis in relation to treatment: study of 850 patients. Cancer 1985;56:918-928.
12. K. Nakakuma, S. Tashiro, T. Hiraoka. Hepatocellular carcinoma and metastatic cancerdetected by iodized oil. Radiology 1985;154:15-17.
13. K. Nakakuma, S. Tashiro ,T. Hiraoka. An attempt for increasing effects of hepatic ligation in advanced hepatoma. Jap Deutsh Med Berielite 1979;24:675-682.
14. CI Park, Si Choi, HG Kim. Distribution of lipiodol in hepatocellular carcinoma. Liver 199;10:72-78.
15. S. Maki, T. Konno, H. Maeda, Image enhancement in computerized tomography for sensitive diagnosis of liver cancer and semiquatitation of tumor selective drug targeting with oily contrast medium. Cancer 1985;56:751-757.

HIGH DOSE RATE BRACHYTHERAPY IN BENIGN UTERINE BLEEDING DISORDERS

Chonlakiet KHORPRASERT MD., Chotika JUMPANGERN MSc.

ABSTRACT

A case report of benign uterine bleedings (metropathia) was treated with high dose rate brachytherapy. The radiation doses were 2 fractions of 700 cGy at 1 centimeter from the tandem at four weeks interval. The patient had no bleeding in a month after treatment. She could tolerate the treatment well without any complications. High dose rate brachytherapy should be remembered in cases of uterine bleeding resisted to other therapies especially in cases of high risk for operation. However, long term follow-up should be done to evaluate late radiation effect of high dose rate radiation for benign uterine bleedings.

INTRODUCTION

Radiotherapy was a method of choice for the treatment of benign bleeding disorders (metropathia) in a woman of high surgical risk in the past. The methods of treatments are intracavitary brachytherapy or external irradiation or both. Most of the brachytherapy treatments used radium as a radioactive source.[1,2] Only a report using high dose rate iridium as a radioactive source for brachytherapy in benign uterine bleeding disorders is available.[3]

CASE REPORT

In August 1991, a 35 years old female patient with chronic renal failure presented at the gynecologic clinic because she had bleedings per vagina. Gynecologic examination revealed bleeding per cervical os. The patient was undergone dilatation and curettage procedure, and the pathological report was proliferation of endometrium. The diagnosis of benign uterine bleeding was given. Her hematocrit was 17 %. She was affected with chronic glomerulonephritis since 1986. In 1988, she was diagnosed of having chronic renal failure. In 1990, kidney transplantation was done, but the result was not good. The transplanted kidney deteriorated quickly, and she was diagnosed of having chronic renal failure again shortly after the transplantation.

The gynecologist prescribed 150-mg DMPA (depot medroxyprogesterone acetate) intramuscular injections every 3 weeks for 6 cycles. In February 1992, she still had periodic vaginal bleeding and her hematocrit was 17%. The second course of 150-mg DMPA intramuscular injections every 3 weeks for 4 cycles was prescribed. In December 1992, her hematocrit was 18% with periodic vaginal bleeding. She suffered from periodic vaginal bleeding with low hematocrit level through serveral courses of medical treatments. In July 1995, She was referred to us for intracavitary radiotherapy because her hemoglobin level was too low to be good candidate for kidney transplantation and she had high surgical risks for hysterectomy.

Division of Radiation Oncology, Department of Radiology, Faculty of Medicine, Chulalongkorn University, Bangkok.

TECHNIQUE

The patient was treated using our microSelectron-HDR afterloading machine. Single rigid 3.2-mm diameter intrauterine tube with 30 degrees angled end was inserted into uterine cavity as shown in figure 1.

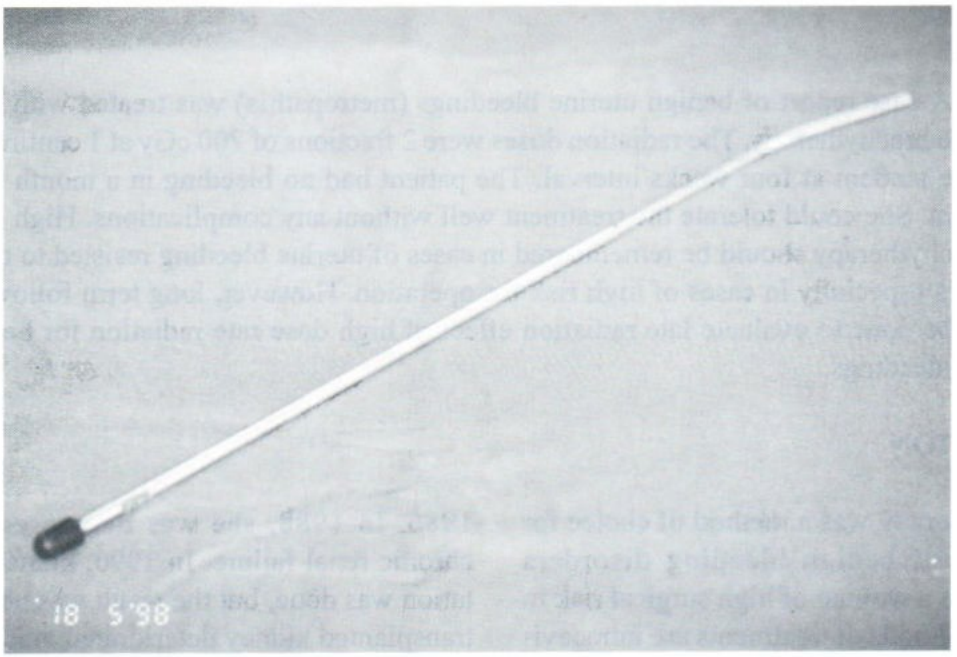

Fig. 1 A rigid 3.2-mm diameter intrauterine tube with 30 degrees angled end.

The intrauterine portion length of the tube was 6 centimeters, and iridium source positions were placed not beyond uterine cavity. Reference isodose for treatment was prescribed at distances of 1 centimeter from axis of applicator. The total treatment consisted of 2 fractions of 700 cGy at four weeks interval. The total rectal dose and bladder dose defined by ICRU were 506 cGy and 830 cGy respectively. Only oral analgesic drug was needed. The treatment procedures were carried out as an out-patient and completed the procedures in 2 hours.

RESULT

The patient tolerated the treatment procedure very well, no immediate complication was found. One month after treatment, the bleeding stopped, and the hematocrit level gradually increased. During 2 years and 8 months follow-up, no bleeding has been observed. In March 1998, her hematocrit was 36.6 %.

DISCUSSION

The availability of computer controlled remote afterloading machines has given impetus to the use of high dose rate brachytherapy. The microSelectron-HDR could be used for outpatient HDR iridium-192 brachytherapy procedures. This machine uses a single high activity iridium-192 source, which can be programmed by its computer

to be selected. It offers several important advantages over low dose rate manual afterloading techniques, including

1. Improved radiation protection to the staff
2. Increased ease of achieving optimized dose distribution
3. Elimination of complications associated with prolonged bed confinement, especially in elderly patients
4. Marked decrease in patient discomfort
5. Administration of the treatment as an outpatient basis
6. Avoidance of general anesthesia in selected patients

Radiotherapy was a method of choice for the treatment of benign bleeding disorders (metropathia) in women of high surgical risk in the past. The methods of treatments are intracavitary brachytherapy or external irradiation or both. Most of the treatments used radium as a radioactive source. Late effects such as cardiovascular deaths, and higher incidence of malignant diseases has been reported.[2,4] In 1989, Ryberg M. and associates published a number of malignant tumors in 107 cases after followed up in 933 women with benign bleeding disorders treated with radiation during 1912 to 1977 period.[2] Inskip PD and associates reported an increased risk of leukemia and other cancer among 4153 women treated with intrauterine radium for benign uterine bleeding disorders between 1925 and 1965. The treatment of benign uterine bleedings by radiotherapy has gradually decreased, but for the selected patients that resist to other treatments, it is an effective treatment. Only a report using high dose rate iridium as a radioactive source for brachytherapy in benign uterine bleeding disorders is available. We demonstrated successful outpatient procedures for treatment of benign uterine bleeding disorders with high dose rate intracavitary radiotherapy.

CONCLUSION

High dose rate iridium intracavitary radiotherapy can be used effectively without any acute complication in cases of uterine bleeding resisted to other therapies especially in cases of high risk for operation. However, long-term follow-up should be done to evaluate late radiation effect of high dose rate radiation for benign uterine bleedings.

REFERENCES

1. Kucera H, Huber H, Weghaupt K. Intracavitry radiotherapy of benign recurrent uterine bleedings. Geburtshife Frauenheilkd 1982 May;42(5):391-393
2. Ryberg M, Lundell M, Petterson F. Radiotherapy in benign uterine bleeding disorders. The Radiumhemmet metropathia cohort 1912-1977. Short and long term results. Ups J Med Sci 1989;94(2): 161-169
3. Kucera H, Huber H, Weghaupt K. Radiomenolysis of the endometrium using high -dose iridium irradiation--clinical and cytologic results. Strahlentherapie 1984 Apr;160(4):220-223
4. Inskip PD, Monson RR, Wagoner JK, Stovall M, Davis FG, Kleinerman RA, Boice JD Jr. Cancer mortality following radium treatment for uterine bleeding. Radiat Res 1990 Sep;123(3):331-344

STIMULATING HAIR GROWTH BY HELIUM-NEON LASER IN RATS

Pichit TRIVITAYARATANA, M.Sc.[1], Wanna TRIVITAYARATANA, M.D.[1], Sanun HORMHUAN, B.Sc.[2], Uriwan JINDEWA, B.Sc.[3]

ABSTRACT

We performed a study to determine whether 632.8 nm helium-neon (He-Ne) laser radiation would affect hair growth of the skin after the hairs had been pull out in 18 female rats, 8 weeks of aged. The four skin areas, 2 cm in diameter each, the hairs were pull out at the back of all rats after ketamine hydrochloride anesthesia. To determine the rate of hair growth and optimum daily energy density irradiance, energy density of 1.35, 2.70 and 4.05 J/cm^2/day of He-Ne laser were delivered for two weeks to area I (15 mins every 24 hrs), area II, two repeated exposures at 12 hrs interval and area III, three repeated exposures at 8 hrs interval, respectively. The control site (area IV) was not irradiated but received placebo light. Additional to the observation of the reaction at all areas where the hairs were pull out, length of hairs on them were measured daily by capillary tube and magnifying lens. The results shown that normal rate of hair growth was 0.27 mm/day while the growth rate at the irradiated areas with 1.35, 2.70 and 4.05 J/cm^2/day were 0.42, 0.62 and 0.36 mm/day, respectively. 2 repeated daily exposures were the optimum energy density for stimulation of hair growth. Hair growth in the control site was the same rate as 1 exposure site and 3 repeated exposures site. Hair follicles needed some energy density of He-Ne laser radiation to initiate hair growth in rats.

INTRODUCTION

Low-energy laser irradiation has been shown to have some bioeffects. Activation of local cellular and humoral level, such as increased formation of ATP,[1,2] fibroblast, mast cells,[3,4] change in prostaglandin level, increased angiogenesis,[5] increased epithelial activity and microcirculation, prevent post traumatic degeneration of nerves [6] were described as the local effect. Systematic effect of low-energy laser were to promote wound healing,[3,7,8] antiinflammation,[2,5] relief pain,[8-12] increased vascularization, increased blood flow and lymphatic drainage.[13] Some authors demonstrated that interaction at tissue level was photochemical in nature, dependent on absorption in a tissue chromophore. Each of these potential chromophores absorbed radiation of some wavelength or wavelengths.[3,4,8,14] The absorption probably increased the energy of this chromophore and its activity was thus altered in relationship to its environment and consequently the metabolism of the cell was changed affecting tissues and organs.[14]

Alopecia is a psychological problem especially in women that play a role in the leading position. Male pattern baldness can affect not only

[1] Department of Radiological Technology, Faculty of Medical Technology, Mahidol University.
[2] Department of Diagnostic Radiology, Bumrungraj Hospital.
[3] Lopburi Cancer Center.

in men, but also in women. In patients with early male pattern baldness, the subcutaneous blood flow was 2.6 times lower than the values found in the normal individuals.[15] Aging results in a reduction of the maximal conductance of the cutaneous vasculature.[16] Stimulating hair growth by many substances, some microorganisms, immunosuppressive drugs, vasodilator drug have been reported.[17-27] Minoxidil is a potent vasodilator that has been used to stimulate cutaneous blood flow in human balding scalps.[28] If this hypothesis is true, it means drugs or substances that causes cutaneous vasodilation, will promote hair growth. He-Ne laser is a non-ionizing radiation and low -energy laser that shows vasodilation effect and angiogenesis.[5,29] It is very interesting thing whether He-Ne laser irradiation would affect hair growth. We proposed an in vivo study in rats in order to measure the rate of hair growth and to decide an optimum laser energy density per day.

MATERIALS AND METHODS

18 white female Wistar rats aged 8 weeks from National Laboratory Animal Center, Mahidol University were introduced in the same environment, same food supplement for 4 weeks before starting the experiment. Theirs mean weights were 324 ± 17.8 g ranging from 300-400 g. These rats were grouped by means of simple random sampling into 3 groups that consisted of 6 rats in each group. All rats were anesthetized with ketamine hydrochloride (25 mg/kg) intramuscularly 5 mins before pulling the hair off from the back. Each of the 4 area was 2 cm in diameter as shown in Fig 1.

Placing these rats in a control environment and food supplement for 24 days, thus the hair follicles grow into telogen stage.[30] The hairs at the same area were pull off again to induced anagen stage of hair follicles. Each skin without hair was irradiated by He-Ne laser (Professional laser: power 30 mW) of monochromatic 632.8 nm. Daily energy density was delivered to various sites according to the following programs:

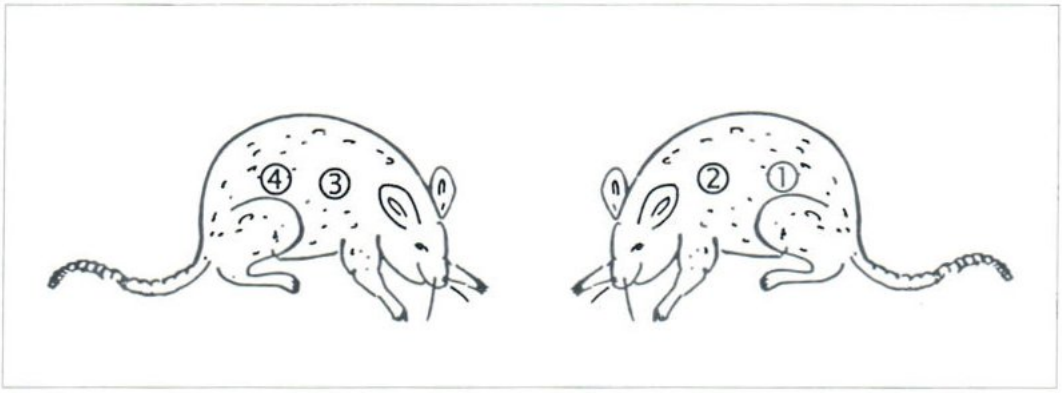

Fig. 1 4 areas of skins at the back of rat, after the hairs were pull off

Table 1. Number of fractions per day and energy density delivered to various sites

site	number of fractions (15 mins/fraction)	energy density/day (J/cm^2/day)
1	0	0.00
2	1	1.35
3	2	2.70
4	3	4.05

Area at site 1 was control, the site 2, 3 and 4 were daily treated with 1, 2 and 3 fractions of He-Ne irradiation for two weeks, respectively. Apart from the observation of the reaction at the 4 areas where the hairs were pull off, length of hairs were also measured by capillary tube and magnifying lens.

RESULTS

Pigmentation was observed on day 3 at site 3, on day 4 at site 2 and 4, on day 6 at the control site.

For 14 days, hair length were 3.9, 5.9, 8.8 and 5.1 mm on site 1, 2, 3 and 4, respectively, as shown in table 2. Daily hair growth in rats group 1, 2 and 3 were plotted versus various sites in figure 3, 4 and 5, respectively.

Table 2. Mean hair length (mm) on various sites from 3 groups of rats

day	site 1	site 2	site 3	site 4
3	0.0	0.0	0.5	0.0
4	0.0	0.0	0.8	0.0
5	0.0	0.6	1.7	0.5
6	0.0	1.3	2.5	1.0
7	0.0	1.8	3.3	1.5
8	0.6	2.4	4.1	2.0
9	1.1	3.0	4.9	2.6
10	1.6	3.6	5.7	3.0
11	2.2	4.2	6.4	3.6
12	2.7	4.8	7.2	4.0
13	3.3	5.3	8.0	4.6
14	3.9	5.9	8.8	5.1
mean /day	0.27	0.42	0.62	0.36

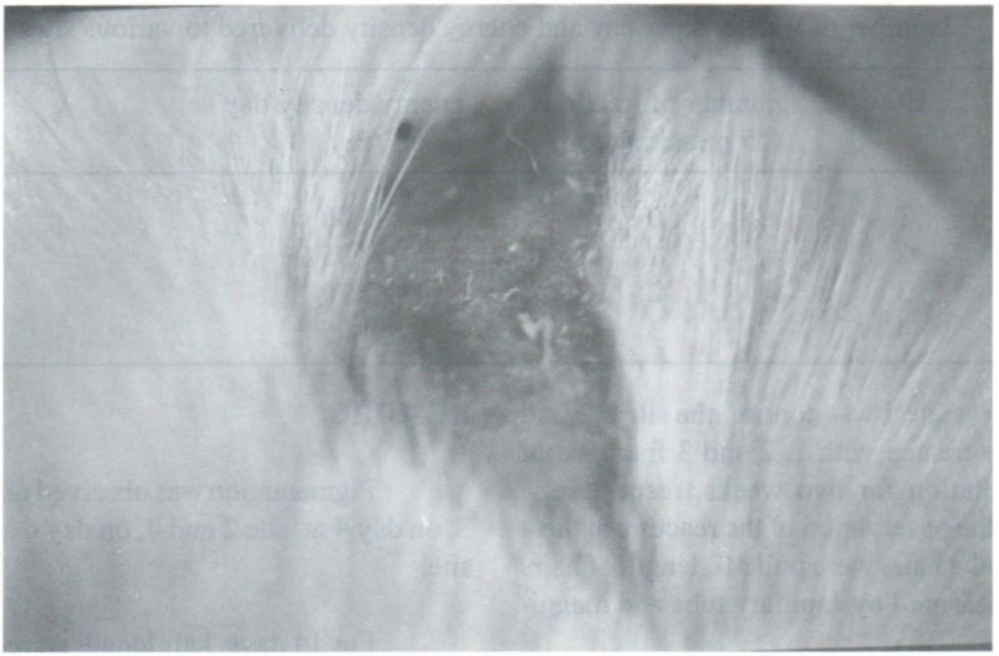

A.

Fig. 2 Observation on day 3 A. no pigmentation at control site

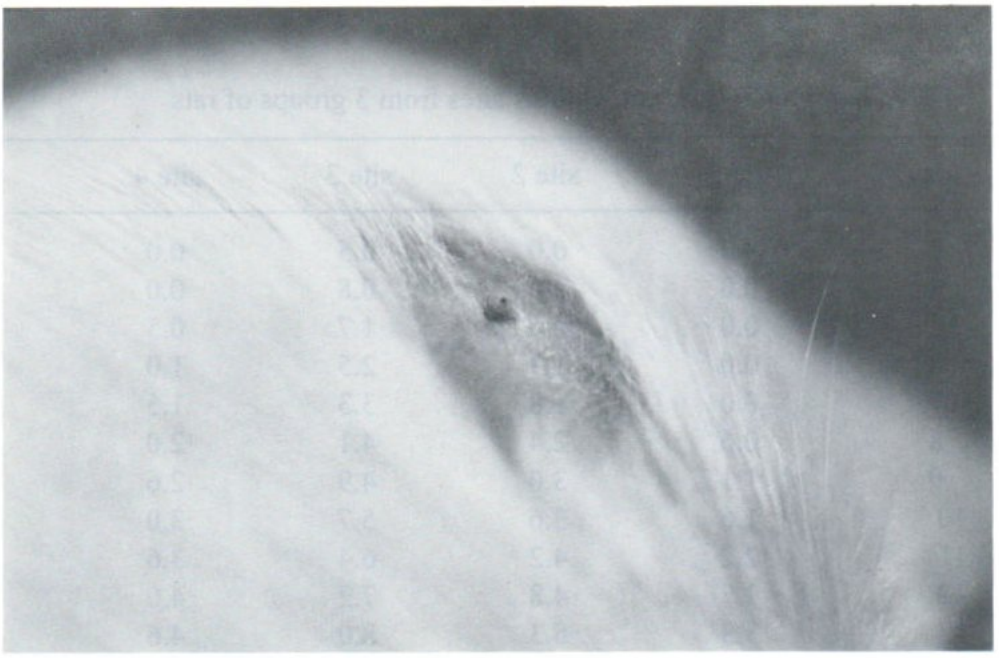

B.

Fig. 2 Observation on day 3 B. pigmentation was observed on site 3

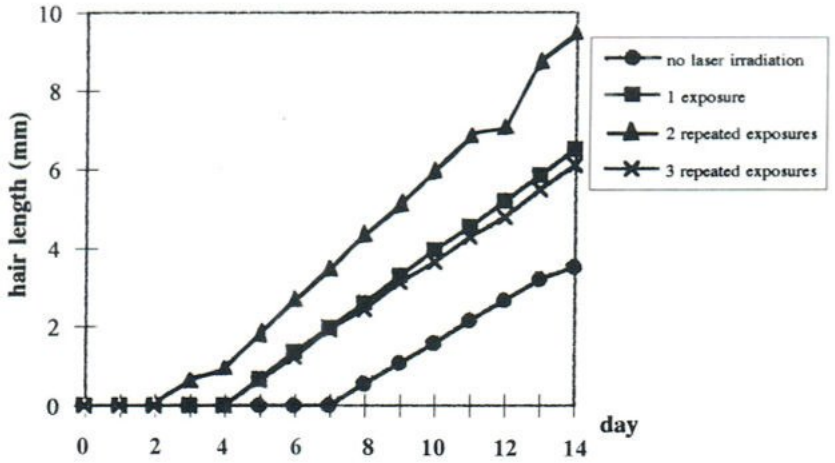

Fig.3 Mean daily hair length on various sites in rats group 1

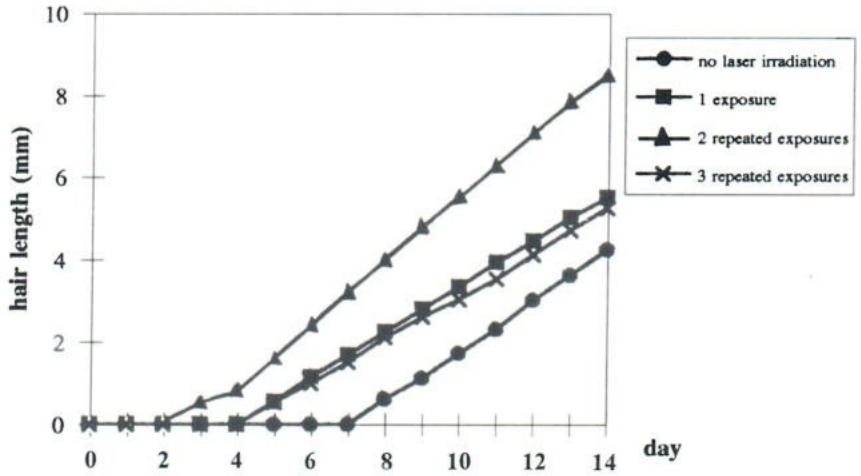

Fig.4 Mean daily hair length on various sites in rats group 2

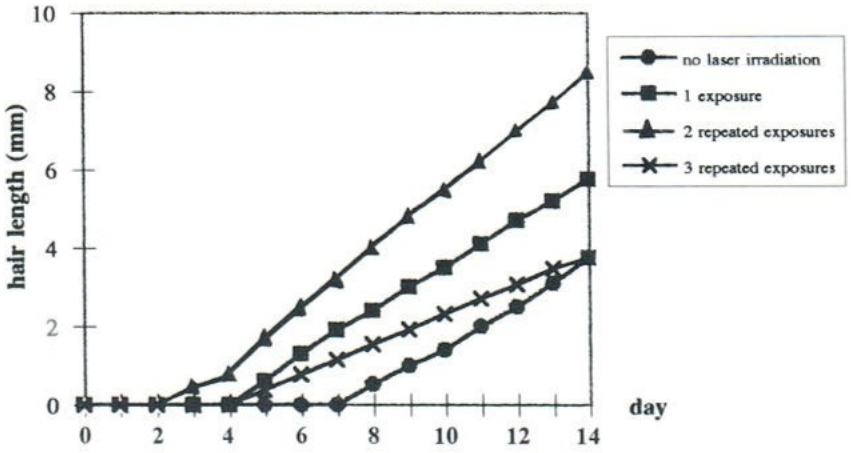

Fig.5 Mean daily hair length on various sites in rats group 3

Analysis of variance was used to analyze the differences between mean of hair length on 4 sites. From 3 groups of rats, the mean at site 1 (μ_0), 2 (μ_1), 3 (μ_2) and 4 (μ_3) were significantly different (p-value = 0.027) as shown in table 3 and hair length on site 3 that was irradiated by He-Ne laser 2 times a day was longer than site 1, 2 and 4 (p-value = 0.005, 0.04 and 0.03), respectively. Hair growth on the control site was the same rate as site 2 and 4 (p-value = 0.190 and 0.239)

Table 3. ANOVA Table

source	d.f.	sum of square	mean of square	F
treatment	3	72.58	24.19	4.54*
error	40	195.90	4.89	
total	43	268.48		

* p-value = 0.027, significant at $\alpha = 0.05$

Table 4. Comparison of means of hair length in each site

treatment	$t = \frac{\lvert (\bar{X}_i - \bar{X}_j) \rvert}{\sqrt{MSE\{(1/n_i) + (1/n_j)\}}}$	p - value
μ_0 , μ_1	0.94	0.190
μ_0 , μ_2	2.70	0.005*
μ_0 , μ_3	0.71	0.239
μ_1 , μ_2	1.76	0.040*
μ_1 , μ_3	0.22	> 0.250
μ_2 , μ_3	1.98	0.030*

* significant at $\alpha = 0.05$

DISCUSSION

The rate of hair growth is supposed to be influenced by such factors as spicies, race, sex, age, season of year, nutrition and hormones.[31,32] Observations have been made mainly on animal hair by the reason of the short cycle of its hair growth. The capillary method was used to measured the rate of hair growth. This method could be used daily with an error rate of 2.82% at 25-30°C.[30] The results showed that normal rate of hair growth was 0.27 mm/day, but the growth rate in the irradiated site with 2.7 J/cm^2/day laser energy was 0.62 mm/day (Table 2). The linearity of hair growth of the 4 areas of the skin were found in all groups (Fig. 3, 4 and 5).

Many chemicals, microorganisms, drugs, immunosuppressive agents, monochromatic light were conducted to stimulate hair growth.[17-27] Daily repeated exposures to high doses of monochromatic 260 nm radiation results in the initiation of active hair growth in telogen phase of hair follicles by occurrence of pigmentation in day 5, with hair protruding above the surface approximately two weeks after the first exposure.[17,18] The 632.8 nm monochromatic light of laser in various power energy were delivered to the various sites of rat-skin. The pigmentation were observed at day 3-4, hairs were protuded at day 4-5 with higher rate than the control site (no laser irradiation). Pigmentation can be observed at the control site on the skin at day 6 with hair protruding above the skin at day 8 after the first exposure (Table 2).

2 repeated exposures doses per day (2.7 J/cm^2) was the optimum energy density for stimulation of hair growth in all 3 groups of rats with mean length 8.8 ± 0.5 mm. This value was significantly longer than hair length at the 1 exposure site (1.35 J/cm^2) and 3 repeated exposures site (4.05 J/cm^2) (p-value = 0.04 and 0.03, respectively). With single exposure dose of 632.8 nm radiation, neither the radiation nor the concentration of protease at the level of the hair germ would be sufficient to initiate hair growth. The highest rate of hair growth was occured at 2 repeated exposures site, It is possible that a second exposure at about 12 hours after the first would release newly formed protease in the recovering cells of the epidermis and that it is this, in combination with the earlier released enzyme or acting on primed target, which caused the initiation of hair growth. The hair germ at 3 repeated exposures site will be destroyed when the third exposure was given. The thymine dimer in DNA of nuclei separate from the matrix cell and telogen hair follicle was dead.[32] It indicated that hair follicles need some energy density of monochromatic light to initiate hair growth.

Excessive dose of He-Ne laser may be harmful to the cell. In rabbit, giving an irradiance of 4.42 W/cm^2 for daily 3-30 min, the mitotic rate of corneal epithelium was reduced and finally damaged. Severe epithelial damage after 30 seconds (0.13 J/cm^2) daily irradiation and 20 min irradiation destroyed most of the epithelium. Endothelial damage occured after irradiation periods of 1 min (0.26 J/cm^2). In cat, corneal thickness increased but endothelial cell density decreased by 21% and 12%, respectively.[33] The bioeffects of low-energy laser irradiation on wound healing have been shown to be ineffective (0.37 and 0.45 J/cm^2/day)[34] or stimulating (3.8 J/cm^2/day) depending on doses.[3] All these experiments revealed that low-energy lasers do have specific bioeffects which seem to be changed from stimulation to damaging with increasing doses.

In radiotherapeutic patients, the distress events may affect from the nature of diseases and the radiation-tissue interaction.[35] Radiation induced alopecia in these patients usually appeared because of the decreasing of newly forming hair cortex.[36] He-Ne may be the alternative way to

stimulate hair growth in male pattern alopecia and radiation induced alopecia by photochemical mechanism. However, the mechanism and pathogenesis of alopecia are the important things that affect the success of the treatment.

REFERENCES

1. Herbert KE, Bhusate LL, Scott DL, Diamantopoules C, et al. Effect of laser light at 820 nm on adenosine nucleotide levels in human lymphocytes. Lasers Life Sci 1989; 3: 37- 45.
2. Palmgren N, Jensen GF, Kaae K, Windelin M, et al. Low-power laser therapy in rheumatoid arthritis. Lasers Med Sci 1969; 4: 193-196.
3. Atabey A, Karademir S, Atabey N, Barutcu A. The effects of the helium-neon laser on wound healing in rabbits and on human skin fibroblasts in vitro. Eur J Plast Surg 1995;18:99-102.
4. Basford JR. Low-energy laser therapy : controversies and new research findings. Lasers Surg Med 1989; 9: 1-5.
5. Mester E, Mester AF, Mester A. The biomedical effects of laser application. Lasers Surg Med 1985;5:31-39.
6. Schwartz M, Doron H, Erlich M, Lavie V, et al. Low energy He-Ne laser and the manifestation of post-traumatic degeneration of the rabbit optic nerve. Lasers Surg Med 1987;7:51-55.
7. Kana JS, Hutschenreiter G, Haina D, Waidelich W. Effect of low power density laser radiation on healing of open skin wounds in rats. Arch Surg 1981;116:293-6.
8. Abergel RP, Muker CA, Lam TS, Dwyer RM, et al. Control of connective tissue metabolism by lasers : recent developments and future prospects. J Am Acadamy Dermatol 1984;11:1142-1150.
9. Mokhar B, Baxter GD, Walsh DM, Bell AJ, et al. Double-blind, placebo-controlled investigation of the effect of combined phototherapy/low intensity laser therapy up on experimental ischaemic pain in humans. Lasers Surg Med 1995;17:74-81.
10. Wong E, Lee G, Zucherman J, Mason DT. Successful management of female office workers with " repetitive stress injury or carpal tunnel symdrome " by a new treatment modality-application of low level laser. Intern J Clinical Pharmacol & Therapeutics 1995;33:208-211.
11. Vasseljen OJ, Hoeg N, Kjeldstad B, Johnson A, et al. Low level laser versus placebo in the treatment of tennis elbow. Scand J Rehabil Med 1992; 24: 37-42.
12. Stelian J, Gil I, Habot B, Rosenthal M, et al. Improvement of pain and disability in elderly patients with degenerative osteoarthritis of the knee treated with narrow-band light therapy. J Am Geriatr Soc 1992; 40: 23-26.
13. Karu TI, Letokhov VS. Biological action of low intensity monochromatic light in the visible range. In: photobiology and photomedicine. Edited by Martelluci S, Chester AN. New York : Plenum, 1985:57-66.
14. Belkin H, Schwartz M. New biological phenomena associated with laser radiation. Health Physics 1989;56:687-690.
15. Klemp P, Peters K, Hamsted B. Subcutaneous blood flow in early male pattern baldness. J Invest Dermatol 1989;92:725-726.
16. Rooke GA, Savage MV, Brengelmann GL. Maximal skin blood flow is decreased in elderly men. J Appl Physiology 1994;77: 11-14.

17. Argyris TS, Argyris BF. Stimulation of hair growth during skin regeneration Developmental Biol 1959;1:269-280.
18. Johnson BE. Potentiation of hair growth by ultraviolet light. Nature 1960;187:159-160.
19. Maurer M, Handjiski B, Paus R. Hair growth modulation by topical immunophilin ligands: induction of anagen, inhibition of massive catagen development, and relative protection from chemotherapy induced alopcia. Am J Pathol 1997;154:1433-1441.
20. Michelet JF, Commo S, Billoni N, Mahe VF, et al. Activation of cytoprotective prostaglandin synthase-1 by minoxidil as a possible explanation for Its hair growth-stimulating effect. J Invest Dermatol 1997; 108:205-209.
21. Philpott MP, Sanders DA, Bowen J, Kealey T. Effects of interleukins, colony - stimulating factor and tumour necrosis factor on human hair follicle growth in vitro: a possible role for interlenkin-1 and tumour necrosis factor alpha in alopecia areata. Br J Dermatol 1996;135: 942-948.
22. Nixon AJ, Broad L, Saywell DP, Pearson AJ. Transforming growth factor-alpha immunoreactivity during induced hair follicle growth cycles in sheep and ferrets. J Histochem Cytochem 1996;44:377-387.
23. Guo L, Degenstein L, Fuchs E. Keratinocyte growth factor is required for hair development but not for wound healing. Genes Dev 1996;10:165-175.
24. Jindo T, Tsuboi R, Imai R, Takamori K, et al. The effect of hepatocyte growth factor/ scatter factor on human hair follicle growth. J Dermatol Sci 1995; 10: 229-232.
25. Yamamoto S, Jiang H, Kato R. Stimulation of hair growth by topical application of FK506, a potent immunosuppressive agent. J Invest Dermatol 1994; 102:160-164.
26. Inaoka Y, Shakuya A, Fukazawa H, Ishida H, et al. Studies on active substances in herbs used for hair treatment. I. Effects of herb extracts on hair growth and isolation of an active substance from Polyporus Umbellatus F. Chem Pharm Bull(Tokyo) 1994;42:-533.
27. Lutz G. Effects of cyclosporin A on hair. Skin Pharmacol 1994;7:101-104.
28. Wester RC, Maibach HI, Guy RH, Novak E. Minoxidil stimulates cutaneous blood flow in human balding scalps: pharmacodynamics measured by laser doppler velocimetry and photopulse plethysmography. J Invest Dermatol 1984;82:515-517.
29. Colls J. Laser therapy today. Urdorf: Lasotronic, nd.
30. Montagna W, Dobson RL. The biology of hair growth. New York: Academic, 1958.
31. Wilkinson DS, Ebline FJG, Champion RH, Burton JL. Text book of dermatology. 4th ed. London: Butler & Tammer, 1986.
32. Montagna W, Dobson RL. Advance in biology of skin. 3rd ed. Oxford: Pergamon, 1969.
33. Deutsch D, Landsman N, Belkin M. Ef fects of repeated low energy laser irradiation in the anterior segment of the eye. Proc. Ist. Int. Cong. Laser Technol Ophth 1987;24.
34. Colver CB, Priestley GC. Failure of a helium-neon laser to affect components of wound healing in vitro. Br J Dermatol 1989;121:179-186.
35. Kim TH, Kim SH, Kim JH, Lee YS, et al. Measurement of apoptotic fragments in growing hair follicles following gamma -ray irradiation in mice. Anticancer Res 1996;16:189-192.
36. Potten CS, Burt PA, Roberts SA, Deshpande NA, et al. Changes in the cellularity of the cortex of human hairs as an indicator for radiation exposure. Radiat Environ Biophys 1996;35:121-125.

Message from

Professor Dr. Kawee Tungsubutra

Editor-in-Chief, The Asean Journal of Radiology.

This is the No. III of Vol. IV of the Asean Journal of Radiology published by the co-operation of the Radiologists both from the Asean and from other countries outside Asean. We have only another 1 year to keep the standard and the regularity of publishing of the Journals so that it can be accepted in the Index Medicus. In this issue we have the first paper from Indonesia. Dr. Cholid Badri had kindly sent his interesting paper which appeared in the first article of this Journal. Unfortunately the last few packs of air-parcels to Singapore, Indonesia and Philippines were sent back to me with different reasons. Anyhow, with the help of Dr. Zaini Ibrahim of the Bracco International B.V. and the other representatives of the Bracco International in different countries, I was furnished with the advices which I hope to overcome the problems of delivering the Journals to the appropriate persons in different countries. We will continue to co-operate and hope to have our journals accepted to be published in the Index Medicus next year, 1999-2000 !

Kawee Tungsubutra.

Kawee Tungsubutra

September-December 1998.

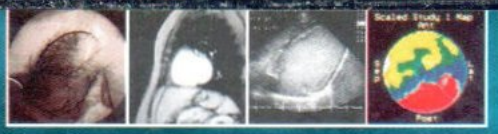

Keeping an eye on imaging

X-ray

MRI

US

NM

Magnetic Resonance Imaging

Ultrasound

Nuclear Medicine

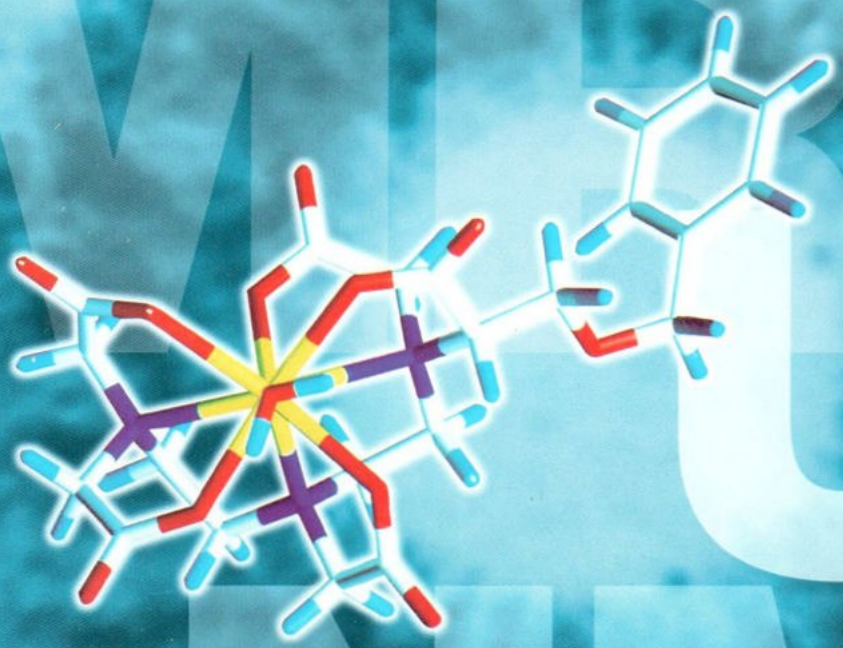

BRACCO IMAGING

Harmony in contrast